Distributed Control Approaches for Power Systems

by

Hajir Pourbabak

A dissertation submitted in partial fulfillment
of the requirements for the degree of
Doctor of Philosophy
(Electrical and Computer Engineering)
in the University of Michigan-Dearborn
2019

Doctoral Committee:

Associate Professor Wencong Su, Chair
Assistant Professor Junho Hong
Assistant Professor Zhen Hu
Assistant Professor Samir Rawashdeh

Hajir Pourbabak

hpourbab@umich.edu

ORCID iD: 0000-0002-1252-1546

DEDICATION

When I start finding out people in my memory who have supported me to be at the point where I am today, I always get to these people due to their endless love and continuing support.

This thesis is proudly dedicated:

To my father and mother, *Hojabr Pourbabak* and *Enji Ansari*, who have taught me that it is always important to be a human, no matter what. They truly sacrificed their life and future to unconditionally support me. It's impossible to thank them adequately for everything they have done for me. God bless them.

To my lovely wife, *Neda*, without her unconditional love and always support, I wouldn't be where I am today.

To my little sister, *Shaghayegh*, who is a true meaning of "there is no better friend than a sister and there is no better sister than you".

ACKNOWLEDGEMENTS

I would like to express my special appreciation and thanks to my advisor Professor *Wencong Su*, who has been a tremendous mentor for me through all the four years of my Ph.D. study. He's the best advisor and one of the smartest people I have ever worked. He has been supportive and has given me the freedom in my research to stimulate my creativity and professional growth while provided insightful discussions about the research. There have been many successes and failures during the last four years. He always supported me when I failed and encouraged me for more progress when I succeeded. I greatly appreciate the amount of time and effort he invested in my professional growth and all the opportunities he gave me. Without his help and support, I would not be where I am today.

I am greatly thankful to the excellent cooperation of committee members of my Ph.D. final defense Assistant Professor *Samir Rawashdeh* (ECE department), Assistant Professor *Junho Hong* (ECE department), and Assistant Professor *Zhen Hu* (IMSE). Their valuable advice and constructive comments truly improve my dissertation. I have to thank the members of my preliminary exam, Associate Professor *Kevin Bai* and Assistant Professor *Stanley Baek* for their helpful advice and constructive comments on my research. I especially thank *Mariann Brevoort* and *Amanda Donovan*, administrative assistants from ECE department for their great help and valuable support through all years of my Ph.D. Of course, there are many people and friends who supported me deeply. I don't have space or time to thank everyone I met in my doctoral journey, but they have all made me become myself.

TABLE OF CONTENTS

LIST OF TABLES

LIST OF FIGURES

ABSTRACT

The energy industry is undergoing through a reconstruction from a monopolistic electricity market to a more open and transactive one. The next-generation grid is a level playing field in terms of electricity transactions, where all customers have an equal opportunity. The emerging concepts of electricity prosumers are expected to have a significant impact on the retail electricity market. As a result, there is an urgent need to control the interactions among numerous consumers and prosumers. The existing control approaches can be divided into three categories, namely, centralized control, decentralized control, and distributed control. The majority of existing literature focuses on the centralized control. In most cases, the dedicated communication links are required to exchange data between the central controller and the local agents. The centralized control approaches are suitable for relatively small-scale systems without reconstructing the existing communication and control networks. However, as the number of consumers and prosumers are increasing to hundreds of thousands, there are some technical barriers on the centralized control-based economic operations such as heavy computation burden and single point of failure. The decentralized control is an intermediate solution to address the above mentioned challenges. The overall objective is to maximize the benefits of local agents and there is no guarantee that the decisions made by each local agents can contribute to the global optimal decision of the entire system. The distributed control has the potential to solve the economic operation problems of multiple consumers and prosumers. Local agents can share information through two-way communication links in order to find the global optimal decision. Application of distributed control methods in power system increase system's scalability, alleviate monopoly and monopsony, improve the privacy and distribute computational load among various entities.

CHAPTER 1
Introduction

In recent years, the high penetration of distributed generations, energy storage devices, dispatchable loads and advanced communication networks increases the customer and prosumers participation in the electricity market. This reconstruction is exerting considerable both positive and negative impacts in power systems. Distributed generations and energy storage devices provide energy resiliency, improve environmental benefit and enhance power quality/reliability of the power systems.

However, as the number of consumers and prosumers are increasing to hundreds of thousands, there are some technical barriers on the centralized control-based operations such as heavy computation burden and single point of failure. Additionally, a comprehensive communication networks are required to exchange data between the central controller and the local agents. The legacy centralized approach would not be able to cope with the huge amount of data and the system operators are facing a tough challenge to support ever-increasing demand with minimum cost due to the high complexity of the power dispatch among numerous power generators with respect to the transmission overloading. In other words, the centralized control approaches are suitable for relatively small-scale systems without reconstructing the existing communication and control networks.

Distributed control approaches are a practical alternative solution to reduce computational burden, remove a single point of failure and improve interoperability [2]. This type of methods iteratively shares information through a two-way communication channel with other agents to find an optimal solution. The main features of the proposed distributed algorithm in this dissertation can be summarized as follows: *Accuracy*: the accuracy achieved by distributed methods is as much as the accuracy of traditional centralized methods, while computational load is dramatically reduced.

Scalability and Interoperability: as the number of agents increases to hundreds of thousands, the legacy centralized method faces certain challenges such as computational burden while distributed algorithm is particularly suitable for solving large-scale optimization problems within a short period of time. *Privacy*: private information (e.g., revenue functions parameters) of agents is not released to others. *Fast Convergence*: due to distributed computational load among all agents in a system, fast convergence is one of the important feature of distributed algorithms. *Monopoly and monopsony*: the absence of central controller and nature of distributed control methods resolve issues raised by monopoly and monopsony.

This chapter provides a detailed discussion about the different control methods and a high-level literature review. Before that a list of required concepts such as microgrids, smart grids, the energy Internet, SCADA etc are provided.

1.1 Concepts

1.1.1 Microgrid

The U.S. Department of Energy defines a microgrid [3] as "a group of interconnected loads and distributed energy resources (DER) within clearly defined electrical boundaries that act as a single controllable entity with respect to the grid. A microgrid can connect and disconnect from the grid to enable it to operate in both grid connected and island mode." It is interesting to mention that the concept of a microgrid has been around for more than a hundred years. Around 1880, Thomas Edison founded and established the first investor-owned electric utility on Pearl Street in lower Manhattan of New York City [4]. On September 4th, 1882, the Pearl Street power station went into operation. This small electric utility was allowed to operate its 27-ton "Jumbo" constant-voltage dynamo (steam generator) and serve 82 local customers without being connected to a main grid, which did not exist yet. This investor-owned electric utility can be considered as the very first version of the microgrid, as shown in Figure 1.1.

In the early 1900s, the first statewide regulation of electric utilities emerged [5]. Due to the evolution of interconnected power grids through long transmission lines, the electric utilities were mov-

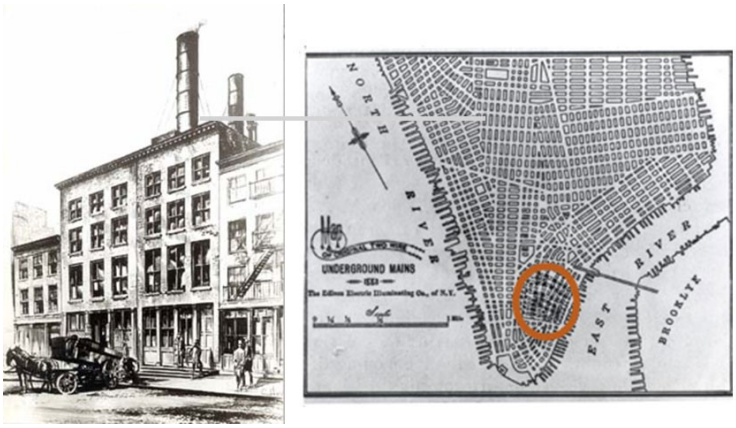

Figure 1.1: Edison strategically located the station in the densely populated area of lower Manhattan. (Photo credit: ConEd)

ing from a microgrid-like independent system to a highly centralized and regulated one. Across the world, the development of the microgrid had been fairly silent until the early 2000s. In the past two decades, however, the original microgrid concept has drawn increased attentions to address the limited electricity access issues for in remote and less developed communities. Microgrids are often the only practically possible solution or the most cost-effective way for these areas that are not connected with to the utility grid. In addition, the enhanced microgrid concept offers new socio-economic benefits that have not even been imagined previously. For instance, non-traditional power generators (e.g., wind turbines, solar panels, small-scale diesel generators) in microgrids are allowed to sell electricity to local consumers, ultimately boosting electricity market restricting activities. In addition, the microgrid no longer relies on a single power source; the on-site generation can be used as an emergency backup in the event of a blackout or brownout in order to mitigate the disturbance and improve power reliability.

Figure 1.2 demonstrates the concept of modern microgrids. Technically speaking, a modern microgrid is a small portion of a low-voltage distribution network that is located downstream from a distribution substation through a point of common coupling (PCC) [6]. Due to the nature of microgrid operations (e.g., ownership, reliability requirement, locations), a major microgrid deployment is expected to be carried out on university campuses and research institutions, military bases, and industrial and commercial facilities. According to Navigant Research (formerly called Pike Re-

search), the global microgrid capacity is expected to grow from 1.4 GW in 2015 to 7.6 GW in 2024 [7]. Modern microgrids not only offer great promise due to their significant benefits, but also result in tremendous technical challenges. There is an urgent need to investigate the sophisticated and state-of-the-art control and energy management systems in microgrids.

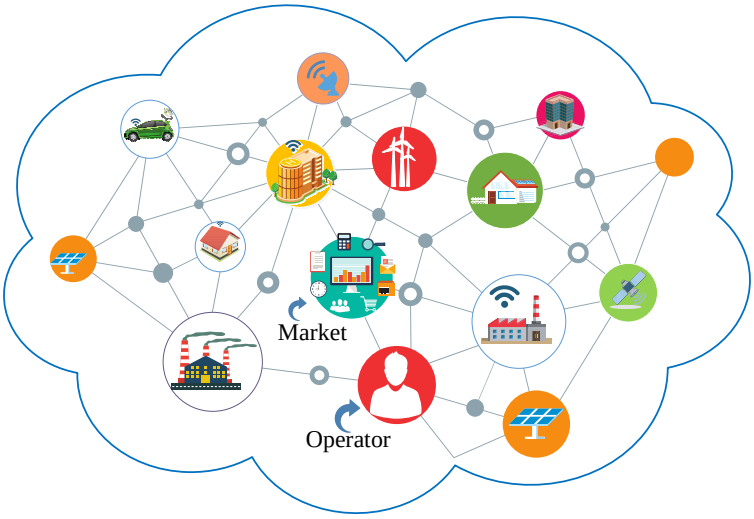

Figure 1.2: An illustrated microgrid system architecture

1.1.2 The Energy Internet and Smart Grids

The data internet (also known as simply the internet) is a network of interconnected networks including, local, private and public computer networks. The internet provides various agents with an opportunity to share data in the information space (World Wide Web) via this complicated network of networks. The energy internet can be considered as a dual of the internet. The (electrical) energy, in the place of information, is shared among various agents in the energy internet networks [8]. In other words, the energy internet is an internet-type network of all the components of a power system, which closely interact with others by sharing both energy and information. Agents or components of this network consist of different prosumers and consumers that have the ability to make decisions by themselves. Microgrids, distributed generations, smart grids, private or governmental energy networks and any community of prosumers and consumers can be a part of this enormous network as agents. The energy internet is also known as the second generation of the power grid because it is equipped with advanced sensing and measurement technology, as well as latest control

and monitoring technology [9]. The energy internet also takes advantage of an advanced communication network to reach a higher level of safety and reliability, and increase the economic and efficient operation of the power system. In addition, the integration of an advanced communication network and smart devices into the power system enables system operators to embed plug-and-play characteristics and intelligent energy management [10]. Figure 1.3 is an internet network used to indicate the concept of the energy internet network.

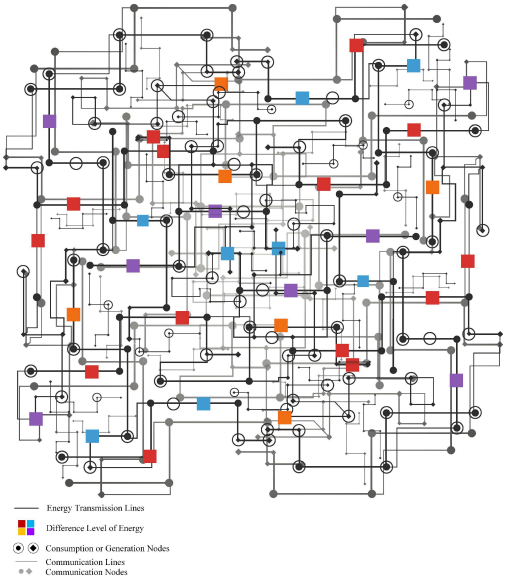

Figure 1.3: A snapshot of the energy internet (Created by Harryarts - freepik.com, customized by authors)

At first glance, there is a slight confusion between the definitions of the smart grid and energy internet because both of them use high technologies and modern methods. The definition of the smart grid itself is confusing, as there are somewhat different definitions because it is not possible to present a singular definition of the smart grid that puts all the various components and concepts together. S. Rahman [11] introduces an adequate definition of the smart grid according to the U.S. Department of Energy's modern grid initiative, "an intelligent or a smart grid integrates advanced sensing technologies, control methods and integrated communications into the current electricity grid." Thus, it provides an opportunity for consumers to have an active role in the electricity market, accommodate various types of energy sources to support system demand, improve energy efficiency

and enhance system security (self-healing) [12].

N. Hatziargyriou *et al.* extracted different features for smart grids from various definitions [13,14]. Thus, the smart grid is:

- **intelligent/smart** because overloads can be determined/predicted to avoid potential outages by rerouting power and doing other preventive measurements.
- **efficient** because the peak shaving technique is used to reduce electrical power consumption during periods of maximum demand on the power utility.
- is able to easily **accommodate** new energy sources and energy storage technologies.
- a good platform for a **competitive electricity market**.
- **quality-focused** due to its technological capabilities to deliver high quality energy.
- a **resilient network** if it uses a new method of controlling and monitoring, such as distributed methods.
- **green** because it is an excellent opportunity to slow the advance of global climate change [15].

The energy internet is a newly developed environment of energy systems. Figure 1.4 shows an evolution timeline of energy systems. Jeremy Rifkin [16] believes "The power grid would be transformed into an info-energy net, allowing millions of people who produce their own energy to share surpluses peer-to-peer." Based on this definition, hundreds of millions of distributed energy resources will eventually produce electricity everywhere and share it with each other through a network of energy internet like, sharing data through information internet. The energy internet integrates smart power grids, advanced distributed control systems, smart devices, smart communication systems, etc. to provide interactive flexibility and efficient energy management.

Therefore, according to [8,17–19], the following are some features that distinguish energy internet from the smart grid:

1. As mentioned earlier, the energy internet is a kind of duality of the internet *i.e.,* all agents, including prosumers and consumers, are able to sell/generate and buy/consume energy.

2. A smart plug-and-play interface is a fundamental requirement of energy internet networks. An intelligent communication interface supports plug-and-play characteristic to detect the connection/disconnection of any device as soon as a plug-and-play happens.

3. The energy internet require efficient management of energy supply and demand in the power grid. Huang *et al.* specify this management as "status monitoring and data collection of all devices as well as providing control references to each device" [17]. Energy routers, as a dual of packet routers, are responsible for dynamically adjusting the energy distribution in the grid by rerouting energy flows in transmission and distribution networks.

4. A regional centralized control method is the dominant control method for smart grids, whereas the energy internet is based on multi-agent (or intelligent agents) approaches. This type of control provides more flexibility for consumers and prosumers to have an active role in the energy system. Customers will be able to choose various services satisfying their budget and preferences.

In sum, the energy internet is an upgraded version of the smart grid, accommodating all types of distributed energy with great flexibility in energy sharing. The major characteristics of an energy internet are its openness, robustness, reliability and competitive environment for the whole procedure of energy generation and consumption.

1.1.3 The Role of Microgrids in the Structure of the Energy Internet

As mentioned earlier, microgrids are one of the parts of the energy internet network, which act as agents. Microgrids have considerable potential to be the main element of infrastructure of the energy internet networks, as they are a promising technology that can increase the reliability and profitability of an energy supply to end consumers [20]. A microgrid, technically, is a low-voltage

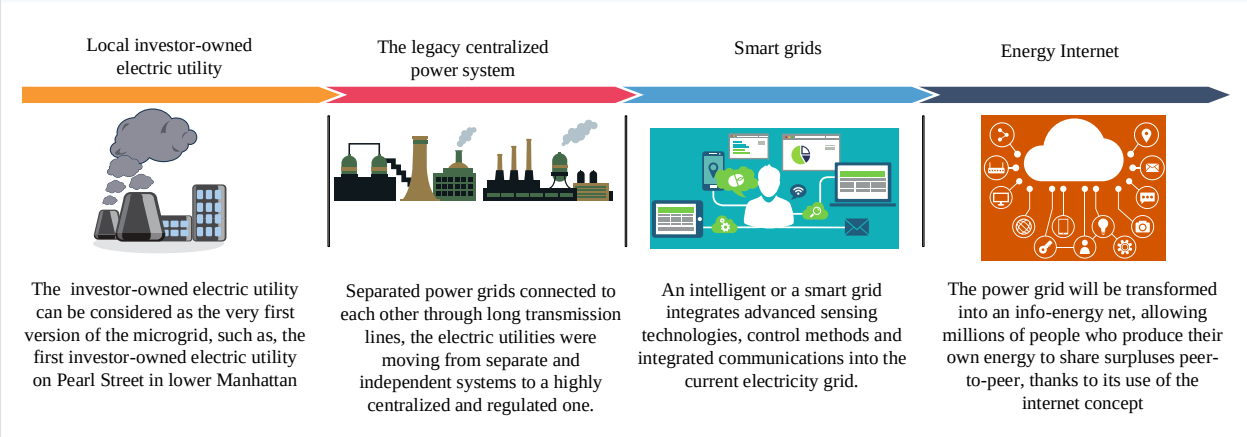

Figure 1.4: The evolution of grids

distribution network that is located downstream of a distribution system and connected to the distribution grid through a point of common coupling (PCC). Microgrids are small-scale power systems that have distributed energy resources (DER), distributed storage (DS) and local loads, which are able to work in islanding mode in the electrical distribution system [21, 22]. According to [17], energy internet networks should have three main features: smart plug-and-play characteristics, intelligent energy management and distributed grid intelligence (see figure 1.5).

A microgrid, as an extension of distributed generation, can be easily integrated with a two-way communication network, smart devices and metering, energy storage, energy monitoring and management system, and load management tools to serve the energy internet as the main element of its infrastructure.

The attractive features of a microgrid that enable it to be an unignorable component of future energy management systems can be listed as in [23]:

1. A microgrid is comprised of various distributed power sources such as solar, wind, fossil fuels, and biomass, fuel cells, internal-combustion engines, and energy storage units.

2. A microgrid can play the role of a controllable power supply or a flexible load because of its greater flexibility in the use of various power sources, its cost-efficient scheduling, and smart management.

3. A microgrid can operate separately as an island to guarantee uninterrupted power supply to users inside of the island until achieving the safe grid-connected mode.

4. A microgrid provides efficient energy utilization for users and satisfies their energy requirements as long as it provides great system reliability.

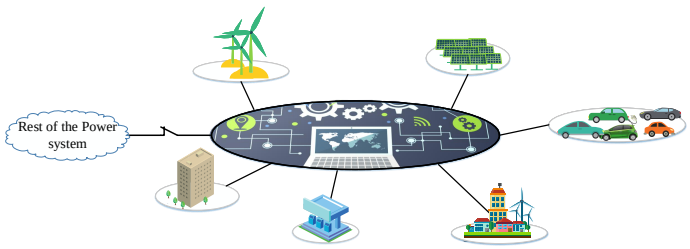

Figure 1.5: A simple representation of a microgrid structure

1.1.4 Data Acquisition in the Legacy Power System and Energy Internet

Supervisory control and data acquisition (SCADA) systems have been widely used to monitor and control plants and equipment in industry since the 1980s. SCADA is an advanced automation control system, which is centrally responsible for the management of power system energy, wide-area data gathering, and the operation of entire electrical power systems [24,25]. Figure 1.6 shows a general diagram of SCADA and simply depicts how SCADA can access wide-area data. SCADA is a well stabilized system and widely use in the legacy power system.

For a successful mission, various parameters should be monitored, such as nodal voltages, line power flows, active/reactive power, system demand, frequency, switch statuses and system topology [26]. Digital and analog parameters and data are usually gathered by a remote terminal unit (RTU) [27]. Then, they are transmitted to the central monitoring/control station. This huge amount of data imposes a heavy computational load on both the monitoring/control system and communication network [28], and then introduces its own technical problems. For example, transmission and analysis of such broad information requires a complicated communication infrastructure. Thus, the SCADA system may not easily support plug-and-play characteristics of distributed generations/storage and scalability.

Furthermore, for any economic analysis, more financial information is required. Any access to private financial information of various prosumers and consumers by a third party such, as SCADA, can easily violate their and the system's overall privacy. This type of data acquisition and sharing makes the legacy power system extremely vulnerable. In sum, the SCADA system suffers from a heavy computational burden, vulnerable privacy and a single point of failure. In [29] Y. Yan *et al.* mention the SCADA based power systems (monitoring and control systems) may only be restricted to transmission systems and the SCADA are not suitable for larger scale monitoring and control of the entire electrical grid.

As is well known, information sharing and collection play a vital role in energy internet networks because most of the functionalities of energy networks depend on wide-area data collection and sharing. Consequently, however, the privacy of prosumers and consumers can at the severe risk as agents share information. Load monitoring is a common method for determining energy consumption for any devices/units in a power system. There are two important methods for load monitoring: intrusive and non-intrusive monitoring methods [30]. Intrusive and non-intrusive monitoring methods are, respectively, referred to as the distributed sensing and single point sensing methods. Accurate data can be obtained through intrusive load monitoring (ILM) by connecting power meters to each appliance in a unit, but this method suffers from some drawbacks, such as high cost, complicated sensor configuration, and installation complexity [31]. In addition, this method is barely trusted in the energy internet environment because it collects each individual appliance's energy consumption.

An immediate alternative method for ILM is non-intrusive load monitoring (NILM), which only uses a single meter per user. NILM is an alternative and effective method for discovering the energy consumption of individual appliances based on analysis of the aggregate load measured by the main power meter in a building. It would seem to better protect privacy because it does not require to violate the private information of an individual when measuring the power consumption of different appliances [30]. However, a study by C. Hui *et al.* [32] shows that the analysis of electrical data gathered by NILM can intrude on privacy because the economic behavior of users can be inferred by

some analytical study. Thus, non-intrusive load monitors and smart meter data may reveal precise user information. On the other hand, battery-based load hiding (BLH), a practical and cost-effective solution, ensures the protection of prosumers, and consumers' privacy against information leakage by third parties or neighbors [33].

In battery-based load hiding method, a battery is installed in the consumer or prosumer's side. This battery is charged and discharged in a strategic way to hide accurate data that can be obtained by the analysis of consumption data [34]. This process removes the detailed load profile information needed by NILM algorithms to detect a user's behavior. This method has some limitations because it completely depends on a battery, whereas the alternative methods can be categorized as non-battery. The non-battery methods can be grouped as cryptology [35, 36] and differential privacy [37].

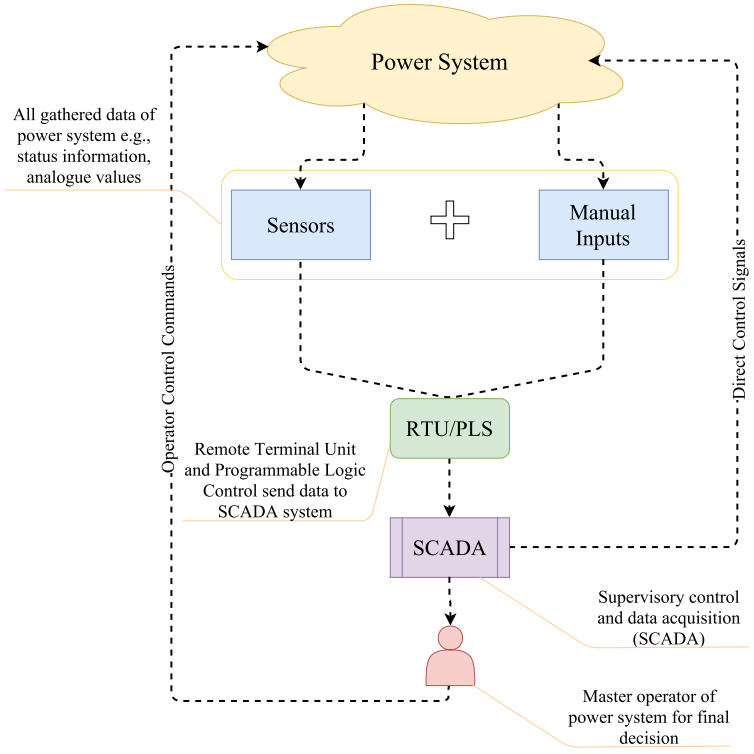

Figure 1.6: General system configuration of supervisory control and data acquisition (SCADA)

1.2 Energy Management Approaches in Energy Networks

In the 1980s and 1990s, the computer industry gradually used the distributed computing approach in place of the centralized computing approach, thanks to the worldwide internet platform. This alteration in the structure of computer network infrastructure led to computation cost reductions, avoidance of a single point of failure and data privacy improvement [17]. As the penetration of distributed energy resources is continuously growing, altering power systems in the same way as the computer network can revolutionize their future [28]. The energy internet, as a technological revolution, can apply a new approach to the energy delivery and management of power systems.

In this section, all three major control methods-centralized, decentralized and distributed control methods-will be investigated in detail for figuring out the pros and cons of applying them to energy internet.

1.2.1 Centralized Control

In a centralized method, all agents, *i.e.*, prosumers and consumers, will independently communicate and directly interact only with a central operator. This center should be able to monitor, gather and analyze real-time data and provide all components with appropriate control signals as long as it records events in a log file. Figure 1.7 shows a simple schematic of the communication structure of a power system. It is worth mentioning that the centralized structure is only applied to the communication network, and the energy system is a pool-based system.

For almost the last two decades, the centralized control approaches were evolving, thanks to the high technology of communication networks and powerful computers. Optimization of microgrid operation is one of the well known problems that has been frequently addressed by various centralized control approaches. The work of A.G. Tsikalakis et al . is one of the earliest methods which proposed a centralized controller to maximize the value of microgrid and the optimization of its operation during interconnected operation, i.e., the production of local generators and energy exchanges with the distribution network are maximized [38]. Unit Commitment (UC) is an optimization problem that is responsible to determine the least-cost of the operation commitment of

generation units [39]. UC problem is one the most complex optimization problem which could be extended over some period of time [40]. Independent system operator (ISO) as a third party handles wholesale electricity markets to find their day-ahead market schedules based on centralized unit commitment [41]. The energy management system (EMS) is a sophisticated administrative controlling system in the power system which also is benefiting from the centralized control methods to monitor, control, and optimize the performance of the generation and transmission system. D.E. Olivares et al. introduce a centralized control architecture and mathematical formulation of the microgrid's energy management problem. Their proposed centralized EMS for an isolated microgrids features a detailed three-phase (unbalanced) model of the system [42]. A novel EMS for a microgrid based on a rolling horizon (RH) strategy is developed by [43]. This EMS provides the online set points for generation units while minimizing the operational cost and considering the forecast of renewable resources and loads.

Unfortunately, the penetration of distributed generation, distributed energy storage, renewable energy sources and prosumers/consumers is continuously growing, meaning the centralized algorithms are no longer effective [44, 45] because they are incapable of operating, monitoring and controlling future power systems, which includes tremendous numbers of agents [46, 47].

Although the centralized methods are mature and established approaches for control of many systems in recent decades, they are not a practical solution for energy internet systems. The reasons behind of this are:

1. Heavy computation burden is a technical barrier for a centralized control as the number of agents increases to hundreds of thousands [24].

2. Centralized methods are not easy to expand and are not appropriate for smart grids as they need to expand very fast [48].

3. Due to the single point of failure of one center-based control systems, these approaches are suitable only for relatively small-scale systems. Thus, a small number of users is affected in the case of the failure of a center [49].

4. The centralized algorithms are not well designed to support plug-and-play functionalities of a large number of participants [50].

5. Finally, the centralized approaches need a high level of connectivity because each agent should directly interact with the center.

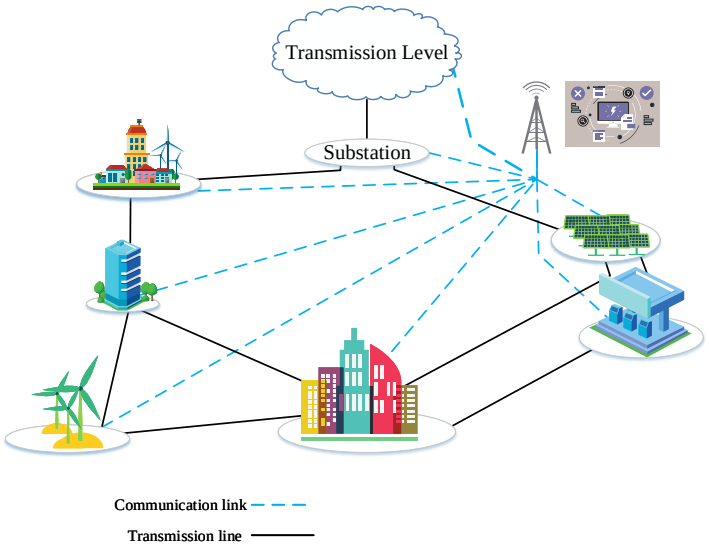

Figure 1.7: Centralized control schematic

1.2.2 Decentralized Control

The two terms, decentralized and distributed methods, are often used in place of each other, but there is a slight difference between these two terms. In this section, the concept of decentralized methods and their pros/cons are reviewed.

In a decentralized control method, each agent or group of agents is controlled by itself or a leader, respectively. Figure 1.8 shows a sample structure of the decentralized approach. The decisions are made based on local measurements, such as voltage and frequency values, and there is a limited number of local connections. It stands to reason, then, that decentralized control methods do not require a high level of connectivity. Furthermore, the decentralized control approach does not need to go through the whole decision-making process of the entire system via one center; therefore, it

is not imposed by a high computation load. On the other hand, because the decentralized approach is mainly based on the local measurements of parameters [51]. The global optimization, stability or reliability of the entire system cannot be assured, due to the lack of communication links and information sharing among agents. However, this feature also enables decentralization with a higher level of privacy protection.

Another strong point of decentralized methods is their robustness against a single point of failure. A system equipped with a decentralized method has a massive redundancy in the number of controllers because, in contrast to the centralized method, there are some leaders/controllers in a decentralized system. For example, if some leaders lose their connection with other agents or an agent fails to operate, the entire system can still remain stable.

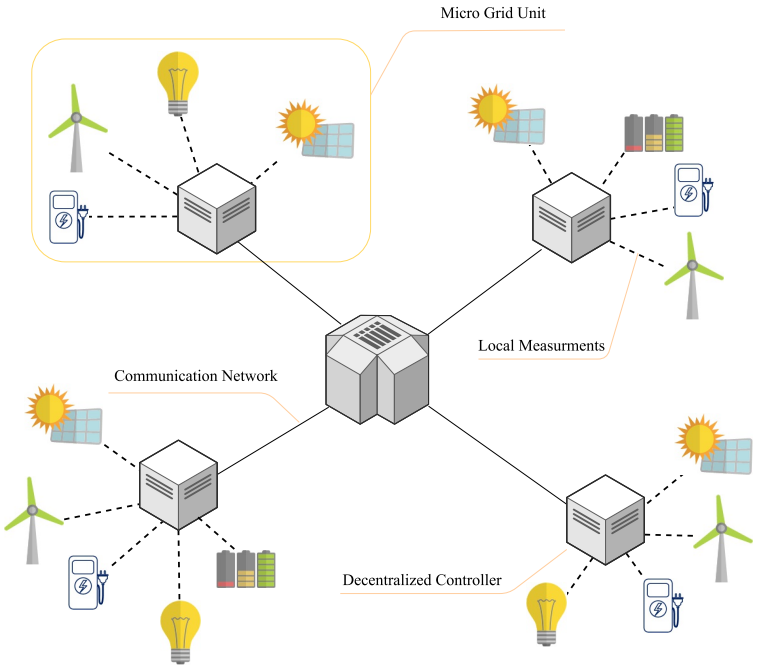

Figure 1.8: Decentralized control schematic

1.2.3 Distributed Control

The difficulties of both the centralized and decentralized methods can be overcome by the distributed control approaches. In this section, the concept of the distributed control approaches and their difference compared with decentralized control approaches are studied.

In contrast to the system being controlled by a decentralized method, in which agents use local measurements, agents of a system equipped with a distributed control method are allowed to share their information with neighbors. In other words, agents in a system with distributed methods not only use local measurements, but also are able to send and receive required information. Therefore, this type of control system can reach the global optimization, reliability and stability like as centralized control methods [52, 53].

The security of the communication networks of the energy internet is the most important factor, which depends on the privacy of agents. Privacy technologies and encryption standards/algorithms are well matured now and provide energy systems with one of highest levels of security [54]. However, sharing the private and confidential information may provide third parties or other agents with the opportunity to intrude on privacy. New algorithms and protocols of distributed control methods [28, 55–57] preserve the privacy of each agent and the entire system by sharing minimal pieces of information. It is worth mentioning that none of the agents share information with a center as a third party.

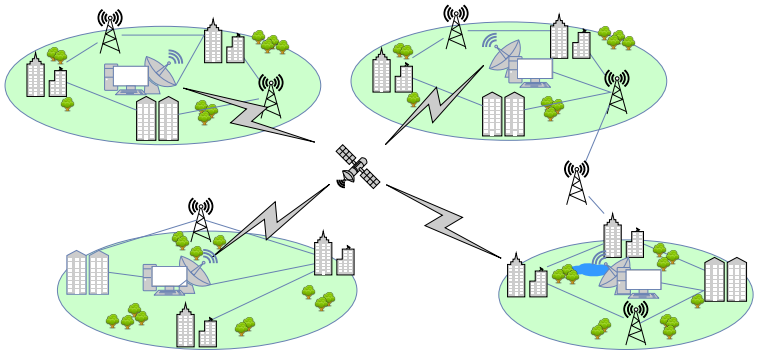

Figure 1.9: Distributed control schematic

As discussed in the introduction section, the energy internet, which is the integration of an advanced communication network and smart devices into the power system, provides the system with plug-and-play characteristics [10]. This ability enables the system to not be influenced by the dynamic topology of the energy internet network. Additionally, it would be easy to extend as new agents arbitrarily connect to the network. The energy infrastructure, including 10,000 power plants, 131 million customers, and 157,000 miles of transmission lines, is one of the most complex infrastruc-

tures ever built by the humans. Based on what is discussed here, the best method to manage such a system is a distributed multi-agents based approach. A mature multi-agent environment with the right set of protocols that allows all agents to locally/globally interact with each other can overcome the drawbacks of the centralized control approach [8].

In sum, distributed methods/algorithms for multi-agent systems, as one of the great revolutions in the energy industry, are very effective tools for energy management of the energy internet because:

- Energy internet networks are easy to expand and support scalability.
- Computational cost is distributed among multi-agents over the energy internet network.
- Energy internet would not be affected by a single point of failure.
- Energy internet would not be affected by the dynamic topology.
- Energy internet support a plug-and-play characteristics.

Distributed control approaches have a wide variety of applications in the power system management such as, power flow control, demand management, reliability and stability study. H. Dagdougui et al. proposed a distributed control strategy for a network of smart microgrids. In this method, an agent i.e., smart microgrid can share information about their internal load and generation. The objective is to minimize the cost of energy storage and exchanged power among smart microgrids when the internal load being supported. One important feature of the proposed approach is that the cooperation among the agents was achieved with no direct knowledge of the others [58]. In [59], a two-level cooperative optimization multi-agent system is designed for distributed energy resources economic dispatch . In this paper, a multi agent-based optimal microgrid control using a fully distributed diffusion strategy solves an economic dispatch problem. The lower level implements an adaptive droop scheme based on online no-load frequency adjustments. There is a peer-to-peer communication among the agents, which simultaneously performs resource optimization while regulating the system frequency.

In a nutshell, distributed optimization techniques could be classiffied into main two groups: based on Lagrangian decomposition and based on Karush-Kuhn-Tucker necessary conditions [60]. Lagrangian decomposition-based techniques can also categorized in some famous group of methods such as Dual decomposition [61] and Alternating Direction Method of Multipliers (ADMM) [62]. Some novel cooperative distributed algorithms that solves the constrained nonlinear optimization problem using Karush-Kuhn- Tucker (KKT) conditions and consensus networks are discussed in [63, 64].

1.3 Characteristics of Energy Internet's Communication Networks

A mature communication network is a vital part of the energy internet and effectively improves the performance of future smart grids. The communication network should be changed and developed as fast as the development of the energy internet and its requirements [9, 54], such as stability, reliability, and profitability of the entire system. The major features of communication networks are:

1. **Two-way and pervasive communication:** The next generation power grid should be supported by advanced two-way and pervasive communications to bring efficiency, reliability and safety for the entire system.

2. **Wide bandwidth:** The communication infrastructure should be able to support the increasing number of agents and help them share their information seamlessly.

3. **Cyber security and privacy:** Privacy and information security, including confidentiality, entity authentication, authorization, validation, etc. are essential for every competitive system. Therefore, communication channels should have some level of security to ensure that there is no leakage of private information to third parties and no preferences are given to one or more agents in a competitive environment. [28].

4. **Interoperability:** Interoperability among the various agents of an energy internet network is the ability of the agents to cooperate and share information to perform tasks without con-

siderable effects on their operations. In other words, agents of a multi-agent system should have integration, effective cooperation, and two-way communications to reach their common goals. The National Institute for Standards and Technology (NIST) is working on protocols and standards for information management and communication standards to provide a comprehensive interoperability for energy internet systems.

5. **Scalability:** Scalability is an essential attribute of a network, system, or process that can support and accommodate increasing number of users, amount of workload, or more complicated process. In an energy system, the communication network should have the ability to easily support new users, new devices and new control methods [65].

6. **Smart plug-and-play:** An intelligent communication interface should support a smart plug-and-play characteristic to detect connection/disconnection of any device as soon as plug-and-play happens.

7. **Self-healing:** One of the approaches for enhancing the system reliability is a self-healing ability. The communication network plays an important role to provide the power system with this self-healing ability.

The structure for the rest of this dissertation is organized as follows: Chapter 2 discusses a consensus-based distributed algorithm for economic dispatch in detail [28]. Chapter 3 comprehensively studies a distributed alternative current power flow (ACPF) for distribution systems [66]. Chapter 4 proposes distributed optimal power flow for DC distribution system [67] while Chapter 5 demonstrates a distributed optimal power flow for their AC counterparts [68]. Chapter 6 reviews the future trends of distributed control methods for Energy Internet.

CHAPTER 2

Consensus-based Distributed Algorithm for Economic Dispatch

2.1 Introduction

This chapter proposes a consensus-based distributed control algorithm for solving the economic dispatch problem of distributed generators. A legacy central controller can be eliminated in order to avoid a single point of failure, relieve computational burden, maintain data privacy, and support plug-and-play functionalities. The optimal economic dispatch is achieved by allowing the iterative coordination of local agents (consumers and distributed generators). As coordination information, the local estimation of power mismatch is shared among distributed generators through communication networks and does not contain any private information, ultimately contributing to a fair electricity market. Additionally, the proposed distributed algorithm is particularly designed for easy implementation and configuration of a large number of agents in which the distributed decision making can be implemented in a simple proportional-integral (PI) or integral (I) controller. In MATLAB/Simulink simulation, the accuracy of the proposed distributed algorithm is demonstrated in a 29-node system in comparison with the centralized algorithm. Scalability and a fast convergence rate are also demonstrated in a 1400-node case study. Further, the experimental test demonstrates the practical performance of the proposed distributed algorithm using the VOLTTRON™ platform and a cluster of low-cost credit-card-size single-board PCs.

2.2 Literature Review

Future power systems are equipped with a great number of distributed generators (DGs), distributed energy storage devices, dispatchable loads and advanced communication networks, which increases the customer participation in the electricity market. As a result, the optimal economic dispatch (ED)

of future power systems is becoming much more challenging. A sophisticated control is needed to fully address the increasing customer participation at the edge of the electric power system and the inability of existing practices to accommodate these changes [69–72].

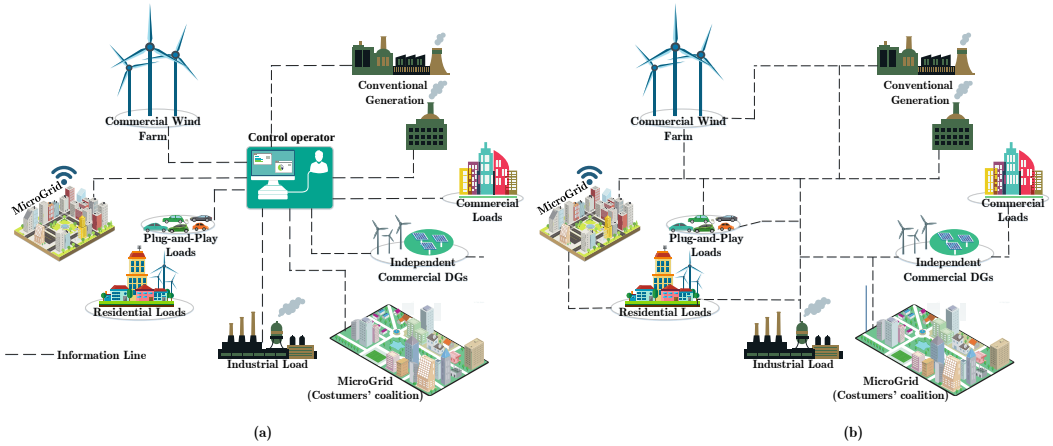

Figure 2.1: Different approaches for power grids. (a) centralized approach, (b) distributed approach (peer-to-peer connections)

In a centralized ED, all participants (DGs and consumers) must release their information to the central controller. As the market penetration of DGs and consumers is continuously growing, the centralized algorithms are no longer suitable due to the heavy computational burden [47]. Moreover, the centralized algorithms are not designed to support plug-and-play functionalities of a large number of participants.

Consensus-based distributed approaches have been found to be practical in many multi-agent applications, such as industrial systems, automated high way systems, and computer networks [73]. Consensus-based distributed approaches are to find the global optimal decision by allowing local agents to iteratively share information through two-way communication links. All agents reach a consensus when they agree upon the value of the information state [49, 53, 74–76]. The information state can be physical quantities or control signals such as voltage, frequency, output power, incremental cost, and estimated power mismatches [77]. Figure 2.1 compares the centralized and distributed methods for solving the ED problem in power systems [24]. The major advantages of distributed methods are summarized as follows:

Scalability and Interoperability: As the number of agents increases to hundreds of thousands, the legacy centralized method faces certain challenges such as computational burden. As more DGs are integrated into power systems, the centralized methods are not suitable for such heterogeneous systems [77, 78].

Monopoly and Monopsony: A central organization usually has a kind of monopoly over the consumers and a monopsony toward the electrical energy DGs. However, as it is discussed in various research papers and academic notes, consumers have a much more apathetic role than DGs do in electrical energy markets under centralized control [79, 80].

Privacy and Stealth Protection: One of the essential and notable features of every competitive system is the equal opportunity for competition for all players. Therefore, it should be ensured that no private information is released by a third-party and no preferences are given to one or more DGs in a competitive market [69].

Computational Cost: Heavy computational load is imposed on the central controller when dealing with a large multi-agent network [77, 81]. However, the computational load can be shared among agents using distributed approaches.

Single Point of Failure: A distributed approach is robust to the single point of failure because there is no need for a center for the supervisory of the entire system [78, 82].

Network Topology: In future power systems, the communication network and power network are subject to frequent change [83]. Accordingly, there are serious doubts about the ability of centralized methods to handle the variable topology.

The literature review shows a growing interest in distributed algorithms in the field of power systems. A distributed algorithm for solving the ED problem that considered thermal generation and random wind power was discussed in [84] for a smart grid. A distributed optimization problem with local constraints was studied in [64] to obtain the optimal solution for a load sharing problem. Hug and Kar [56] introduced a consensus-based distributed energy management approach to handle loads of a micro-grid. Rahbari-Asr *et al.* investigated an incremental welfare consensus-based

algorithm that manages both loads and DGs [63]. In addition, they developed a cooperative distributed demand management system in [57] based on Karush–Kuhn–Tucker conditions for plug-in electric vehicle charging. A distributed optimal power flow was introduced for a large-size distribution system in [85]. Mudumbai *et al*. [47] worked on the distributed algorithm for both optimal ED and frequency control with a large number of intermittent energy sources. The authors in [55] proposed a distributed real-time demand response for a multi-agents system to maximize social welfare. They defined sub-problems by decomposing the main optimization problem and locally solving each sub-problem. Binetti *et al*. [75] presented a distributed method to solve the ED problem considering power losses of transmission lines. Two consensus protocols were run in parallel to reach the consensus and estimate the power-mismatch considering the lines' losses. Elsayed and El-Saadany proposed a fully decentralized method that can solve both the convex and the practical non-convex ED problem. They also considered transmission losses in [86]. In [87], a distributed constrained gradient approach was proposed to consider both the equality and inequality constraints for online optimal generation control. Another algorithm has been introduced in [88] to help energy producers to collect information regarding power mismatch between generation and consumption. This mechanism finally converges incremental cost to an optimal value. N. Cai *et al.* [89] offers a decentralized approach for the economic dispatch problem of a micro-grid in which, various agents use local information or receive some information from their immediate neighbors. However, this paper does not cover the power balance within micro-grid because it is assumed that power balance has already been met. One of the distributed techniques for solving non-convex economic dispatch problem has been introduced in [75]. In this technique, a leader-less consensus based distributed algorithm share bids among different agents based on an auction mechanism. G. Binetti *et al*. considered transmission losses, valve-point loading effect, multiple fuel, prohibited operating zones in non-convex ED problem. A primal-dual perturbation method is proposed by T.H Chang *et al*. [90] enabling multi-agents system to reach a global optimum. In this method, all agents try to estimate functions of global cost and constraints based on distributed approach.

From the control algorithm's point of view, one common issue with existing distributed consensus

algorithms is their slow convergence (high iteration numbers), privacy, high connectivity requirement and complexity. For instance, in most of previous works the incremental cost (λ) and output power are shared [55], which violate privacy principles. While agents in a multi-agent system may not share private information with center (third-party), they share the private information with other agents and it could be even worse than the centralized method. In addition, distributed methods cannot attract serious attentions in case of implementation if they suffer from high connectivity, slow convergence and complexity. To address the aforementioned limitations of existing distributed methods, we propose a novel consensus-based distributed algorithm to maintain data privacy and reduce computational time while solving for a large-scale ED problem. The proposed approach need to share minimum information (Power mismatch) among different agents in a multi-agent network, thus, the privacy of all agents will definitely be improved. In other words, the parameter of cost function, utility function, incremental cost (λ) and output power etc. will not be shared among agents and, also, third-party are not at all able to access to these parameters. In addition, computational cost will be decreased that make the scalability possible for enormous multi-agent system. Figure 2.2 shows a general view of the communication network for the proposed method. The main features of the proposed distributed algorithm are as follows:

1. ***Accuracy***: The ED problem is solved in a fully distributed manner without relying on a central controller. The solution accuracy is validated by the benchmark results achieved by traditional centralized methods.

2. ***Privacy***: DGs and consumers do not need to disclose any private information (e.g., cost functions and utility functions) with others. The estimated power mismatch between the total generation and the total demand is the only information to be shared among all DGs. In addition, consumers are not required to have a communication channel between one another or to exchange information with all DGs. They only need to connect to local DGs.

3. ***Fast Convergence***: The proposed algorithm outperforms some existing distributed methods in terms of number of iteration and computational time.

4. ***Scalability***: The proposed distributed algorithm is particularly suitable for solving large-scale optimization problems (e.g., >1,000 agents) within a short period of time.

5. ***Easy Implementation***: This salient feature makes it possible to deploy the proposed distributed methods in the field at scale.

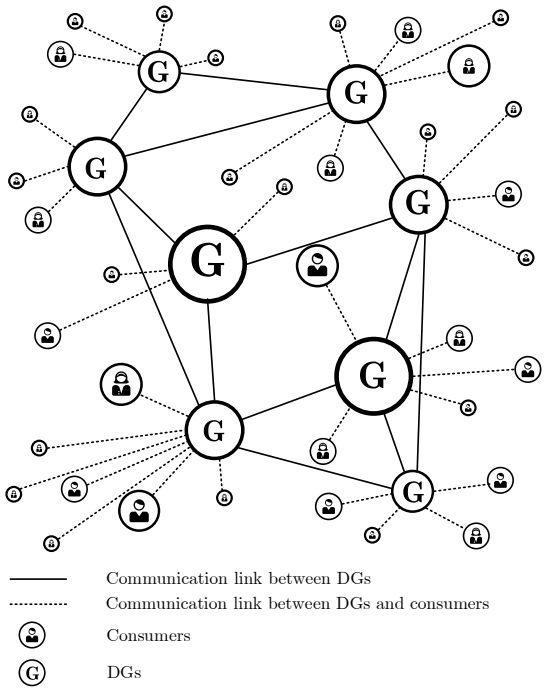

Figure 2.2: The illustrated communication network for the proposed distributed method.

The structure for the rest of this chapter is organized as follows: Section 2.3 formulates the ED problem as a global objective function, considering cost functions, utility functions and constraints. Section 2.4 discusses graph theory, consensus-based distributed protocols, optimality and convergence analysis of proposed algorithm . Section 2.5 evaluates the solution performance using software simulation and experimental testing. Section 2.6 summarizes this chapter and presents the concluding remarks.

2.3 System Modeling and Problem Description

The ED problem is a short-term resource allocation of a number of DGs to meet the load requirement in a most cost-effective way. The utility function of consumers, the cost function of DGs

and their surplus function are defined in this section. Then, the overall optimization problem is formulated based on the defined model of economic players in an electricity market.

2.3.1 Utility Function, Marginal Benefit and Consumer's Surplus

Each consumer in an electricity market has its own preferences for energy consumption during different times of a day. These preferences cause various levels of requested demand within an operation period. There are some factors affecting the preferences of consumers in an electricity market such as the instantaneous or average price of electricity, temperature changes, the type of user and comfort level. The different demand levels requested by consumers in response to these diverse factors can be modeled by utility functions for mathematical purposes [46, 55, 80]. In other words, the utility function measures the satisfaction level or welfare of consumers as a function of different types of performance (*i.e.,* demand level) to represent a consumer's preferences. In a typical electricity market, the utility function $U_j(P_j^{Load})$ shows the level of satisfaction of the $j-th$ energy consumer, where P_j^{Load} is the demand of $j-th$ consumer.

Marginal benefit is an additional utility that an electrical consumer will gain by getting one more unit (MW) of electrical energy. The consumption of more power increases the utility function if the marginal benefit has a positive value; however; the consumption of more power decreases the level of satisfaction if the marginal benefit has a negative value [91]. The common utility functions are non-decreasing functions; thus, the marginal benefit is a non-negative function. It means [92]:

$$\frac{\partial U_j(P_j^{Load})}{\partial P_j^{Load}} \geq 0, \qquad j \epsilon S_D \tag{2.1}$$

It is evidently proven that the marginal benefit of electrical consumers is a non-increasing function because the marginal benefit will normally decrease as users consume more energy. Thus, we have [92]:

$$\frac{\partial^2 U_j\left(P_j^{Load}\right)}{\partial\left(P_j^{Load}\right)^2} \leq 0, \qquad j \epsilon S_D \tag{2.2}$$

There are various types of utility function for single and multiple goods, such as: *Cobb-Douglas Utility Function*, *Perfect Substitutes*, *Perfect Complements* and *Quasilinear*. In this chapter, a quadratic mathematical model satisfying (2.1) and (2.2) is used in Equation (2.3) as a utility function of the consumers. This utility function is customized for different consumers based on parameters b \$/kWh^2 and ω \$/kWh. The larger ω is, the higher the utility function.

$$U_j\left(P_j^{Load}\right) = \begin{cases} \omega_j P_j^{Load} - b_j (P_j^{Load})^2 & P_j^{Load} \leq \omega_j / 2b_j \\ \frac{\omega_j^2}{4b_j} & P_j^{Load} \geq \omega_j / 2b_j \end{cases} \tag{2.3}$$

Consumer's surplus measures the welfare on the consumers' side; hence, it is a measurement of the benefit, derived from the electricity market, of an economic player on the consumption side [63]. A consumer's surplus will be represented by (2.4), if the $j-th$ consumer pays λ \$/kWh for P_j^{Load} kW of the electrical energy.

$$\mathcal{S}_j^{Load}\left(P_j^{Load}\right) = U_j\left(P_j^{Load}\right) - \lambda P_j^{Load}, \qquad j \epsilon S_D \tag{2.4}$$

Consumers attempt to maximize their own welfare in the market. Therefore, they consume power at the maximum value of their concave surplus function. Figure 2.3 shows the graphical representation of equations (2.3) and (2.4).

2.3.2 Cost Function and DG's Surplus

Generally speaking, a multiple piecewise linear or quadratic function, known as cost function, is used to estimate the total cost of the output-power of the energy providers, such as DGs. Using a proper cost function is the best way to pre-evaluate the performance of a DG and to solve an ED problem [79]. Here, we consider a quadratic mathematical equation to model a typical DG. α \$/kWh^2, β \$/kWh and γ \$/h are coefficients that customize the cost function for each DG and P_i^{Gen} is power generated by the $i-th$ DG.

$$C_i\left(P_i^{Gen}\right) = \alpha_i (P_i^{Gen})^2 + \beta_i P_i^{Gen} + \gamma_i, \qquad i \epsilon S_G \tag{2.5}$$

A DG's surplus (commonly known as profit) measures the welfare of a DG. In other words, it is a benefit gained by DG, when the sale price of energy is more than the costs spent to produce the energy. If the $i-th$ DG sells P kW of electrical energy at λ \$/kWh, the DG's profit is expressed as in (2.6).

$$\mathcal{S}_i^{Gen}\left(P_i^{Gen}\right) = \lambda P_i^{Gen} - C_i\left(P_i^{Gen}\right), \qquad i \epsilon S_G \tag{2.6}$$

Unlike consumers, DGs tend to produce as much electricity as possible. Figure 2.4 shows the surplus curve of a DG. The more power DGs produce, the higher surplus they obtain.

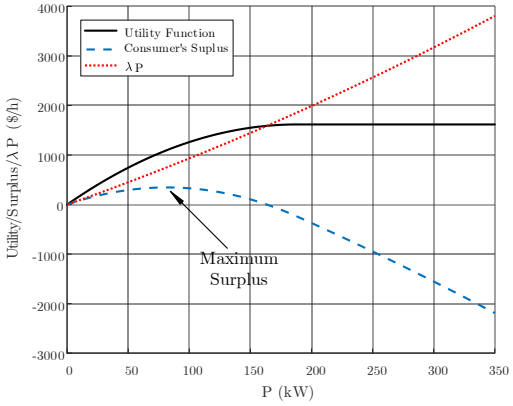

Figure 2.3: Consumer's surplus and utility function

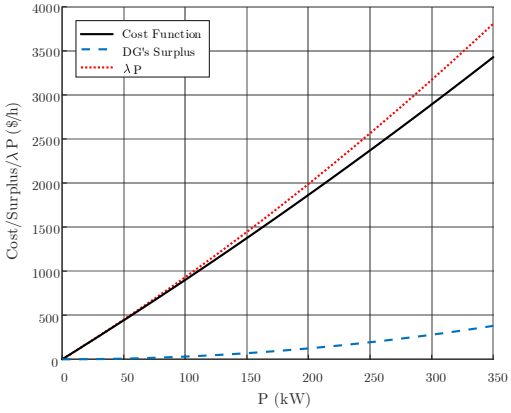

Figure 2.4: A DG's surplus and cost function

2.3.3 Global Optimization Problem

The objective function in this chapter is to maximize the welfare of all consumers and DGs. In other words, the objective function is to maximize the summation of the utility functions (2.3) and minimize the summation of the cost functions (2.5). Thus, the overall objective function can be written as:

$$Min\left(\sum_{i\epsilon S_G} C_i\left(P_i^{Gen}\right) - \sum_{j\epsilon S_D} U_j\left(P_j^{Load}\right)\right) \tag{2.7}$$

Note that the current version of the proposed distributed algorithm does not consider the power losses and the maximum capacity of the power lines. This objective function is also subject to constraints of power balance between the aggregated generations ($\sum_{i\epsilon S_G} P_i^{Gen}$) and consumption ($\sum_{j\epsilon S_D} P_j^{Load}$) as in (2.8).

$$\sum_{i\epsilon S_G} P_i^{Gen} = \sum_{j\epsilon S_D} P_j^{Load} \tag{2.8}$$

In addition, the output-power of each DG and the consumption of each consumer cannot go beyond their maximum capacity. These two constraints can be applied to the optimization problem as in (2.9).

$$\begin{aligned} 0 \leq P_i^{Gen} \leq P_{i,max}^{Gen} \qquad & i\epsilon S_G \\ 0 \leq P_j^{Load} \leq P_{j,max}^{Load} \qquad & j\epsilon S_D \end{aligned} \tag{2.9}$$

2.4 Distributed Algorithm for Economic Dispatch

As previously mentioned, consensus-based distributed approaches offer a great solution for solving optimization problems such as economic dispatch. In this section, we review the conception of the graph theory and elaborate on the proposed distributed algorithm in details.

2.4.1 Graph Theory

We can model the agents' interaction through the communication network by (un)directed graphs denoted by $\mathcal{G}(\mathcal{V}, \xi)$. Consider a network of n connected agents in which nodes are designated by $\mathcal{V} = \{v_1, v_2, ... v_p\}$ and $\xi \subseteq \mathcal{V} \times \mathcal{V}$ shows a set of edge. The directed edge $\vec{e_{ij}} = (v_i, v_j)$ shows that agent i share it's information state with agent j. Also, undirected edge $e_{ij} = (v_i, v_j)$ indicates that agents i and j can share information with each other. Two matrices will commonly be

used to represent the communication topology of a multiple-agents network. The adjacency matrix denoted by $\mathcal{A} = \{[a_{ij}] \, | a_{ij} \in \mathcal{R}^{\mathcal{P}\times\mathcal{P}}\}$ of an undirected graph $\mathcal{G}$ is symmetric. The entry a_{ij} of an adjacency matrix is a positive value if $e_{ij} \in \xi$ and $a_{ij} = 0$ for $e_{ij} \notin \xi$. Otherwise, the entry a_{ii} is assumed to be zero. The second matrix is Laplacian matrix $L = \{[l_{ij}] \, | l_{ij} \in \mathcal{R}^{\mathcal{P}\times\mathcal{P}}\}$ in which entry $l_{ii} = \sum_{j} a_{ij}$ and $l_{ij} = -a_{ij}$ for $i \neq j$. Equation (2.10) shows matrices $\mathcal{A}$ and L [84].

$$A = \begin{bmatrix} a_{11} & a_{12} & \cdots & a_{1n} \\ a_{21} & a_{22} & \cdots & a_{2n} \\ \vdots & \vdots & \ddots & \vdots \\ a_{n1} & a_{n2} & \cdots & a_{nn} \end{bmatrix} \quad , and \quad L = \begin{bmatrix} \sum_{j} a_{1j} & -a_{12} & \cdots & -a_{1n} \\ -a_{21} & \sum_{j} a_{2j} & \cdots & -a_{2n} \\ \vdots & \vdots & \ddots & \vdots \\ -a_{n1} & -a_{n2} & \cdots & \sum_{j} a_{nj} \end{bmatrix} \tag{2.10}$$

2.4.2 Consensus-based Distributed Protocols

In consensus-based distributed approaches, a network of agents shares information via communication channels between agents to reach a consensus. Node i and node j have reached a consensus if and only if the value of the state of the $i-th$ node (x_i) and the state of the $j-th$ node (x_j) are equal [73, 74]. Thus, multiple agents reach a consensus when all of them agree on the coordination information or variable. The Laplacian potential for a graph is delineated by (2.11) which represents a kind of virtual energy stored in a graph [93].

$$\mathcal{L}_{\mathcal{P}} = \sum_{i,j} a_{ij}(x_j - x_i)^2 = 2x^T L x \tag{2.11}$$

In other words, the Laplacian potential could be used as a measure that shows the total disagreement among all agents in a network. If the agents of a network tend to reach a consensus, they should at least interact with their neighbors to minimize Laplacian potential ($\mathcal{L}_{\mathcal{P}}$) as a disagreement [73]. In fact, a general consensus for a multi-agent system will be reached if and only if $\mathcal{L}_{\mathcal{P}} = 0$ or $x_i = x_j$.

The "consensus" being used for the proposed method is defined as zero-power-mismatch. Based on the definition of Laplacian potential, the whole power mismatch is a virtual energy stored in the network that must be minimized. Consensus is reached by converging towards

$$\Delta P_1^T = \Delta P_2^T = \cdots = \Delta P_n^T = 0 \tag{2.12}$$

where ΔP_i^T is a power mismatch of the whole system estimated by the $i-th$ DG.

Considering that all agents have single-integrator dynamics [73, 93], a standard linear consensus protocol is defined as (2.13).

$$\dot{x_i}(t) = \sum_j a_{ij}(x_j - x_i) \tag{2.13}$$

Equation (2.13) can be written for all agents as a vector: $\dot{x}(t) = -Lx$, which is equivalent to the gradient of the Laplacian potential of a graph as shown in Equation (2.14). It represents a gradient-descent algorithm that is able to find the minimum of the Laplacian potential function. As previously discussed, the minimum Laplacian potential happens at $\Delta P_i = 0, \quad \forall i$.

$$\dot{x_i}(t) = -\nabla \mathcal{L}_{\mathcal{P}} \tag{2.14}$$

A discrete-time version of the linear consensus protocol of a first-order integrator can be represented by (2.15)

$$\begin{aligned} x_i(k+1) - x(k) = u_i(k) \Longrightarrow \\ x_i(k+1) = x_i(k) + u_i(k) \end{aligned} \tag{2.15}$$

where $u_i(k)$ depends on the information state of neighbors of $i-th$ agent (*i.e.*, $u_i = f_i(x_1, x_2, ..., x_j)$) and can be shown by (2.16).

$$u_i(k) = \sum_j a_{ij}(x_j(k) - x_i(k)) \tag{2.16}$$

Equation (2.17) is obtained from (2.15) and (2.16), where I is unit matrix.

$$x_i(k+1) = x_i(k) + \sum_j a_{ij}(x_j(k) - x_i(k)) \Longrightarrow$$
$$x_i(k+1) = x_i(k) - Lx_i(k) = (I - L)x_i(k) \tag{2.17}$$

Given that the sum of row of adjacency matrix A is one (*i.e.*, A is a stochastic matrix), Equation (2.18) can be derived from (2.17). Equation (2.18) explicitly indicates that the next state of each agent depends on the current states of other agents.

$$x_i(k+1) = \sum_j a_{ij}x_j(k) \tag{2.18}$$

Now, we consider ΔP as information coordination that needs to be shared among agents. Equation (2.19) shows that ΔP of each agent is calculated by the current estimated ΔP of other neighbors. It is worth mentioning that ΔP, the only information shared among different agents, does not include any private information. The consumers do not need to launch any communication link among themselves for information coordination. Thus, the elements associated with the connectivity between any pair of consumers are zero in "Matrix A". Moreover, consumers do not have to establish a communication channel with more than one DG. They are connected to a local or nearest DG if there is a physical connection (transmission and distribution line). Since the power mismatch is the only shared information among DGs, a DG and its associated loads/consumers can be viewed as an aggregate node. The "Reduced Matrix A" being used in Equation (19) is only an adjacency matrix of DGs' communication network. In sum, the A matrix has many zero elements that most of them could be ignored for the sake of simplicity. The A matrix that used in Equation (19) is only an adjacency matrix of DGs' communication network without zero elements of consumers' network and communication channel among consumers and DGs. Thus, we omitted zero

elements. The A matrix is reduced by dimension in comparison with A matrix of the entire system.

$$\begin{bmatrix} \Delta P_1(k+1) \\ \Delta P_2(k+1) \\ . \\ . \\ . \\ \Delta P_n(k+1) \end{bmatrix} = [A] \begin{bmatrix} \Delta P_1(k) \\ \Delta P_2(k) \\ . \\ . \\ . \\ \Delta P_n(k) \end{bmatrix} \Longrightarrow \vec{\Delta P}(k+1) = A\vec{\Delta P}(k) \tag{2.19}$$

Each DG uses its own estimated power mismatch as a feedback. By adding the vector $\vec{P}^{L}(k) - \vec{P}^{Gen}(k)$ to Equation (2.19), Equation (2.20) is obtained as a consensus protocol for this chapter.

$$\vec{\Delta P}^{T}(k+1) = A\vec{\Delta P}(k) + \vec{P}^{L}(k) - \vec{P}^{Gen}(k)$$

$$\Longrightarrow \begin{bmatrix} \Delta P_1^T(k+1) \\ \Delta P_2^T(k+1) \\ . \\ . \\ . \\ \Delta P_n^T(k+1) \end{bmatrix} = [A] \begin{bmatrix} \Delta P_1(k) \\ \Delta P_2(k) \\ . \\ . \\ . \\ \Delta P_n(k) \end{bmatrix} + \begin{bmatrix} P_1^L(k) - P_1^{Gen}(k) \\ P_2^L(k) - P_2^{Gen}(k) \\ . \\ . \\ . \\ P_n^L(k) - P_n^{Gen}(k) \end{bmatrix} \tag{2.20}$$

Where P_i^L is the summation of all local loads connected to $i-th$ DGs. Every iteration, the DGs need to go through a simple process to update incremental cost λ internally. This λ does not need to be shared with neighbors. Once gain, the only information that will be shared through the communication network is ΔP.

The discrete-time equation (2.21) shows proposed protocol for λ in this chapter, where $\Delta x > 0$ shows the interval of discrete-time integration, and K_I is the controller coefficient.

$$\lambda_i(k+1) = K_I \sum_k \left(\Delta P_i^T(k+1) + \Delta P_i^T(k)\right) \times \frac{\Delta x}{2} \tag{2.21}$$

The incremental cost λ is used to calculate output-power (P_i^{Gen}) of a DG, The parameters of cost function (2.5) such as α, β and the calculated λ inside the controller of each agent are used to estimate output-power using Equation (2.22). In fact, other agents and third-parties are not at all able to access these parameters.

$$P_i^{Gen}(k+1) = \begin{cases} 0 & P_i^{Gen} \leq 0 \\ \frac{\lambda_i(k+1)-\beta_i}{2\alpha_i} & 0 < P_i^{Gen} < P_{i,max}^{Gen} \\ P_{i,max}^{Gen} & P_i^{Gen} \geq P_{i,max}^{Gen} \end{cases}, \tag{2.22}$$

When a DG estimates its output-power, it can determine the estimated power mismatch by Equation (2.23), and share this estimate with its neighbors at each iteration.

$$\Delta P_i(k+1) = P_i^{Gen}(k+1) - P_j^L(k+1), \qquad i \epsilon S_G \tag{2.23}$$

When a DG determines its λ in accordance with its output-power, it shares λ with the local consumers. Then the consumers calculate their demands based on the λ offered by the DG. It is not, however, necessary to share λ among consumers; in other words, each consumer just needs to receive λ from one DG. Then, the consumer can determine its best and most cost-effective demand based on the maximum level of the consumer's surplus function represented by (2.4). The maximum of consumer's surplus can be achieved by $\frac{\partial \mathcal{S}_j^{Load}}{\partial P_j^{Load}} = 0$, which is shown in (2.24). The utility function of consumers in Equation (2.3) and Figure 2.3 show that if a consumer uses power more than $\omega_j/2b_j$, its level of satisfaction will not be increased. Thus, the maximum load of $j-th$ consumer is considered as $P_{j,max}^{Load} = \omega_j/2b_j$.

$$P_j^{Load}(k+1) = \begin{cases} 0 & P_j^{Load} \leq 0 \\ \frac{\omega_j - \lambda_i(k+1)}{2b_j} & 0 < P_j^{Load} < P_{j,max}^{Load} \\ P_{j,max}^{Load} & P_j^{Load} \geq P_{j,max}^{Load} \end{cases}, \tag{2.24}$$

The consumer sends the amount of estimated demand to a local DG if there is a physical connection (i.e., distribution lines) between them. The consumers do not need to disclose any properties of its utility function. In addition, consumers do not need to establish any communication channel among themselves to coordinate any information state or with more than one DG. The above-mentioned features significantly reduce the computing complexity and the upfront cost of new communication infrastructure

Figure 2.5 illustrates the interaction between a specific DG and other agents (DGs and consumers).

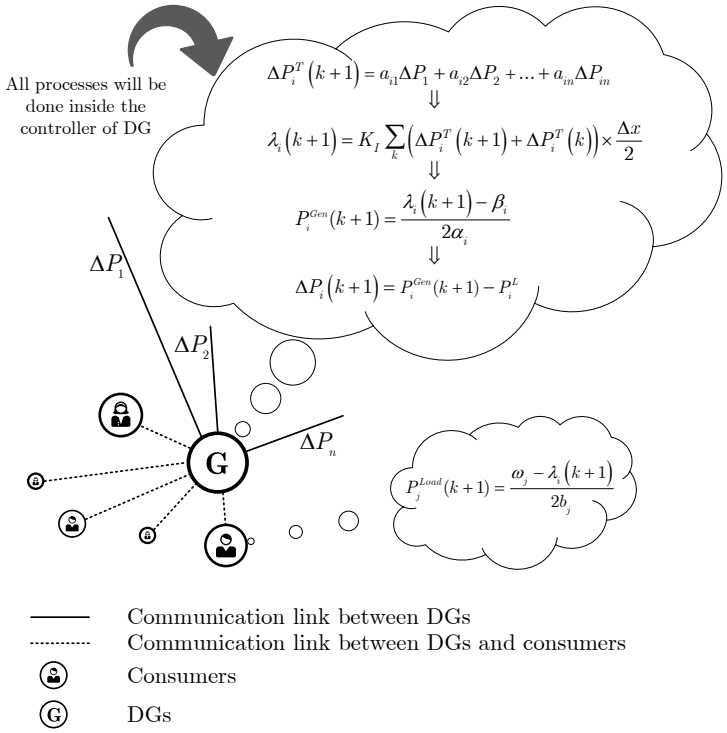

Figure 2.5: Distributed decision making for a DG at every iteration.

The optimality and convergence analysis of the proposed distributed algorithm will be discussed in the rest of this section.

2.4.3 The Optimality Analysis

As mentioned before, P_i^L is the summation of local loads connected to $i-th$ DG. Equation (2.25) shows the $(k+1)-th$ iteration of total P_i^L and ψ_i indicates the portion of total load connected

to $i-th$ DG. θ_i^L and φ_i^L are used in the place of $\psi_i \sum_j \frac{\omega_j}{2b_j}$ and $\psi_i \sum_j \frac{1}{2b_j}$, respectively, for more simplicity. $(k+1)-th$ iteration of DG's output is calculated by (2.26). In addition, θ_i^{Gen} and φ_i^{Gen} are used in the place of $\frac{\beta_i}{2\alpha_i}$ and $\frac{1}{2\alpha_i}$, respectively.

$$\begin{aligned} P_i^L(k+1) = \psi_i \sum_j P_j^{Load}(k+1) &= \psi_i \sum_j \frac{\omega_j}{2b_j} - \psi_i \sum_j \frac{1}{2b_j} * \lambda_i(k+1) \\ &= \theta_i^L - \varphi_i^L \lambda_i(k+1); \quad \sum_j \psi_i = 1 \end{aligned} \tag{2.25}$$

$$P_i^{Gen}(k+1) = \frac{\lambda_i(k+1) - \beta_i}{2\alpha_i} = \frac{\lambda_i(k+1)}{2\alpha_i} - \frac{\beta_i}{2\alpha_i} = \varphi_i^{Gen}\lambda_i(k+1) - \theta_i^{Gen} \tag{2.26}$$

Finally, the power mismatch $\Delta P_i(k+1)$ calculated by $i-th$ DG is achieved by (2.27) where, $\varphi_i^c = \varphi_i^{Gen} + \varphi_i^L$ and $\theta_i^c = \theta_i^{Gen} + \theta_i^L$.

$$\begin{aligned} \Delta P_i(k+1) = P_i^{Gen}(k+1) - P_i^L(k+1) &= \left(\varphi_i^{Gen} + \varphi_i^L\right)\lambda_i(k+1) - \left(\theta_i^{Gen} + \theta_i^L\right) \\ &= \varphi_i^c \lambda_i(k+1) - \theta_i^c \end{aligned} \tag{2.27}$$

λ_i, ΔP_i^T of $i-th$ agent for $k=0$ can be calculated by (20), (23) and (25) .

$$\Delta P_i^T(1) = \Delta P_1(0) + \Delta P_2(0) + \cdots = \Delta_1 \tag{2.28}$$

$$\Delta P_i^T(0) = \Delta P_1(0^-) + \Delta P_2(0^-) + \cdots = \Delta_0 \tag{2.29}$$

$$\lambda_i(1) = K_I(\Delta P_i^T(1) + \Delta P_i^T(0)) = K_I(\Delta_1 + \Delta_0) \tag{2.30}$$

By continuing this process for $k = 1, 2, \cdots$, equations (2.31), (2.32) will be obtained.

$$\Delta_{k+1} = \Delta P_i^T(k+1) = \sum_i K_I \varphi_i^c \Delta_k - \Delta_k \quad \forall i \epsilon S_G \tag{2.31}$$

$$\lambda_i(k+1) = K_I(\Delta_k + \cdots + 2\Delta_2 + 2\Delta_1 + \Delta_0) \quad \forall i \epsilon S_G \tag{2.32}$$

In Equation (2.31), $||\Delta_{k+1}||$ merges to zero *i.e.;* $||\Delta_{k+1}|| \to 0$ if $||1 - \sum_i K_I \varphi_i^c|| \leq \varepsilon < 1$, where where ε is a positive number. Then, we have $\lambda_i(k+1) \leq (\varepsilon^k \Delta_0 + 2\varepsilon^{k-1}\Delta_0 \cdots + 2\varepsilon^2 \Delta_0 + 2\varepsilon\Delta_0 + \Delta_0), \quad \forall i \epsilon S_G$. Therefore, if $k \to \infty$, $\lambda_i$will not approach infinity; hence, $\lambda_i(k+1) \leq \frac{1}{1-\varepsilon}\Delta_0 + \frac{\varepsilon}{1-\varepsilon}\Delta_0 = \frac{1+\varepsilon}{1-\varepsilon}\Delta_0$. The smaller $||1 - \sum_i K_I \varphi_i^c||$ is, the faster the power mismatch will converge to 0. K_I is the parameter that can control/change the size of $||1 - \sum_i K_I \varphi_i^c||$ to be less than 1.

Finally, Equation (2.33) indicates that λ_i for all DG ($\forall i$) will be same and $\Delta P_i^T(k+1)$ of $i-th$ of DG will converge to zero for $\forall i \epsilon S_G$. We consider all $\lambda_i \quad \forall i$ as λ because they are identical. In the next step, we will show (2.33) will satisfy the KKT conditions.

$$\begin{aligned} \lim_{k\to\infty} \lambda_i(k+1) &= \lambda; \qquad \forall i \epsilon S_G \\ \lim_{k\to\infty} \Delta P_i^T(k+1) &= \Delta_{k+1} = 0; \qquad \forall i \epsilon S_G \end{aligned} \tag{2.33}$$

Assumption 1: All local cost functions utility functions (2.3) and (2.5) are strictly concave and convex, respectively. Accordingly, the total objective function (2.7) is strictly convex.

Assumption 2: In addition, all equality and inequality constraint functions, represented by (2.8) and (2.9), are affine.

Lemma 1: The optimization problem represented in this chapter through (2.3)-(2.9) is a convex optimization problem with differentiable objective and constraint functions satisfying Slater's condition (*assumption 1 and 2 guarantee Slater's condition*), thus the KKT conditions provide ***necessary and sufficient conditions*** for optimality [94].

The remaining of this section makes certain that the fixed-point of proposed iterative consensus algorithm obtained by (2.20)-(2.24) is a global optimal solution of (2.7) if it is satisfying the following KKT conditions [64].

Lagrangian:

$$L(P,\lambda,\mu,\zeta)=\left(\sum_{i\epsilon S_G}C_i\left(P_i^{Gen}\right)-\sum_{j\epsilon S_D}U_j\left(P_j^{Load}\right)\right)+\lambda\left(\sum_{j\epsilon S_D}P_j^{Load}-\sum_{i\epsilon S_G}P_i^{Gen}\right)$$
$$+\sum_{i\epsilon S_G}\mu_i\left(P_i^{Gen}-P_{i,max}^{Gen}\right)+\sum_{i\epsilon S_G}\zeta_i\left(-P_i^{Gen}\right)+\sum_{j\epsilon S_D}\mu_j\left(P_j^{Load}-P_{j,max}^{Load}\right)+\sum_{j\epsilon S_D}\zeta_j\left(-P_j^{Load}\right) \tag{2.34}$$

Lagrangian stationarity ($\nabla_P L(P,\lambda,\mu,\zeta)$=0):

$$\begin{aligned}&\frac{\partial C_i\left(P_i^{Gen}\right)}{\partial\left(P_i^{Gen}\right)}-\lambda+\mu_i-\zeta_i=0; \qquad \forall i\epsilon S_G\\ &-\frac{\partial U_j\left(P_j^{Load}\right)}{\partial\left(P_j^{Load}\right)}+\lambda+\mu_j-\zeta_j=0; \qquad \forall j\epsilon S_D\end{aligned} \tag{2.35}$$

Complementary slackness:

$$\begin{aligned}&\mu_i\left(P_i^{Gen}-P_{i,max}^{Gen}\right)=0\,, \quad \zeta_i\left(-P_i^{Gen}\right)=0; \qquad \forall i\epsilon S_G\\ &\mu_j\left(P_j^{Load}-P_{j,max}^{Load}\right)=0\,, \quad \zeta_j\left(-P_j^{Load}\right)=0; \qquad \forall j\epsilon S_D\end{aligned} \tag{2.36}$$

Dual feasibility:

$$\begin{aligned}&\mu_i\geq 0\,, \quad \zeta_i\geq 0; \qquad \forall i\epsilon S_G\\ &\mu_j\geq 0\,, \quad \zeta_j\geq 0; \qquad \forall j\epsilon S_D\end{aligned} \tag{2.37}$$

All local constraints presented by (2.9) for generation and consumption level of DGs and loads are considered as the primal feasibility.

Let consider fixed point of the proposed iterative consensus algorithm as optimal point, $\Delta P_i^T = \Delta P_1+\Delta P_2+\cdots\Delta P_n=0$, where $\Delta P_i = P_i^{Gen}-P_i^L$ and $\lambda_1=\lambda_2=\cdots=\lambda_n=\lambda,\ \forall i.\ \Delta P_i^T=0$ satisfies the equality constraint, as the load balance of the entire system, to ensure that the demand will be supported. As mentioned before, there is only one equality constraint (2.8); thus, all agents

should reach the same λ and (2.25)-(2.33) guarantee the identical λ for all agents.

If the optimal solution of the objective function does not violate local constraints (inequality functions) represented by (2.9), then these constraints will never play any role in changing the minimum compared with the problem without the inequality constraints. The DG's profit is maximized when $\partial \mathcal{S}_i^{Gen}/\partial P_i^{Gen} = 0;\ \forall i \epsilon S_G$. It means $\lambda_{opt} - \partial C_i/\partial P_i^{Gen}|_{P_{i,opt}^{Gen}} = 0;\ \forall i \epsilon S_G$. The Lagrangian stationarity (2.35), complementary slackness (2.36) and dual feasibility (2.37) are satisfied by taking $\lambda = \partial C_i/\partial P_i^{Gen}|_{P_{i,opt}^{Gen}};\ \forall i \epsilon S_G$ and $\mu_i = \zeta_i = 0,\ \forall i$. Thus, λ obtained by algorithm is λ_{opt} because it satisfies the KKT condition.

The local constraints can affect the optimal solution in two ways:

If the optimal points are greater than maximum limitation, $P_{i,opt}^{Gen} \geq P_{i,max}^{Gen}$, in this case, the maximum level is considered as an optimal solution, hence $P_{i,opt}^{Gen} = P_{i,max}^{Gen}$ and $\partial C_i/\partial P_i^{Gen}|_{P_{i,max}^{Gen}} - \lambda_{opt} \leq 0$. Thus, the Lagrangian stationarity (2.35), complementary slackness (2.36) and dual feasibility (2.37) are satisfied by taking $\lambda = \lambda_{opt};\ \forall i, j, \mu_i = \lambda_{opt} - \partial C_i/\partial P_i^{Gen}|_{P_{i,max}^{Gen}}$ and $\zeta_i = 0,\ \forall i$.

If the optimal points are less than minimum limitation, $P_{i,opt}^{Gen} \leq 0$, in this case, the minimum level is considered as optimal solution, hence $P_{i,opt}^{Gen} = 0$ and $\partial C_i/\partial P_i^{Gen}|_0 - \lambda_{opt} \geq 0$. Thus, the Lagrangian stationarity (2.35), complementary slackness (2.36) and dual feasibility (2.37) are satisfied by taking $\lambda = \lambda_{opt};\ \forall i, j, \zeta_i = \partial C_i/\partial P_i^{Gen}|_0 - \lambda_{opt}$ and $\mu_i = 0,\ \forall i$.

The same procedure could be considered for consumers' side. If all local constraints (inequality functions) represented by (9) are ignored, the consumer surplus is maximized when $\partial \mathcal{S}_j^{Load}/\partial P_j^{Load} = 0; \forall j \epsilon S_D$. It means $\partial U_j/\partial P_j^{Load}|_{P_{j,opt}^{Load}} - \lambda_{opt} = 0; \forall j \epsilon S_D$. The Lagrangian stationarity (2.35), complementary slackness (2.36) and dual feasibility (2.37) are satisfied by taking $\lambda = \partial U_j/\partial P_j^{Load}|_{P_{j,opt}^{Load}}; \forall j \epsilon S_D$ and $\mu_j = \zeta_j = 0,\ \forall i$. Thus, λ obtained by algorithm is λ_{opt} because it satisfies the KKT condition.

If the optimal points are greater than maximum limitation, $P_{j,opt}^{Load} \geq P_{j,max}^{Load}$, in this case, the maximum level is considered as an optimal solution, hence $P_{j,opt}^{Load} = P_{j,max}^{Load}$ and $\partial U_j/\partial P_j^{Load}|_{P_{i,max}^{Load}} - \lambda_{opt} \geq 0$. Thus, the Lagrangian stationarity (2.35), complementary slackness (2.36) and dual fea-

sibility (2.37) are satisfied by taking $\lambda = \lambda_{opt};\ \forall j, \mu_j = {}^{\partial U_j}/_{\partial P_j^{Load}}|_{P_{i,max}^{Load}} - \lambda_{opt}$ and $\zeta_j = 0,\ \forall j$.

If the optimal points are less than minimum limitation, $P_{j,opt}^{Load} \leq 0$, in this case, the minimum level is considered as optimal solution, hence $P_{j,opt}^{Load} = 0$ and ${}^{\partial U_j}/_{\partial P_j^{Load}}|_0 - \lambda_{opt} \leq 0$. Thus, the Lagrangian stationarity (2.35), complementary slackness (2.36) and dual feasibility (2.37) are satisfied by taking $\lambda = \lambda_{opt};\ \forall i, j, \zeta_j = \lambda_{opt} - {}^{\partial U_j}/_{\partial P_j^{Load}}|_0$ and $\mu_j = 0,\ \forall j$.

Lemma 2: The optimal solution found by the proposed iterative consensus algorithm is unique.

It is proved that the fixed point of the proposed iterative consensus algorithm satisfies the KKT conditions while objective and constraint functions are both strictly convex and differentiable. Thus, the satisfaction of Slater's condition provides an absolute assurance about global optimality.

2.5 Performance Assessment

In this section, we conduct a performance evaluation of the proposed distributed method through three case studies using software simulations and experimental test. All software simulations are conducted in the MATLAB 2015a environment on an ordinary desktop PC with an Intel(R) Core(TM)i3 CPU @ 2.13 GHz, 4-GB RAM memory. The experiment test is performed using the VOLTTRON™ platform and a cluster of low-cost credit-card-size single-board PCs.

In the first case study, we provide a numerical example to evaluate the algorithm performance (i.e., accuracy) in a relatively small-scale system. The numerical results are compared with the benchmark results found by a traditional centralized economic dispatch. The centralized method is implemented using YALMIP toolbox [95] and MATLAB.

In the second case study, we demonstrate the scalability and fast convergence rate of the proposed distributed algorithm in a large-scale network with 1,400 agents.

In the third case study, we set up an experimental testbed to verify the practical performance of the proposed distributed algorithm using the VOLTTRON™ platform and a group of low-cost credit-card-size single-board PCs.

2.5.1 Case Study I (Evaluation of Accuracy)

In this case study, an IEEE 39-bus test system with 29 agents (10 DGs and 19 consumers) is considered. Their cost functions and utility functions are formulated using Equations (2.5) and (2.3), respectively. Table 2.1 summarizes the parameters of the cost functions and utility functions of the agents [63]. The initial values of the λs are randomly selected. The controller parameters (K_I and K_P) are obtained by trial-and-error. K_I and K_P can be randomly set in the range of zero to one.

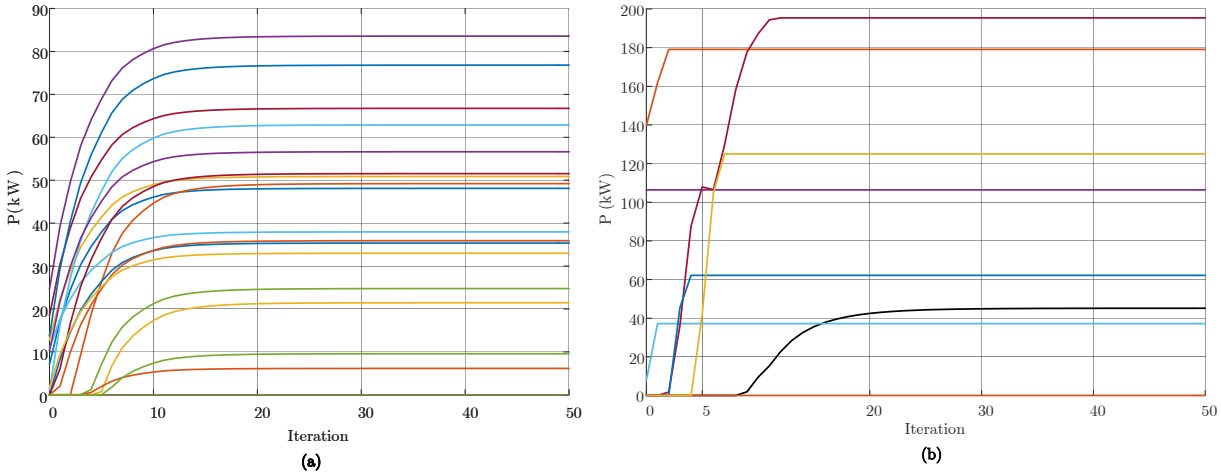

Figure 2.6: Generation output and load demand powers in case study I; (a) demands (kW), (b) DGs (kW)

Figure 2.6 shows the evolution of DG power output and load demand, respectively. Figure 2.6(a) contains 19 consumer demand curves and Figure 2.6(b) includes 10 DG output-power curves. As can be seen in 2.6, the economic dispatch solution converges at the 36-th iteration. The corresponding execution time is about 1.69 seconds. The accuracy of the proposed distributed solution algorithm is validated by the benchmark results found by a centralized method. As shown in Tables 2.2 and 2.3, the solution mismatch between the distributed and centralized methods is less than 0.00201% of the average. As the distributed algorithm proceeds, the incremental cost converges to $8.175\,\$/\text{kwh}$, as shown in Figure 2.7. The evolution of power mismatch, the evolution of total generation and the evolution of total load demand are shown in Figure 2.8. Power mismatch (ΔP) serves as *coordination information* and gradually converges to a consensus *(i.e.,* $0\ kW$*)*. The power

Table 2.1: The coefficients of DGs' cost functions and consumers' utility functions in case study I

	Cost function			Utility function		
i	α_i	β_i	$P_{i,max}^{Gen}$	ω_i	b_i	$P_{i,max}^{Load}$
1	0.0031	8.71	113.23	17.17	0.0935	91.79
2	0.0074	3.53	179.1	12.28	0.0417	147.29
3	0.0066	7.58	90.03	18.42	0.1007	91.41
4	0.0063	2.24	106.41	7.06	0.0561	62.96
5	0.0069	8.53	193.80	10.85	0.0540	100.53
6	0.0014	2.25	37.19	18.91	0.1414	66.88
7	0.0041	6.29	195.4	18.76	0.0793	118.35
8	0.0051	4.30	62.17	15.70	0.1064	73.81
9	0.0032	8.26	143.41	14.28	0.0850	84.00
10	0.0025	5.3	125	10.15	0.0460	110.32
11	–	–	–	19.04	0.0650	146.46
12	–	–	–	06.87	0.0549	62.61
13	–	–	–	15.96	0.0619	128.91
14	–	–	–	14.70	0.0633	116.08
15	–	–	–	17.50	0.0607	144.04
16	–	–	–	10.97	0.2272	24.15
17	–	–	–	16.25	0.1224	66.39
18	–	–	–	17.53	0.0826	106.14
19	–	–	–	09.84	0.0869	56.60

tolerance is set to be 0.001 kW in our case studies. As the incremental cost and power mismatch settle down, the optimal value of social welfare is found to be $5,211.5\,\$/\text{hr}$. It is important to note that the proposed distributed algorithm is able to converge to the near-optima much faster than other distributed methods [56, 63, 84]. For example, one of the published works [63] showed that the same economic dispatch problem was solved after 500 iterations, while our distributed control algorithm is able to find the same results at the 36-th iteration.

2.5.2 Case Study II (Evaluation of Scalability and Fast Convergence)

In order to demonstrate the scalability, we then apply the proposed solution algorithm to a large-scale system, including 1,000 consumers and 400 DGs. The initial conditions of the1,400 agents are randomly selected.

As shown in Figure 2.9, the incremental costs reach consensus within approximately 40 iterations,

Table 2.2: Comparison of the output of DGs achieved by distributed and centralized methods in case study I

Output Power (kW)	Distributed Method	Centralized Method
P_1	0	0
P_2	179.1	179.099
P_3	45.16	45.1614
P_4	106.4	106.409
P_5	0	0
P_6	37.19	37.189
P_7	195.4	195.399
P_8	62.17	62.1699
P_9	0	0
P_{10}	125	124.999
Total	750.4	750.428

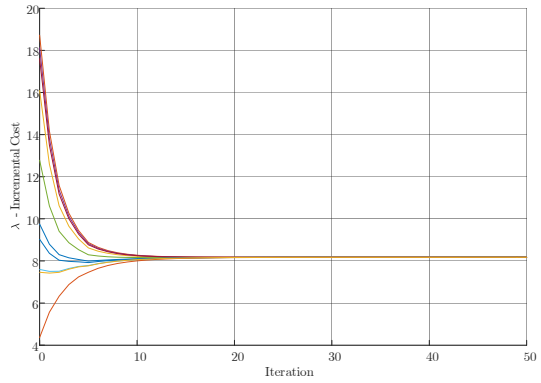

Figure 2.7: Incremental cost of DGs in case study I

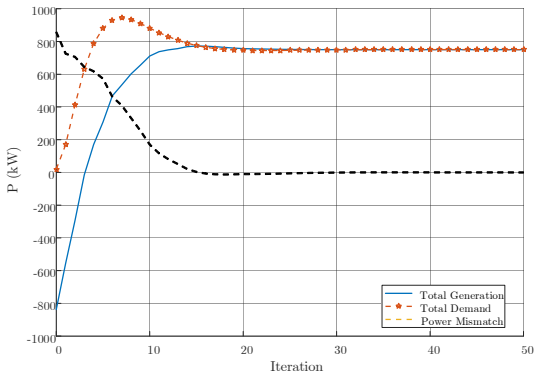

Figure 2.8: Generation, demand and power mismatch in case study I

which is considered a fast convergence rate for a 1,400-agent system. The corresponding execution time is 192.579 seconds. Some simulation for different numbers of agents, 29 (10 DGs and 19 Consumers), 350 (150 DGs and 200 Consumers), 700 (300 DGs and 400 Consumers), 1050 (350 DGs and 700 Consumers), 1400 (400 DGs and 1000 Consumers)), are performed to study the trend in number of iteration for convergence. The Figure 2.10 shows that as the number of agents increase from 29 (case study I) to 1,400 (case study II), the number of iteration is almost constant, demonstrating that the proposed distributed algorithm is particularly suitable for solving large-scale economic dispatch problems. The minimum error criteria for power mismatch tolerance is set to

Table 2.3: Comparison of the demand of loads achieved by distributed and centralized methods

Demand of Loads (kW)	Distributed Method	Centralized Method
L_1	48.1	48.095
L_2	49.21	49.207
L_3	50.86	50.863
L_4	0	0
L_5	24.76	24.758
L_6	37.96	37.955
P_7	66.73	66.733
L_8	35.36	35.356
L_9	35.91	35.905
L_{10}	21.46	21.455
L_{11}	83.57	83.568
L_{12}	0	0
L_{13}	62.87	62.874
L_{14}	51.53	51.531
L_{15}	76.8	76.80
L_{16}	6.148	6.148
L_{17}	32.98	32.981
L_{18}	56.62	56.621
L_{19}	9.573	9.573
Total	750.4	750.428

be $\Delta P = 0.001\ kW$ in our case studies used in Figure 2.10.

As previously emphasized, the power mismatch is the only shared information between agents. It reduces the computational cost because the proposed algorithm only needs a simple updating process on the power mismatch. Besides, consumers do not need to establish any communication channel among themselves to coordinate any information state or with more than one DG. The above-mentioned features contribute to a significantly reduction on the computing complexity.

2.5.3 Case Study III (Evaluation of Practical Performance)

The proposed distributed algorithm is particularly designed for easy implementation and configuration of local agents by using a simple proportional-integral (PI) or integral (I) controller. Equations (2.20)-(2.23) can be easily modeled as a PI or I controller to update the estimated power mismatch iteratively and exchange information (*i.e.*, ΔP) with other agents. Figure 2.11(a) shows a simple

PI controller for a DG. A PI controller is used for each consumer to adjust its own demand based on $\Delta\lambda$ between the current and previous iteration. Figure 2.11(b) shows a simple controller for a consumer. As $\Delta\lambda$ becomes zero, the consumer's surplus is maximized.

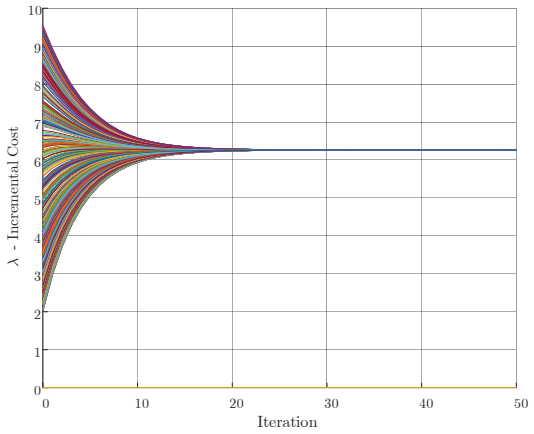

Figure 2.9: Incremental cost ($/kWh) of DGs in case study II

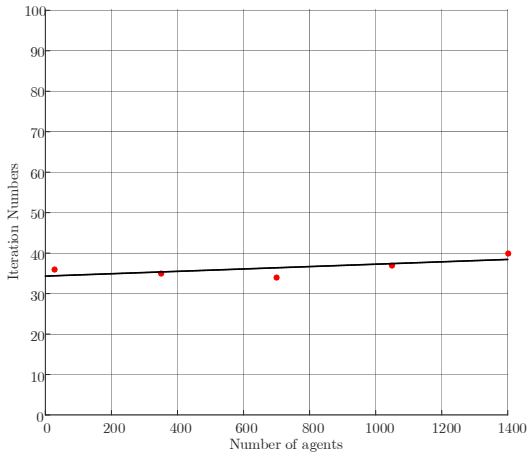

Figure 2.10: The trend in number of iteration for algorithm convergence

In case study III, the communication platform is implemented in VOLTTRON™ which is an innovative distributed control and sensing software platform developed by the Pacific Northwest National Laboratory [96]. The open-source VOLTTRON™ platform makes it possible to deploy distributed control agents at a very low cost. The platform provides various services such as resource management, agent code verification and directory services allowing to manage different assets within the power system. In the large scale, VOLTTRON™ can manage assets within smart grids, facilitate demand response, support energy trading and record grid data.

The VOLTTRON™ platform is implemented on an ordinary Linux desktop with an FX-4100 CPU @ 3.6 GHz, 8-GB RAM memory. The control platform is substantiated into a cluster of low-cost credit-card-size single board PCs (Cubieboard A20). The Cubieboard A20 processor is based on a dual-core ARM Cortec-A7 CPU architecture. We use the Python programming language to implement the proposed consensus-based distributed control algorithms for each agent. In this proof-of-concept implementation, every Cubieboard is emulated as a distributed controller for local agents (DGs and consumers), while the PC with the VOLTTRON™ platform is regarded as an

information exchange bus. The decision making process is conducted in a fully distributed fashion. Figure 2.12a shows the overall system set up. For the demonstration purpose, the proposed distributed algorithm is applied to a relatively small-scale distribution system including 6 DGs and 10 consumers. As shown in figure 2.12a, DGs are labeled as G1, G2, ..., G6 while consumers are labeled as L1, L2, ..., L10. The coefficients of DGs' cost functions and consumers' utility functions are randomly selected.

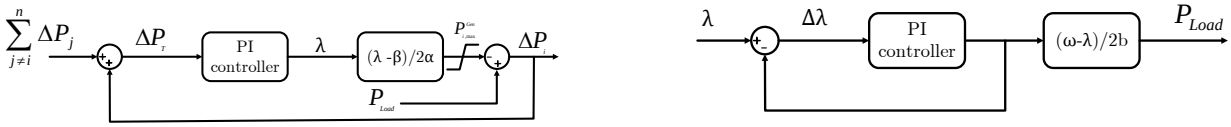

(a) PI-controller for DGs

(b) PI-controller for consumers

Figure 2.11: Local PI-controller for DGs and consumers

Figure 2.12b shows the detailed experimental test results. The output-power of DG3 and DG5 and the demand of L4 are zero. The experimental test results are validated using the benchmark results achieved by a centralized approach. As figure 2.12b shows, the total generation is about 421 kW that satisfies the total load demand. The incremental cost converges to 7.371 $/kwh at the 42-th iteration, which is considered as a fast convergence rate.

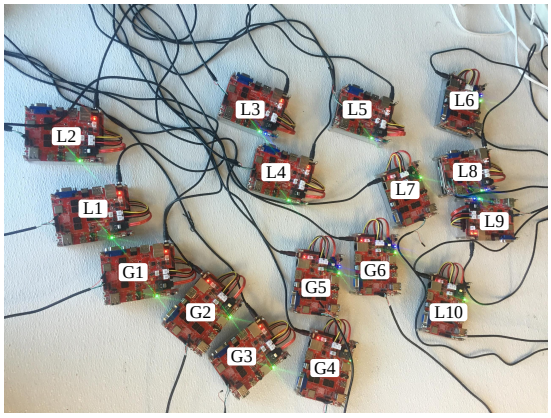

(a) The Proof-of-Concept 16-node Testbed using a Cluster of Single-board PCs ("L" inidicates loads/consumers; "G" inididates DGs)

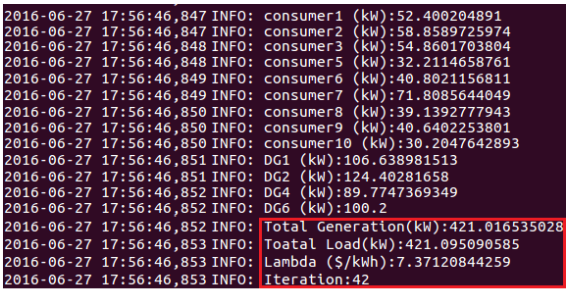

(b) The experimental test results

Figure 2.12: The hardware implementation

2.6 Conclusions

In this chapter, we proposed a novel consensus-based distributed algorithm to solve an optimal dispatch problem of distributed generators. First, we formulated the social welfare problem considering the cost functions of DGs and the utility functions of consumers. Second, we developed the distributed algorithm to find the global optima by allowing the iterative coordination of agents (consumers and DGs) with each other. Agents only share their estimated power mismatch, which does not contain any private information, ultimately contributing to a fair electricity market. Third, we performed software simulation and experimental test to demonstrate the accuracy, privacy, effectiveness, fast-convergence, scalability, and easy-implementation of the proposed distributed algorithm under various conditions.

CHAPTER 3
Distributed AC Power Flow (ACPF) Algorithm

3.1 Introduction

Power flow is one of the basic tools for system operation and control. Due to its nature, which determines the complex nodal voltages, line flows, currents and losses, it enforces a large computation load on a power system. A distributed/decentralized algorithm unburdens the central controller and shares the total computation load with all agents. Therefore, such algorithms are an effective method for dealing with power flow complexity. In this chapter, a distributed method based on a linearized AC power system is proposed. First, the linearization procedure of a comprehensive non-linear AC power flow is detailed. Second, a distributed method is presented based upon the linear AC power flow equations. Three case studies are presented to evaluate the overall performance of the proposed method. In the first case study, the accuracy level of both linearized AC power flow and distributed AC power flow is assessed. In the second case study, the dynamic performance of distributed AC power flow is investigated based on the load sudden changes. In the third case study, the scalability of the proposed distributed AC power flow is evaluated by applying it to a larger power system.

3.2 Literature Review

The Power flow problem (known as load flow) is an important tool for power system monitoring, control and decision making. As a result, researchers are currently working to find an effective method for solving the power flow problem from emergence of power systems. Naturally, the power flow imposes a heavy computation load on the power system because it determines the complex nodal voltages from which line flows, currents and losses can be derived [97]. Typical

power flow solutions were first introduced about 50 years ago. W. F. Tinney and C. E. Hart in [98] present Newton's method for solving the power flow problem as one of the earlier methods. Furthermore, [99, 100] suggest several different methods for solving the AC power flow problem. R. P. Klump *et al.* propose an approach in [101] for solving the low-voltage power problem, showing the effectiveness of their method in the speed and frequency of convergence. [102] introduces an iterative process for the power flow of radial grids based on the exact power flow solution. Recently, N. Ghadimi in [103] presents two different methods for solving the power flow based on the proportional sharing assumption and circuit laws to find the relationship between power inflows and outflows through all elements. In addition, many attempts have been made to linearize the power flow problem. Linearization helps us to achieve a reduction in the overall computation needed for comprehensive AC power flow; however, the accuracy level will be reduced as well [1, 40, 104].

In recent years, the penetration of distributed generators (DGs), including renewable energy resources and other local fossil fuel generators is increasing, exerting both the positive and negative impacts on power systems. These local generators provide energy resiliency, improve environmental benefit (carbon emissions reduction) and enhance the power quality/reliability of power systems. However, the presence of local generators and the market reconstruction result in significant challenges in power system operation, control, and protection [2, 83, 105]. Protection of the system would be very challenging because the power flow direction of the distribution grid would be changed from single to bidirectional with the integration of distributed generation. Thus, the conventional protection system cannot protect this modified power system as it would a traditional power system [106]. Additionally, comprehensive communication networks are required to exchange data between the central controller and the local agents. As the number of agents increases to the hundreds of thousands, the control system is confronted with some technical barriers, such as the computational complexity and a single point of failure [46, 107].

In the traditional power system, various agents (e.g. DGs and loads) are controlled by a center. A wide range of signals and information is gathered through supervisory control and data acquisition (SCADA) from all over the system and is sent to a center. SCADA is an advanced automation con-

trol system that centrally manages the power system by gathering data and monitoring the system's operation. Then the central controller carries out a power flow or optimal power flow computations and sends control and operational commands back to the operators spread over a wide geographical area. A two-way complex communication channel for each agent is required to support all data transmission between the center and agents [25,28]. Consequently, this system suffers from a technical communication barrier and cannot be effective for future smart grids due to the variation in topology of both the communication and electrical network of a smart grid. Moreover, the legacy centralized approach would not be able to cope with the huge amount of data. In other words, this kind of approach is suitable for relatively small-scale systems without reconstructing the existing communication and control networks. Thus, a centralized method cannot carry out operational and control responsibilities for a large number of agents because of the high penetration of DGs, load volatility, market deregulation, etc.

Power flow computation is negatively affected in systems that are integrated with numerous DGs and loads, suffering from computational complexity. Furthermore, a single point of failure is always an imminent threat to a system with a centralized controller. That is, if the central controller fails to connect to the system, the entire system will experience failure. These kinds of challenges can be completely addressed by introducing a fully distributed control approach to future power systems [24]. Therefore, an immediate and effective replacement for the centralized control approaches, which addresses the challenges raised by the launching of smart grids, is a distributed approach [53]. In this type of method, each agent makes its own operation decisions based on information exchanged with its neighbors and/or local measurements. In distributed methods, it is not required to share all information globally or send it to a central control; thus, computational load will be distributed among all agents.

Recently, many researchers have given their attention to the distributed methods for controlling and operating power systems. Power flow, as an important numerical analysis, could considerably benefit from the use of a distributed algorithm, playing a constructive role in determining the best operation of existing systems. A distributed power flow can provide a reliable and fast control

system for power systems. A distributed power flow can be used for power system restoration, distribution system management, load shedding, microgrid control, etc. [108]. In recent years, many attempts have been made to develop a distributed method for power system operation, such as distributed power flow, distributed economic dispatch and distributed optimal power flow. A distributed multi-phase power flow for the distribution grids is introduced in [109]. This method divides and separates the distribution network using several partitions based on the control capabilities of each area. A power flow of the entire grid is carried out by iteratively running centralized local power flows on each partition. This method uses distributed intelligence to share information. C.P. Nguyen *et al*. applied an agent-based distributed power flow to the unbalanced radial distribution systems considering the network's complete models. The power flow problem is solved by an iterative backward/forward sweep technique added to the distributed smart agents [110]. M. Warnier *et al*. in their recent paper [45] presented a new distributed computation method used for real-time monitoring to avoid cascading failures in a power system. A reduced decentralized calculation method, based on an iterative procedure, has been presented in [111] to solve the power flow problem. It helps operators have an appropriate estimation of the state of the neighboring system. H. Dagdougui *et al*. proposed a decentralized control strategy of power flow to minimize the cost of energy storage and power exchanged between smart microgrids, as well as enable the system for demand support [58]. In [112], K. Nakayama *et al*. present a distributed approach to minimize power flow loss function of the transmission and distribution lines. Their algorithm is designed based on updating the loop variables. T. Erseghe introduced a fully distributed algorithm for optimal power flow based on the alternating direction multiplier method (ADMM), which does not need a central controller. ADMM helps author reach a scalable and distributed algorithm [62]. In [113], the authors presented a distributed version of DC optimal power flow (DC-OPF) for radial distribution systems based on a partial primal-dual algorithm.

In this chapter, we propose a distributed AC power flow based on a linearized AC power flow. Contributions of this work can be considered as follows:

- AC linearized power flow benefits from a high accuracy in comparison with that of typical

DC power flow. Thus, the driven distributed AC power flow obtains power flow results as accurately as AC power flow. In the first case study, the simulation results show the accuracy of the distributed method. The results are compared with those of a centralized method as a benchmark.

- The proposed distributed AC power flow can be applied to the distribution system because our approach does not assume the small ratio of R/X for the sake of generality.
- The proposed distributed AC power flow can cope with load profile changes. The second case study shows that the distributed AC power flow is readily able to follow the load changes.
- The proposed distributed AC power flow is reliable to scale up. The third case study, including a 37-bus IEEE test system and a 2000-bus Texas synthetic system, confirms that the distributed method is scalable and can easily deal with a large number of agents.
- In addition, the distributed approach improves privacy because agent information is not being shared with a central controller or the whole system. Each agent is informed by its neighbors' data. Moreover, the single point of failure, which is common in centralized methods, is removed due to the nature of distributed methods.

This chapter is organized as follows. The next section defines the power flow problem and all necessary equations. Section (3.4) provides the linearization procedure of the power flow problem, including all assumptions, approximations and steps. Section (3.5) proposes a distributed power flow driven by the linearized power flow. Section (3.6) provides three case studies to demonstrate the accuracy, dynamic performance and scalability of the proposed distributed AC power flow. Finally, Section (2.6) reviews the research opportunities and possible applications.

3.3 General Formulation of Power Flow

The values of the voltage magnitude and phase angle at each bus of a power system are calculated using the power flow under steady-state conditions. In addition, the active (P) and reactive (Q)

power flows of all power lines and buses are computed at the same time. Figure (3.1) shows the delivered net active and reactive power to a bus, as well as its generated powers, consumed powers and other parameters [1]. At each bus, four variables, including P_k (net injected active power), Q_k (net injected reactive power), V_k (bus voltage) and δ_k (bus phase angle) are involved in the power flow computation. Two of them are considered as input information for power flow in order to calculate the other two. V_k and δ_k are known for slack bus and are $1pu$ and $0°$, respectively. Thus, P_k and Q_k should be determined. In PV buses, the power flow problem determines Q_k and δ_k based on known P_k andV_k. In addition, P_k and Q_k of PQ buses are known ; thus, the V_k and δ_k of all PQ buses are calculated during the power flow computation.

Equation (3.1) prepares the nodal equations for a power system network, where Y_{Bus} is the power grid admittance matrix and $\mathcal{I}$ and $\mathcal{V}$ are $N \times 1$ vectors of buses' current and voltage. The net complex power injected into bus k is shown by (3.2), where I_k^* indicates the conjugate of the vector of the injected current at the $k-th$ bus.

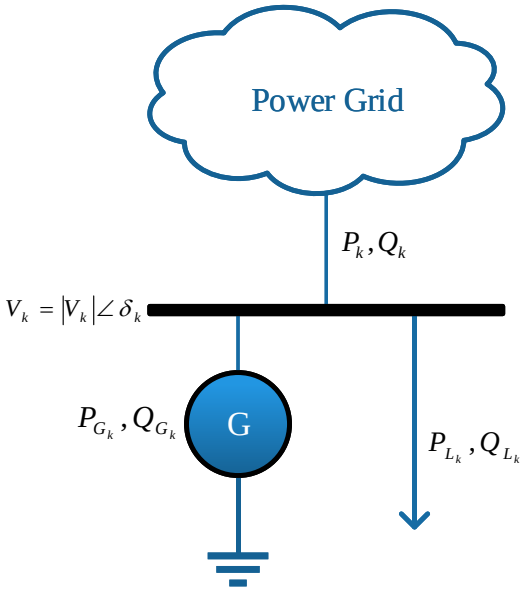

Figure 3.1: Bus configuration

$$\mathcal{I} = Y_{Bus}\mathcal{V} \tag{3.1}$$

$$P_k + jQ_k = V_k I_k^* \tag{3.2}$$

$$P_k = P_{G_k} - P_{L_k},\ Q_k = Q_{G_k} - Q_{L_k} \tag{3.3}$$

Equation (3.4) is another representation of the nodal equations based on elements of Y_{Bus}.

$$I_k = \sum_{n=1}^{N} Y_{kn} V_n \tag{3.4}$$

Substituting (3.2) in (3.4) and by taking $V_k = |V_k| \angle \delta_k$ and $Y_{kn} = |Y_{kn}| \angle \theta_{kn}$, equations (3.5) and (3.6) are obtained.

$$P_k + jQ_k = V_k \left[\sum_{n=1}^{N} Y_{kn} V_n \right]^*, \quad k = 1,\ 2,\ 3, ... \tag{3.5}$$

$$P_k + jQ_k = |V_k| \sum_{n=1}^{N} |Y_{kn}|\, |V_n|\, e^{j(\delta_k - \delta_n - \theta_{kn})} \tag{3.6}$$

In equation (3.7), active and reactive power balance can be achieved as the real and imaginary parts of (3.6), where G_{kn} and B_{kn} are the real and imaginary parts of Y_{Bus} matrix elements *i.e.*, $Y_{kn} = G_{kn} + jB_{kn}$.

$$\begin{aligned} P_k &= |V_k| \sum_{n=1}^{N} |V_n| \left[G_{kn} \cos(\delta_k - \delta_n) + B_{kn} \sin(\delta_k - \delta_n) \right] \\ Q_k &= |V_k| \sum_{n=1}^{N} |V_n| \left[G_{kn} \sin(\delta_k - \delta_n) - B_{kn} \cos(\delta_k - \delta_n) \right] \end{aligned} \tag{3.7}$$

In addition, the power flows transmitted by a line between bus k and n are calculated by (3.8), where g_{kn} and b_{kn} are the conductance and susceptance of the power line, respectively, both measured in Siemens.

$$P_{kn} = |V_k|^2 g_{kn} - |V_k||V_n| g_{kn} \cos(\delta_k - \delta_n) - |V_k||V_n| b_{kn} \sin(\delta_k - \delta_n)$$
$$Q_{kn} = -|V_k|^2 (b_{kn} + b_k) - |V_k||V_n| g_{kn} \sin(\delta_k - \delta_n) + |V_k||V_n| b_{kn} \cos(\delta_k - \delta_n) \quad (3.8)$$

3.4 Linearized AC Power Flow

In many linearization approaches used for power flow, such as typical DC power flow [1, 40], the line resistances and active power loss are subsequently neglected. DC power flow is non-iterative and, of course, a convergent method. However, the accuracy is ignored in this method because of some underlying assumptions, such as a flat voltage profile and small differences of voltage phase angles [104]. DC power flow is not appropriate for a distribution system because the assumption of $R \ll X$ is no longer valid.

In this chapter, a set of assumptions and approximations are considered to have a linearized AC power flow without neglecting reactive power, voltage differences, power losses and line resistances.

As can be seen in equations (3.5) and (3.7) we have two different operators that make our equation non-linear. First operator is the multiplication term between voltage variable such as $V_n * V_k$. The second operator is trigonometric, such as $\sin(\delta_k - \delta_n)$ and $\cos(\delta_k - \delta_n)$.

For most typical operating conditions, the difference angles of voltage phasors at two buses connected by a power line is less than 10-15 degrees. Therefore, equation (3.7) can be written as (3.9)

$$P_k = |V_k| \sum_{n=1}^{N} |V_n| [G_{kn} + B_{kn}(\delta_k - \delta_n)]$$
$$Q_k = |V_k| \sum_{n=1}^{N} |V_n| [G_{kn}(\delta_k - \delta_n) - B_{kn}] \quad (3.9)$$

After eliminating the trigonometric operations, we try to remove the multiplication operations between voltage variables in active and reactive power equations.

First, the reactive power formula mentioned in equation (3.9) can be rewritten as equation (3.10)

$$Q_k = |V_k|^2 (G_{kk}(\delta_k - \delta_n) - B_{kk}) + \sum_{\substack{n=1 \\ n\neq k}}^{N} |V_k|\,|V_n|\,[G_{kn}(\delta_k - \delta_n) - B_{kn}] \tag{3.10}$$

The imaginary part of the Y_{Bus} elements can be written as: $B_{kk} = b_k + \sum_{\substack{n=1 \\ n\neq k}}^{N} b_{kn}$ and $B_{kn} = -b_{kn}$, where b_k is the shunt capacitors/reactors at bus k. In addition, we have $G_{kn} = -g_{kn}$.

Finally reactive power can be presented by (3.11):

$$\begin{aligned} Q_k &= -|V_k|^2 b_k - \sum_{\substack{n=1 \\ n\neq k}}^{N} \left(|V_k|^2 b_{kn} + |V_k|\,|V_n|\,[g_{kn}(\delta_k - \delta_n) - b_{kn}]\right) \\ &= -|V_k|^2 b_k - \sum_{\substack{n=1 \\ n\neq k}}^{N} \left(|V_k|^2 b_{kn} + |V_k|\,|V_n|\,g_{kn}(\delta_k - \delta_n) - |V_k|\,|V_n|\,b_{kn}\right) \\ &= -|V_k|^2 b_k - \sum_{\substack{n=1 \\ n\neq k}}^{N} (|V_k|\,b_{kn}(|V_k| - |V_n|) + |V_k|\,|V_n|\,g_{kn}(\delta_k - \delta_n)) \end{aligned} \tag{3.11}$$

In a per-unit system, the numerical values of voltage magnitudes $|V_n|$ and $|V_k|$ are very close to 1.0. In fact, the voltage magnitudes are usually between 0.95 and 1.05. In addition, We can consider a reasonable approximation for all product terms ($|V_k|\,|V_n|$); thus, this term is almost $1.0pu$. It is worth mentioning that this is only an approximation and it is not an assumption. Therefore, we do not consider a flat voltage profile, and voltage magnitude is not assumed to equal $1.0pu$

However, the difference between voltage variables ($|V_k| - |V_n|$) cannot be neglected. Based on this assumption, equation (3.10) can be written as

$$Q_k = -b_k - \sum_{\substack{n=1 \\ n\neq k}}^{N} (b_{kn}(|V_k| - |V_n|) + g_{kn}(\delta_k - \delta_n)) \tag{3.12}$$

Now, the active power equation can be converted to a linear one based on the same approximation. The active power equation in (3.9) can be written as equation (3.13). Equations (3.14) and (3.15)

can be obtained by substituting the equivalent of G_{kn} and B_{kn}.

$$P_k = |V_k|^2 (G_{kk} + B_{kk} (\delta_k - \delta_k)) + \sum_{\substack{n=1 \\ n \neq k}}^{N} |V_k| |V_n| [G_{kn} + B_{kn}(\delta_k - \delta_n)] \tag{3.13}$$

$$P_k = |V_k|^2 \sum_{\substack{n=1 \\ n \neq k}}^{N} g_{kn} + \sum_{\substack{n=1 \\ n \neq k}}^{N} |V_k| |V_n| [-g_{kn} - b_{kn}(\delta_k - \delta_n)] \tag{3.14}$$

$$P_k = \sum_{\substack{n=1 \\ n \neq k}}^{N} |V_k| g_{kn}(|V_k| - |V_n|) - |V_k| |V_n| b_{kn}(\delta_k - \delta_n) \tag{3.15}$$

Similar to reactive power, we can simplify equation (3.15) by considering $|V_k|$ and its product terms, *i.e.,* $|V_k| |V_n|$ as $1.0pu$. Then we have:

$$P_k = \sum_{\substack{n=1 \\ n \neq k}}^{N} g_{kn}(|V_k| - |V_n|) - b_{kn}(\delta_k - \delta_n) \tag{3.16}$$

If we put both the reactive and active equations together:

$$P_k = \sum_{\substack{n=1 \\ n \neq k}}^{N} [g_{kn}(|V_k| - |V_n|) - b_{kn}(\delta_k - \delta_n)] \tag{3.17}$$

$$Q_k = -b_k - \sum_{\substack{n=1 \\ n \neq k}}^{N} [b_{kn}(|V_k| - |V_n|) + g_{kn}(\delta_k - \delta_n)] \tag{3.18}$$

δ_k and V_k can be obtained by (3.17) and (3.18), respectively.

$$\left(\sum_{\substack{n=1 \\ n \neq k}}^{N} g_{kn} \right) |V_k| - \left(\sum_{\substack{n=1 \\ n \neq k}}^{N} b_{kn} \right) \delta_k = P_k + \sum_{\substack{n=1 \\ n \neq k}}^{N} g_{kn} |V_n| - \sum_{\substack{n=1 \\ n \neq k}}^{N} b_{kn} \delta_n \tag{3.19}$$

$$\left(\sum_{\substack{n=1 \\ n \neq k}}^{N} b_{kn} \right) |V_k| + \left(\sum_{\substack{n=1 \\ n \neq k}}^{N} g_{kn} \right) \delta_k = -Q_k - b_k + \sum_{\substack{n=1 \\ n \neq k}}^{N} b_{kn} |V_n| + \sum_{\substack{n=1 \\ n \neq k}}^{N} g_{kn} \delta_n \tag{3.20}$$

3.5 Distributed AC Power Flow

Graph theory provides us with the capability to model the various agents' relationships in the grid through undirected/directed graphs denoted by $G(\bar{\vartheta}, \psi)$. The agents are introduced by $\bar{\vartheta} = \{\vartheta_1, \vartheta_2, ..., \vartheta_n\}$ and their interactions are designated by a set of edges i.e., $\psi \subseteq \vartheta \times \vartheta$. The directed edges $\vec{\omega_{ij}} = (\vartheta_i, \vartheta_j)$ and $\omega_{ij} = (\vartheta_i, \vartheta_j)$ show one-way and two-way information transmission between two separate agents (agent i and agent j). The adjacency matrix is used to represent the communication topology of a grid. In this chapter, a two-way communication channel is considered to model interaction between two adjacent buses. Thus, the adjacency matrix, denoted by $A = \{[a_{ij}] \, | a_{ij} \in \mathcal{R}^{\mathcal{P}\times\mathcal{P}}\}$, of an undirected graph G is symmetric. The entry a_{ij} of an adjacency matrix is a positive value if $\omega_{ij} \in \psi$ and $a_{ij} = 0$ for $\omega_{ij} \notin \psi$. Otherwise, the entry a_{ii} is assumed to be zero. The second matrix is Laplacian matrix $L = \{[l_{ij}] \, | l_{ij} \in \mathcal{R}^{\mathcal{P}\times\mathcal{P}}\}$ in which entry $l_{ii} = \sum_j a_{ij}$ and $l_{ij} = -a_{ij}$ for $i \neq j$.

A distributed approach is applied to the power system with the help of the linearized power flow formulas. This distributed approach is based on concepts presented by [73, 74]. Some pieces of information are shared among agents in the power system network to have them reach a consensus, *i.e.*, power balance. The admittance matrix (Y_{Bus}) of a power system surprisingly corresponds to this Laplacian matrix. Thus, the elements of this matrix can be used as the elements of the Laplacian matrix to model the data transmission network.

Equation (3.21) is used as a distributed protocol for this chapter. x_i shows the state of the $i-th$ agent in a network. Agent i can receive agent j's information or share its own information with agent j, as it has a communication channel with it, *i.e.*, $a_{ij} \neq 0$.

$$x_i(k+1) = \sum_j a_{ij} x_j(k) \tag{3.21}$$

All a_{ij} are defined based on the real and imaginary parts of elements of Y_{Bus} to exchange voltage magnitudes and phase angles among agents. It is important to mention that each agent shares information only with its neighbors. In other words, the communication network is defined based

on the power system topology because the Laplacian matrix corresponds to admittance matrix. Let us rewrite equations (3.19) and (3.20):

$$G_k \left|V_k\right| - B_k \delta_k = P_k + V'_{G_k} - \delta'_{G_k} \tag{3.22}$$

$$B_k \left|V_k\right| + G_k \delta_k = -Q_k - b_k + V'_{B_k} + \delta'_{B_k} \tag{3.23}$$

where G and B are constant values for the $k-th$ bus and are obtained by equation (3.24) :

$$G_k = \sum_{\substack{n=1 \\ n \neq k}}^{N} g_{kn}, \quad B_k = \sum_{\substack{n=1 \\ n \neq k}}^{N} b_{kn} \tag{3.24}$$

V'_{G_k} and V'_{B_k} are so-called shadow voltages. They are the shadows, of adjacent buses' voltages, cast on the $k-th$ bus. V'_{G_k} and V'_{B_k} are cast by the conductance and susceptance of the power line, respectively, connected to the $k-th$ bus.

$$V'_{G_k} = \sum_{\substack{n=1 \\ n \neq k}}^{N} g_{kn} \left|V_n\right|, \quad V'_{B_k} = \sum_{\substack{n=1 \\ n \neq k}}^{N} b_{kn} \left|V_n\right| \tag{3.25}$$

There are the same definitions for δ'_{G_k} and δ'_{B_k}, both of which are shadow phase angles of adjacent buses' phase angles on the $k-th$ bus.

Equation (3.26) shows the related formulas:

$$\delta'_{G_k} = \sum_{\substack{n=1 \\ n \neq k}}^{N} b_{kn} \delta_n, \quad \delta'_{B_k} = \sum_{\substack{n=1 \\ n \neq k}}^{N} g_{kn} \delta_n \tag{3.26}$$

Equation (3.22)-(3.26) are based on the distributed protocol previously presented by equation (3.21). They guarantee that each agent only needs the voltage and phase angle values of its neighbors. Figure (3.2) clearly shows data sharing based on the provided protocol.

In addition, the closed-form of $\left|V_k\right|$ and δ_k for the $k-th$ bus can be shown by equations (3.27) and

(3.28), where $C = P_k + V'_{G_k} - \delta'_{G_k}$ and $D = -Q_k - b_k + V'_{B_k} + \delta'_{B_k}$.

$$|V_k| = \frac{CG_k + DB_k}{G_k^2 + B_k^2} \tag{3.27}$$

$$\delta_k = \frac{DG_k - CB_k}{G_k^2 + B_k^2} \tag{3.28}$$

In summary, G_k, B_k, P_k, Q_k are known, constant and private information for each bus and not necessary to be shared. It is worth mentioning that G_k and B_k are from lines connected to the $k-th$ bus. The agents do not need to access the information of the entire system configuration. The only information that needs to be exchanged between the buses are V and δ of adjacent buses. In other words, if an agent connects through one line to the distribution system it will access information through a point of common coupling (PCC).

3.6 Performance Evaluation

In this section, three case studies are presented to assess the performance of the proposed distributed AC power flow. All software simulations are conducted in the MATLAB 2017a environment on an ordinary desktop PC with an Intel Core(TM)i7 CPU @ 2.13 GHz, 8-GB RAM memory.

In the first case study, we provide a numerical example to evaluate the algorithm performance from accuracy prospective in a relatively small-scale system (five-buses). The numerical results are compared with typical AC power flow, linearized AC power flow and DC power flow as the benchmark results.

In the second case study, we tested the changes in load level to see how distributed AC power flow copes with real-time changes in load.

In the third case study, a larger system (texas 2000-buses) is considered to demonstrate the scalability of proposed the AC power flow.

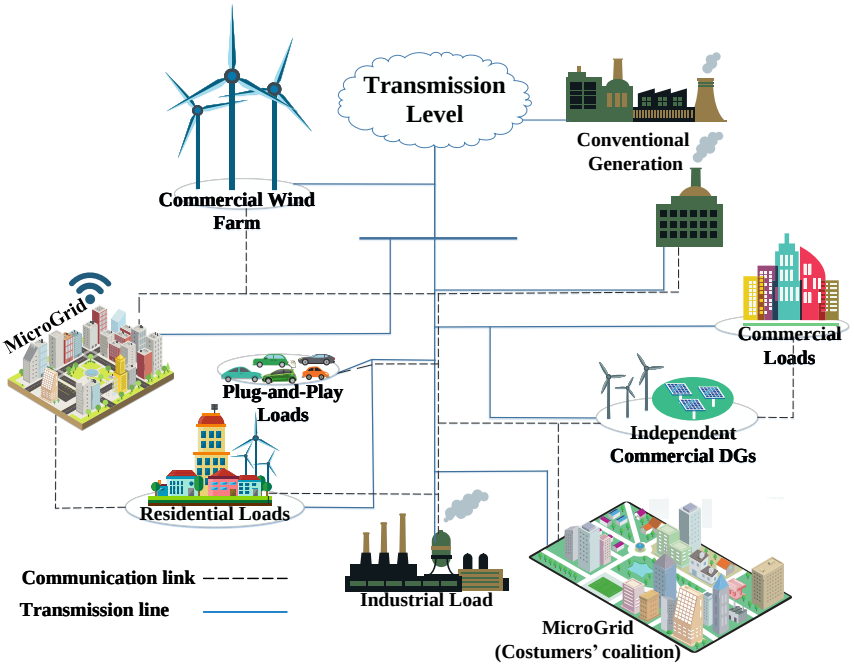

Figure 3.2: Demonstration of the communication network for the applied distributed method

3.6.1 Accuracy Analysis

In this section, a numerical proof for the accuracy analysis of both the proposed linearized power flow and distributed protocol are provided. A sample power system is selected from the power flow example of the PowerWorld software [1]. Figure (3.3) shows a five-buses system, including two generators, transformers and loads. The elements of Y_{Bus} are: $Y(1,1) = 13.73 - j49.72$, $Y(1,5) = -3.73 + j49.72$, $Y(2,2) = 2.68 - j28.46$, $Y(2,4) = -0.89 + j9.92$, $Y(2,5) = -1.79 + j19.84$, $Y(3,3) = 7.46 - j99.44$, $Y(3,4) = -7.46 + j99.44$, $Y(4,4) = 11.92 - j147.96$, $Y(4,5) = -3.57 + j39.68$, $Y(5,5) = 9.09 - j108.58$.

In addition, Table (3.1) provides injected active and reactive powers at each bus of five-buses system. Buses 1 and 3 are the slack and PV buses of the system, respectively. The desired voltage for the slack bus and PV bus are $1pu$ and $1.05pu$, respectively.

Table (3.2) shows a comprehensive comparison between AC power flow (ACPF), linearized AC power flow (L-ACPF), DC power flow (DCPF) and the proposed distributed AC power flow (D-ACPF). As can clearly be seen, the results of the proposed linearized AC power flow are much

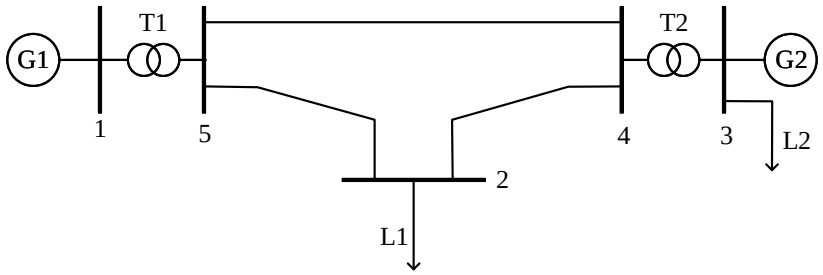

Figure 3.3: Five-bus power system

Table 3.1: Injected active and reactive power of each bus

Bus	P_G MW	P_L MW	Q_G MVar	Q_L MVar
1	Slack	0	Slack	0
2	0	800	0	280
3	520	80	PV	40
4	0	0	0	0
5	0	0	0	0

more precise than those of the typical DCPF. The voltage profile of L-ACPF is no longer flat as it is in DCPF because both the active and reactive powers' equations are incorporated into the power flow formulas. However, voltages of L-ACPF are slightly different from those of conventional AC power flow due to some approximations used for the linearization of non-linear AC power flow.

Table 3.2: Comparison of ACPF, L-ACPF, D-ACPF

Bus	i	1	2	3	4	5
ACPF	V pu	1.000	0.834	1.050	1.019	0.974
	δ deg	0.00	-22.41	-0.60	-2.83	-4.55
L-ACPF	V pu	1.00	0.815	1.050	1.004	0.963
	δ deg	0.00	-19.0686	0.2978	-2.1682	-4.2144
DCPF	V pu	1.00	1.00	1.00	1.00	1.00
	δ deg	0.00	-18.6948	0.5238	-1.9972	-4.1253
D-ACPF	V pu	1.000	0.816	1.050	1.004	0.963
	δ deg	0.00	-19.0812	0.3384	-2.1654	-4.2340

In addition, phase angles of L-ACPF are closer to that of ACPF. Therefore, L-ACPF can reach more accurate results with lighter mathematical calculation. Furthermore, the proposed D-ACPF has the appropriate results that are more precise than those of DCPF and are very close to those

of ACPF and L-ACPF. The solution mismatch between the distributed AC power flow (D-ACPF) and centralized AC power flow (ACPF) methods is less than $0.95\,\%$ and $1.95\,\%$ of the average for voltages and phase angles, respectively.

3.6.2 Dynamic Performance Test

As mentioned earlier, AC power flow imposes a heavy computational load on the system. Continuous monitoring of a large system is one of the technical issues raised by AC power flow. D-ACPF, however, shares computational load among various agents; therefore, continuous running of AC power flow is theoretically possible meaning the results of D-ACPF can follow loads variations.

In the second case study, the dynamic performance of D-ACPF is studied by intentional changes in the level of demand in PQ buses. The active demand (P_L) and reactive demand (Q_L) are suddenly changed from 800 MW and 280 MVAR to 280 MW and 120 MVAR, respectively. The goal of this test is to indicate that D-ACPF easily follows the change of load and calculates AC power flow based on the new demand level. As can be see in Figure. 3.4, D-ACPF can carry out real-time power flow based on real demand profile. Thus, D-ACPF can be a very effective tool for system operation and control because it can easily provide operators and agents with real-time AC power flow results.

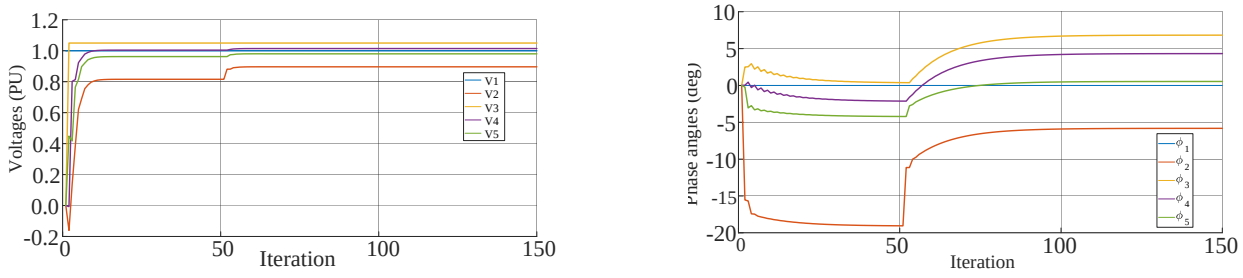

(a) (b)

Figure 3.4: Dynamic performance test for voltage and phase angle (five Buses)

3.6.3 Scalability Test (37 and 2000-bus System)

Scalability testing evaluates the performance of an algorithm in the case of a higher number of agents to measure how much it can be scaled up. Sometimes, new algorithms work very well with

a relatively small-scale system. However, they may not be able to cope with a larger system because of the heavier computations, accumulated error and more uncertainties.

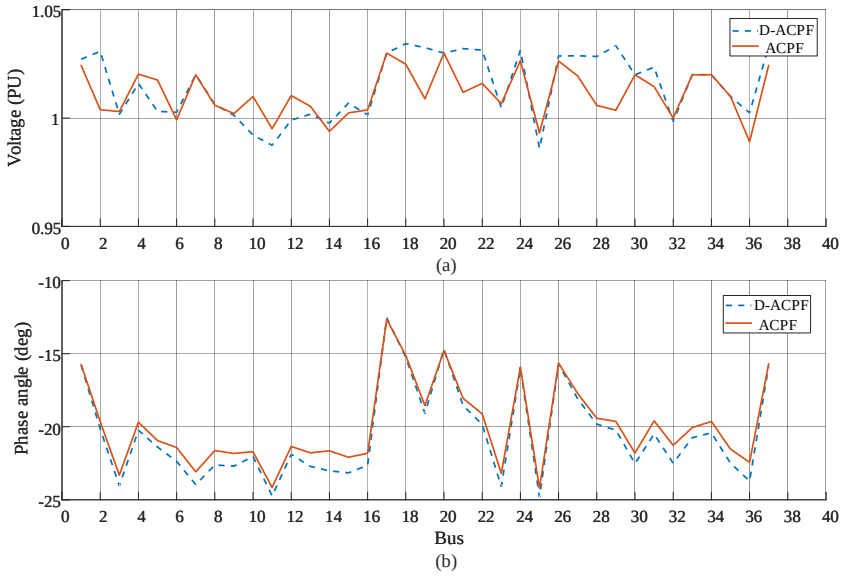

Figure 3.5: 37-bus power system

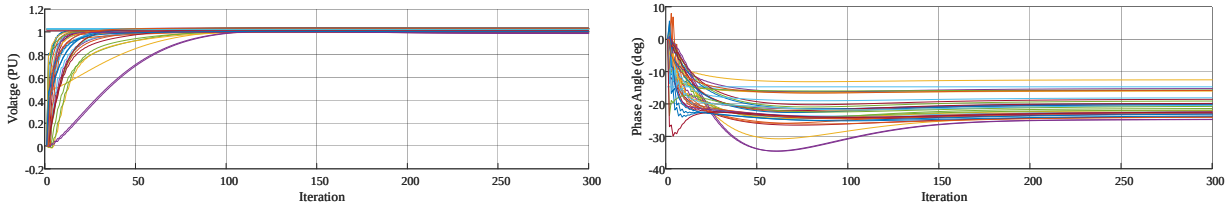

(a) (b)

Figure 3.6: Buses voltage and phase angle convergence of 37-bus power system

In this chapter, the investigation of scalability is carried out by a 37-bus IEEE test system and a 2000-bus Texas synthetic system. IEEE test system includes 9 generators, 26 loads, 8 shunt capacitors, 43 power lines and 14 transformers. Detailed information can be found in Chapter 6 of [1]. For this system, we also examine accuracy. Figure (3.5) shows the voltage and phase angle profile of this system. As can be seen, D-ACPF can meet the benchmark criteria based on ACPF because its calculated voltages and phase angles are very close to those of AC power flow. The solution mismatch of the power flow results between the distributed AC power flow (D-ACPF) and

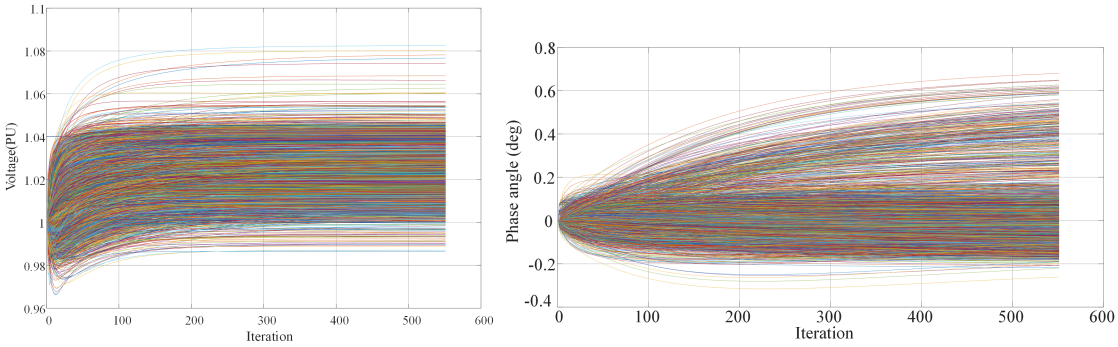

(a) (b)

Figure 3.7: Buses voltage and phase angle convergence of 2000-bus power system

centralized AC power flow (ACPF) methods is $0.86\,\%$ and $2.66\,\%$ of the average for the voltage and phase angle profile, respectively. Texas synthetic system, which is built from public information and a statistical analysis of real power systems, includes 2007 buses, 282 generators, 1417 loads, 41 shunt capacitors, 2481 lines and 562 transformers. Figure. 3.7 shows the convergence of the results for this huge system. As can be seen, both voltage amplitude and voltage angle successfully converged. The simulation results of this test and the small mismatch between results of D-ACPF and those of typical AC power flow demonstrate that D-ACPF can be an effective replacement for a typical AC power flow in the case of scalability.

3.7 Conclusions

In this chapter, we proposed a distributed approach (D-ACPF) based on a linearized AC power flow. The distributed method can easily be applied to a power system based on the distributed protocol and can benefit from the accuracy of L-ACPF. The proposed L-ACPF provides us with a simple power flow formulation that is much more precise than that of DCPF. The simulation results shows that regular AC power flow can be replaced by the proposed distributed AC power flow. Three different simulation tests are provided to confirm accuracy, dynamic performance and scalability of the proposed distributed AC power flow. The proposed D-ACPF can be applied to other studies of power systems, as well, such as load shedding and demand response.

CHAPTER 4

Distributed Optimal Power Flow Algorithm for DC Systems

4.1 Introduction

The optimal power flow problem over direct current (DC) grids is to minimize the cost of active power generation considering all power flow equations, the maximum capacitance of the lines, and voltage limited boundaries of all the buses. It is one of the famous non-convex problems in the power system area. In this chapter, a new distributed consensus-based algorithm is proposed for solving optimal power flow for DC distribution systems. As this algorithm is based on semi-definite relaxation (SDR), a mathematical proof is provided to show the exactness of the SDR relaxation technique. Then, it is demonstrated that the proposed distributed method converges to the global optimal point while satisfying all system constraints. A detailed analysis of the proposed algorithm is provided by applying it to a modified version of the IEEE-30 bus system. Finally, this method is applied to different DC power flow case studies, such as 14, 30, 57, 118, 200-bus systems, to provide a strong performance assessment. The simulation results, when compared with the benchmark, are quite promising.

4.2 Literature Review

Direct current (DC) grid systems, invented by Thomas Edison, have a history as long as that of alternating current (AC) grids, invented by Nikola Tesla. In fact, the first power transmission system was operated under DC power, as it was the standard in the United States during the early years of electricity. But soon it was figured out that the DC transmission system is not efficient for long distance energy delivery because it is not easily converted to different voltage levels, due to lacking technology. Despite Edison's unsuccessful endeavor to disgrace the AC system, electricity

systems were mostly dominated by AC power in the 90s [114]. Today, the electricity grid is mainly powered by alternating current, but distribution part of the power systems is experiencing serious challenges due to the integration of distributed generations and storage units into the power grid.

While the electrical energy is widely distributed among end-users by alternating current (AC) grids, most of the appliances used in the consumer side are operated by DC power [115]. Moreover, many types of distributed generators, such as renewable resources generate DC electrical energy and storage units are charged and discharged with DC power. This unfortunate situation forces two or more steps of DC/AC and AC/DC conversions, which dramatically reduce energy efficiency. Therefore, in the near future, distribution systems will no longer be operated the way they used to be.

A DC distribution system, in place of a conventional AC distribution system, can smoothly and efficiently interact with loads, distributed generations and storage units while eliminating any unnecessary DC/AC and AC/DC conversions [116, 117]. One of the earliest DC distribution systems, as an effective replacement for an AC power distribution system, has been successfully brought into full operation in electric propulsion ships [118]. The successful applications of DC grids are currently restricted to data centers, telecommunication, buildings, and ships. However, DC grids have enough potential to be employed in the distribution level of the power system due to developments in power electronics, renewable energy, and storage systems [119]. The overall advantages of DC distribution systems will be higher efficiency, easier integration of DC components, no need for frequency stabilization, etc.

Optimal power flow (OPF), as a fundamental optimization problem in power systems [120], determines a cost-effective dispatch of all energy resources supporting the requested demand in a system while satisfying all local/global constraints at the same time [121, 122]. With regard to the emergence of DC distribution systems, OPF on DC grids is drawing much more attention now because of the unique features of DC grids such as, direct P-V coupling. In other words, due to the lack of reactive power, there is no way to locally regulate voltage. Generally speaking, in an OPF problem over AC or DC grids, an economic dispatch (ED) problem [28] considering all power flow

equations, the maximum capacitance of the lines, and voltage limited boundaries of all the buses, is solved. In the following paragraphs of the literature review, OPF problems and various solving methods are discussed for both AC and DC power systems in two main categories, centralized and distributed methods.

Centralized AC OPF methods have been studied since the early 1960s, when the typical OPF problem was first formulated [123]. In a centralized method, all components directly communicate with a central operator, *e.g.* SCADA. This center should be able to monitor, gather and analyze real-time data and provide all components with appropriate control signals while it records events in a log file. Many methods, including interior point, quadratic programming, Lagrangian relaxation, gradient methods, mixed integer programming, and Newton-based methods, have been reviewed and classified several times [124, 125]. S. Galvani *et al*. propose a probabilistic optimal power flow (P-OPF) in order to maximize the predictability of a system while minimizing the cost of total power generation considering the power generation of its generators, tap changer position of its regulator transformers, voltage magnitude at its generators and reactive power compensation sources as the control variables [126]. In [127], a novel method, as a general solution framework, is proposed to derive an approximate optimal solution satisfying the rank-one constraint for the SDP relaxation of the AC OPF problem. Z. Yang *et al.* introduce a new OPF method for hybrid AC-DC grids using a linear approximation method for the power flow equations to overcome the convexity of the problem's nature [128]. W. A. Bukhsh *et al.* cover an interesting and challenging topic, the possible existence of local optima, in their paper. They show that standard local optimization techniques can converge to these local optima [129]. Chance-constrained AC OPF can handle stochastic OPF, ensuring secure system operation despite inevitable increasing uncertainties [130, 131]. [132] offers a real-time AC-OPF based on a quasi-Newton algorithm to provide a fast control, overcoming randomness and fluctuations in the power system.

As discussed earlier, DC distribution grids are becoming more important as more DC energy resources, storage units and loads are connected to low voltage grids. However, intensive study of OPF and PF has not been carried out for DC systems because AC systems have been primarily the

center of research interest since the emergence of the power grids. K. Fleischer *et al*. proposed one of the earliest DC distribution analyses, including PF and short circuit studies [133]. They discussed system modeling including sources, loads and power lines for both PF and short circuit. C. Jayaratha *et al*. reviewed the efficiency of three different LF methods to analyze low voltage DC grids energized by photo-voltaic (PV) panels [134]. L. Mackay conducted extensive research on the modeling of DC grids and their components, fault analysis/detection and OPF analysis in unbalanced bipolar DC distribution grids [119]. L. Gan *et al*. applied a second-order cone programming (SOCP) relaxation to the OPF problem and provide proof of the exactness of this relaxation under two assumptions: unlimited upper bounds of the bus voltages or uniformity of voltage the upper bounds when the power injection lower bounds are negative [135]. J. Li *et al*. proposed SOC relaxation of the OPF problem, as an extension of [135], in stand-alone direct current micro-grids [136]. An OPF strategy and voltage regulation control for DC microgrids based on hierarchical control is proposed in [137] to minimize the transmission loss in a generic dc microgrid. An OPF study of DC distribution grids with network power loss and degree of voltage distribution imbalance as objective functions is done in [138]. This research considers the fact that an increase of distributed energy may affect the grid's stable operation and economic indicators. An exact OPF study, formulated in terms of voltage and current, is conducted for bipolar DC distribution grids with asymmetric loading in [139], which shows the LMP defers between the different polarities depending on the asymmetric loading and congestion.

Due to the high penetration of distributed energy sources, pervasiveness of storage units, required plug-and-play characteristic of loads, and inevitable dynamic topology of the power grid, centralized algorithms are no longer effective [45,47]. Consequently, distributed OPF methods have been offered by researchers because this type of approaches is able to overcome centralized approaches' drawbacks. In distributed methods, agents only need to locally connect with their immediate neighbor(s). They can control the type of shared information. Thus, it can be ensured that no uncontrolled private information is released to a third party. This advantage provides all agents with an opportunity to participate in a fair and competitive market, without any kind of monopoly or

monopsony [28]. Apart from privacy improvement, the single point of failure will naturally be resolved as there is no need for a center to supervise all agents [76, 140]. Moreever, computational load will no longer affect a central controller as it is spread out over the entire network [141]. The dynamic topology of power systems and plug-and-play functionalities will be requisite features of the future open-access power system, which can easily be supported by distributed algorithms. All of these features make it possible for distributed methods to support high scalability as an urgent need in future power systems. A. Engelmann *et al*. propose an application of the augmented Lagrangian alternating direction inexact Newton (ALADIN) method to distributively solve AC OPF. Their proposed method ensures the locally quadratic convergence of AC-OPF [142]. X. Fang *et al*. propose a new distributed chance-constrained OPF to minimize the cost of overall generation while mitigating wind power uncertainty [143]. To the best of our knowledge, there exist only a few studies on distributed control methods for OPF of DC distribution networks. A distributed solution for the OPF problem in DC distribution grids, as an extension of the distributed consensus and innovations approach introduced in [144], is presented in [145]. E. Sindi *et al*. applied a distributed control strategy based on recursive algorithms to address line loss reduction, balancing feeder currents, and voltage profile management in a DC microgrid [146]. N. Meyer-Huebner *et al*. believe that future power grids will be hybrid grids consisting of the conventional AC transmission system partially combined with high voltage DC grids. Therefore, they formulate a separable AC-DC OPF problem, which could distributively be resolved and is suitable for such hybrid systems [147].

In this chapter, we start by reviewing a semi-definite relaxation (SDR) technique, which is known to be a successful method as of the last decade. Then we provide a particular and simple proof to demonstrate its exactness for OPF of DC grids without considering assumptions such as in [136] and [135]. Afterward, we introduce our new distributed consensus-based method for DC distribution systems, which considers all line constraints and voltage limitations. Each agent (*i.e.,* bus) only shares information with its one or more immediate neighbors. The proposed method will be supported by comprehensive performance evaluations and a mathematical proof, ensuring global optimality. The main contributions/features of our work are as follows:

- A simple mathematical proof has been provided to show the exactness of the semi-definite relaxation (SDR) technique.
- A fully distributed consensus-based method for DC distribution systems is proposed. The privacy of each component and the entire system is improved due to very limited sharing of information.
- A single point of failure would not be an area of concern, as there is no need for any kind of aggregator or central controller.
- The proposed approach is suitable for both mesh and radial DC grids.

The structure of the rest of this chapter is organized as follows: Section 5.3 formulates a comprehensive OPF problem as a global objective function, considering cost functions and constraints. Section 4.4 investigates the SDR technique and provides proof of its exactness. Section 5.4 introduces a distributed consensus-based algorithm with a brief review of graph theory and the required optimality analysis. Section 2.5 demonstrates simulation results for various test systems. Finally, section 2.6 summarizes this chapter and presents the concluding remarks.

4.3 Optimal Power Flow Formulation for DC Systems

In this section, the OPF problem for DC grids, including generator cost functions and all equality and inequality constraints, are formulated. Generators are mathematically represented by a strictly increasing cost functions shown in (4.1).

$$\mathcal{C}_k(P_{\mathcal{G}_k}) = \alpha_k P_{\mathcal{G}_k}^2 + \beta_k P_{\mathcal{G}_k} + \gamma_k, \quad \forall k \in \mathbb{N}_{\mathcal{G}} \tag{4.1}$$

where $\alpha\,[\$/(\text{kW})^2\text{h}] \geq 0$, $\beta\,[\$/\text{kWh}] \geq 0$, $\gamma\,[\$/\text{h}] \geq 0$ are coefficients that customize the cost function for each DC generator and are different for various DC energy resources. In general, it represents gas turbines or diesel generators if the coefficients are all non-zero or it may represent any linear function or constant function if $\alpha = 0$, $\beta \geq 0$, $\gamma \geq 0$ or $\alpha = 0$, $\beta = 0$, $\gamma \geq 0$ respectively. In

this chapter, we assume that cost functions are always quadratic functions (i.e., $\alpha > 0$) in order to have a universal distributed algorithm for all types of such functions. We may consider small value for α to have cost functions close to the corresponding linear functions. $\mathrm{P}_{\mathcal{G}_k}$ [kW] is the amount of power generated by the k^{th} DC generator, and $\mathbb{N}_{\mathcal{G}}$ shows a set of buses associated with a generator.

The constraints of the OPF problem can be divided into two main groups, local constraints and global constraints. Nodal KCL for the power flow equations, the buses' voltage amplitude limitations, and the generation maximum and minimum capacity are among the local constraints. In addition, load balance as an equality constraint is among the global constraints.

As shown in (4.2), the total cost function $\mathfrak{F}_{\mathfrak{T}}$ (where $\overrightarrow{P}_{\mathcal{G}} = \left[P_{\mathcal{G}_1}, P_{\mathcal{G}_2}, \cdots, P_{\mathcal{G}_N}\right]^T$) is a summation of all the generators' cost functions. Equation (4.3) indicates a box constraint for the power capacity of each generator, where $P_{\mathcal{G}_k}^{max}$ indicates the maximum possible generation level. The voltage magnitude boundary is shown by (4.7), which makes the optimization problem a non-convex problem. Pre-set values of the slack bus are defined by (4.8). Equation (4.4) shows the power balance between generation and consumption. The first statement on the right side of (4.4) shows the total load installed on the generator and load buses, where $\mathbb{N}_{\mathcal{L}}$ indicates the load-only buses. The second statement on the right side of (4.4) represents the summation of the estimated active power loss of each bus, where $\mathbb{N}_{\mathcal{S}}$ defines the set of all buses, including generator, load, slack and connection buses. $\mathbb{N}_{\mathcal{E}}$ shows a set of distribution lines where each line (l) is determined by an un-directed edge (k, n) and is located between the k^{th} and n^{th} buses.

$$Minimize \quad \mathfrak{F}_{\mathfrak{T}}\left(\overrightarrow{P}_{\mathcal{G}}\right) = \sum_{\forall k \in \mathbb{N}_{\mathcal{G}}}^{N} \mathcal{C}_k(P_{\mathcal{G}_k}) \tag{4.2}$$

$$0 \leq P_{\mathcal{G}_k} \leq P_{\mathcal{G}_k}^{max}, \quad \forall k \in \mathbb{N}_{\mathcal{G}} \tag{4.3}$$

$$\sum_{\forall k \in \mathbb{N}_{\mathcal{G}}}^{N} P_{\mathcal{G}_k} = \sum_{\forall k \in (\mathbb{N}_{\mathcal{G}} + \mathbb{N}_{\mathcal{L}})}^{N} P_{\mathcal{L}_k} + \sum_{\forall (k,n) \in \mathbb{N}_{\mathcal{E}}}^{N} P_{Loss_{kn}} \tag{4.4}$$

$$P_{net_k} = \begin{cases} P_{\mathcal{G}_k} - P_{\mathcal{L}_k} & , \quad \forall k \in (\mathbb{N}_{\mathcal{G}} + \mathbb{N}_{\mathcal{L}}) \\ 0 & , \quad \forall k \notin (\mathbb{N}_{\mathcal{G}} + \mathbb{N}_{\mathcal{L}}) \end{cases} \tag{4.5}$$

$$P_{net_k} = \sum_{\forall n \in (\mathbb{N}_{\mathcal{S}} - \{k\})}^{N} P_{kn}, \ \forall k \in \mathbb{N}_{\mathcal{S}} \tag{4.6}$$

$$V_k^{min} \leq V_k \leq V_k^{max}, \quad \forall k \in \mathbb{N}_{\mathcal{G}} \tag{4.7}$$

$$V_{k_{slack}} = 1, \quad k_{slack} \in \mathbb{N}_{\mathcal{G}} \tag{4.8}$$

$$P_{kn} = G_{kn}(V_k V_k - V_k V_n), \ \forall k, n \in \mathbb{N}_{\mathcal{S}}, \ k \neq n \tag{4.9}$$

$$P_{kn} \leq P_{kn}^{max}, \quad \forall (k, n) \in \mathbb{N}_{\mathcal{E}} \tag{4.10}$$

The injected net active powers are shown by P_{net_k} at the k^{th} bus. G_{kn} indicates the conductance of the line between k^{th} and n^{th} buses. The line flow constraint is formulated by (4.10), where P_{kn}^{max} indicates the maximum power flow through the l^{th} line located between the k^{th} and n^{th} buses.

4.4 Semi-definite Relaxation (SDR)

In SDR, we first determine all sources of non-convexity in a given optimization problem to identify the fundamental difficulties spread through out the problem. Then we transform non-convexity into a specific constraint (*i.e.,* rank constraint) and eventually drop that constraint [148]. Afterwards, the newly convexified problem will be investigated to determine whether it is exact or not.

The non-convexity in the OPF problem for DC grids (5.2)-(4.10) is only linked back to the product term of V_k and V_n. However, all equations that have voltage parameters can be written as linear combinations. Thus, by introducing a new variable $W_{kn} = V_k V_n$ or $W_{nk} = V_n V_k$, we obtain the following equivalent formulation of the above optimization problem by only rewriting our equations:

$$Minimize \quad \mathfrak{F}_{\mathfrak{T}} \left(\overrightarrow{P_{\mathcal{G}}} \right)$$

s.t. (5.3), (5.6), (5.7), (5.9), and (4.10)

$$W_{kn} = W_{nk} = V_k V_n, \quad \forall k \in \mathbb{N}_{\mathcal{G}},\ \forall (k,n) \in \mathbb{N}_{\mathcal{E}} \tag{4.11}$$

$$W_{kk}^{min} \leq W_{kk} \leq W_{kk}^{max}, \quad \forall k \in \mathbb{N}_{\mathcal{G}},\ \forall (k,n) \in \mathbb{N}_{\mathcal{E}} \tag{4.12}$$

$$W_{k_{slack}} = 1, \quad k_{slack} \in \mathbb{N}_{\mathcal{G}} \tag{4.13}$$

$$P_{kn} = G_{kn}(W_{kk} - W_{kn}), \quad \forall k \in \mathbb{N}_{\mathcal{G}},\ \forall (k,n) \in \mathbb{N}_{\mathcal{E}} \tag{4.14}$$

$$P_{Loss_{kn}} = G_{kn}(W_{kk} + W_{nn} - 2W_{kn}) \geq 0,\ \forall (k,n) \in \mathbb{N}_{\mathcal{E}} \tag{4.15}$$

As can be seen, only equation (4.11) has the original non-convexity. This substitution ($W_{kn} = V_k V_n$) introduces four new variables for each $l = (k,n)$ line, including W_{kn}, W_{nk}, W_{kk}, and W_{nn}. It is very obvious that $W_{kn} = W_{nk}$. Consequently, two more constraints can be derived and used in place of (4.11).

$$\begin{bmatrix} W_{kk} & W_{kn} \\ W_{kn} & W_{nn} \end{bmatrix} \succcurlyeq 0, \quad \forall (k,n) \in \mathbb{N}_{\mathcal{E}} \tag{4.16}$$

$$rank \begin{bmatrix} W_{kk} & W_{kn} \\ W_{kn} & W_{nn} \end{bmatrix} = 1, \quad \forall (k,n) \in \mathbb{N}_{\mathcal{E}} \tag{4.17}$$

Constraint (4.16), which satisfies $W_{kn}^2 \leq W_{kk} W_{nn}$, $W_{kk} \geq 0$, $W_{nn} \geq 0$, represents **the inside space of a rotated second-order cone** as a feasible area. It is well known that this space obviously is a convex set, as shown in equation (4.18) and figure (4.1a)

$$\left\| \begin{bmatrix} 2W_{kn} \\ W_{kk} - W_{nn} \end{bmatrix} \right\|_2 \leq W_{kk} + W_{nn}, \quad \forall (k,n) \in \mathbb{N}_{\mathcal{E}} \tag{4.18}$$

The rank constraint (4.17) will be satisfied if and only if the lower-left corner element of the reduced row echelon form (rref) in equation (4.19) is zero, which results in $W_{kn}^2 = W_{kk} W_{nn}$. This equality represents the surface of the rotated second-order cone as a non-convex feasible area (plotted in

figure (4.1a)).

$$rref\left(\begin{bmatrix} W_{kk} & W_{kn} \\ W_{kn} & W_{nn} \end{bmatrix}\right) = \begin{bmatrix} 1 & \frac{W_{kn}}{W_{kk}} \\ W_{kn}^2 - & \\ W_{kk}W_{nn} & 0 \end{bmatrix} \tag{4.19}$$

As is demonstrated by constraint (4.15), the optimal solution of OPF must also be on a plane represented by $P_{Loss_{kn}} - G_{kn}(W_{kk} + W_{nn} - 2W_{kn}) = 0,\ \forall(k,n) \in \mathbb{N}_{\mathcal{E}}$. We refer to this plane as the "active loss plane" for each DC line. The intersection of the active loss plane and the rank constraint is depicted by a red parabola curve in figure (4.1a).

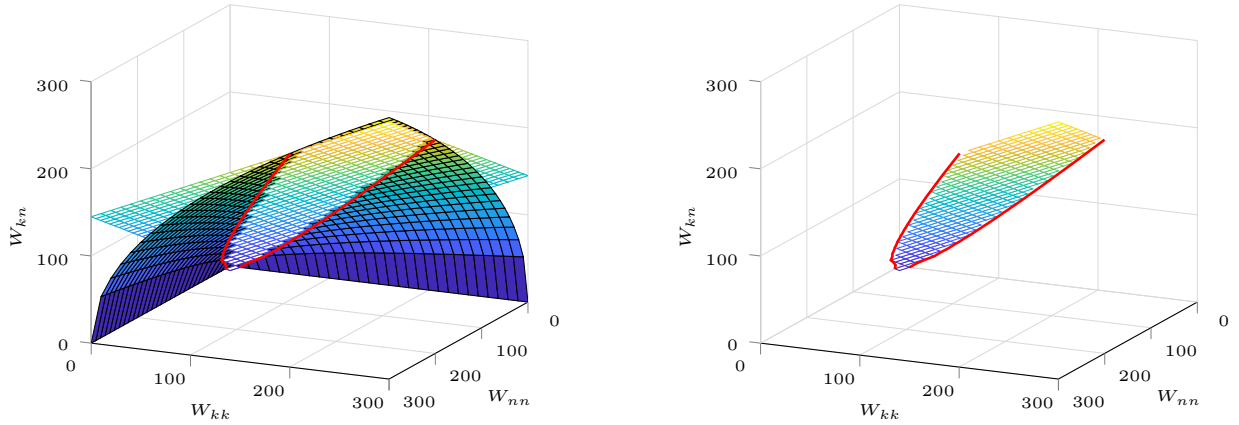

(a) (b)

Figure 4.1: Visual analysis of the problem's feasible area. (a) The intersection of the active loss plane and rank constraint, (b) The convexified feasible area for any set of (W_{kk}, W_{nn}, W_{kn}) , $\forall(k,n) \in \mathbb{N}_{\mathcal{E}}$

It is easy to see that the parabola curve is a non-convex set. Thus, for relaxation, we should consider the inside space of the parabola on the active loss plane, which means the rank constraint should be dropped!

Remark 1. The unique unconstrained minimizer of quadratic cost function is negative (*i.e.*, $^{-\beta_k}/_{2\alpha_k}$), and the generator's output is subject to the box constraints (5.3). Therefore, the quadratic cost functions used in this chapter (5.2) are strictly increasing.

***Assumption**:* We assume that $\pi = [\overrightarrow{P}_{\mathcal{G}}\ W_{kn}\ W_{kk}\ W_{nn}]^T$ is 1) a feasible solution of the relaxed OPF problem and, at the same time, 2) is not a feasible solution of the original OPF problem. In other words, π violates the rank constraint ($W_{kn}^2 \neq W_{kk}W_{nn}$) and exists inside of the parabola (see figure (4.1b)).

***Theorem 1**:* Given the above assumption and the fact that our cost functions are strictly increasing (*Remark* 1), there is always another feasible point on the boundary (the red parabola curve) with the same W_{kk} and W_{nn}, *i.e.,* $\pi' = [\overrightarrow{P}'_{\mathcal{G}}\ W'_{kn}\ W_{kk}\ W_{nn}]^T$ that has a smaller/equal cost relative to $\pi = [\overrightarrow{P}_{\mathcal{G}}\ W_{kn}\ W_{kk}\ W_{nn}]^T$.

***Proof part-I**:* Followed by the assumption, we have $W_{kn}^2 < W_{kk}W_{nn}$ for a feasible point like π. There always exists a positive value like $\varepsilon_{kn} > 0$, such that $W'_{kn} = W_{kn} + \varepsilon_{kn}$ and $(W'_{kn})^2 = W_{kk}W_{nn}$. Using equations (5.7), (5.9), and (4.14), we write the nodal KCL of the power flow equations at π' as:

$$P'_{\mathcal{G}_k} - P_{\mathcal{L}_k} = \sum_{\forall n \in (\mathbb{N}_{\mathcal{S}} - \{k\})}^{N} G_{kn}(W_{kk} - W'_{kn}),\ \forall k \in \mathbb{N}_{\mathcal{S}} \tag{4.20}$$

By substituting $W_{kn} + \varepsilon_{kn}$ for W'_{kn}, the above equation can be re-written as:

$$P'_{\mathcal{G}_k} - P_{\mathcal{L}_k} = \sum_{\forall n \in (\mathbb{N}_{\mathcal{S}} - \{k\})}^{N} G_{kn}(W_{kk} - W_{kn}) - \sum_{\forall n \in (\mathbb{N}_{\mathcal{S}} - \{k\})}^{N} G_{kn}\varepsilon_{kn},\ \forall k \in \mathbb{N}_{\mathcal{S}} \Rightarrow$$

$$P'_{\mathcal{G}_k} - P_{\mathcal{L}_k} = P_{\mathcal{G}_k} - P_{\mathcal{L}_k} - \sum_{\forall n \in (\mathbb{N}_{\mathcal{S}} - \{k\})}^{N} G_{kn}\varepsilon_{kn} \Rightarrow$$

$$P'_{\mathcal{G}_k} = P_{\mathcal{G}_k} - \sum_{\forall n \in (\mathbb{N}_{\mathcal{S}} - \{k\})}^{N} G_{kn}\varepsilon_{kn} \tag{4.21}$$

It is apparent that $P'_{\mathcal{G}_k}$ is less than $P_{\mathcal{G}_k}$ because $G_{kn},\ \varepsilon_{kn} > 0$, thus we finally have:

$$\sum_{\forall k \in \mathbb{N}_{\mathcal{S}}}^{N} P'_{\mathcal{G}_k} < \sum_{\forall k \in \mathbb{N}_{\mathcal{S}}}^{N} P_{\mathcal{G}_k} \tag{4.22}$$

Mathematically, equation (4.22) demonstrates that the total generated power at π' is less than that

at π. According to *Remark 1,* as the total cost functions are strictly increasing in $[0,\ P_{\mathcal{G}}^{max}]$, the value of objective function (5.2) at π' is less than its value at π. This completes *proof part-I.*■

Proof part-II*:* A question arises here: how is the total generation level at π' lower than that at π while the total load is constant? The answer is that the amount of active power loss at $\pi' = [\overrightarrow{P_{\mathcal{G}}'}\ W'_{kn}\ W_{kk}\ W_{nn}]^T$ is less than that at $\pi = [\overrightarrow{P_{\mathcal{G}}}\ W_{kn}\ W_{kk}\ W_{nn}]^T$. Equation (4.23) shows active power loss at π':

$$P'_{Loss_{kn}} = G_{kn}(W_{kk} + W_{nn} - 2W'_{kn}),\ \forall (k,n) \in \mathbb{N}_{\mathcal{E}} \tag{4.23}$$

where $W'_{kn} = W_{kn} + \varepsilon_{kn}$. Then we have

$$P'_{Loss_{kn}} = G_{kn}(W_{kk} + W_{nn} - 2W_{kn}) - 2G_{kn}\varepsilon_{kn} = P_{Loss_{kn}} - 2G_{kn}\varepsilon_{kn}, \quad \forall (k,n) \in \mathbb{N}_{\mathcal{E}} \tag{4.24}$$

It is apparent that $P'_{Loss_{kn}}$ is less than $P_{Loss_{kn}}$ because $G_{kn},\ \varepsilon_{kn} > 0$ and finally

$$\sum_{\forall (k,n) \in \mathbb{N}_{\mathcal{E}}}^{N} P'_{Loss_{kn}} < \sum_{\forall (k,n) \in \mathbb{N}_{\mathcal{E}}}^{N} P_{Loss_{kn}} \tag{4.25}$$

and this completes *proof part-II.*■

4.5 Distributed Consensus-based Algorithm for OPF

A consensus average-based distributed algorithm, which finds the global optimal solution for OPF, is proposed in this section. A brief graph theory shows our assumptions and justifies our model for a communication network. $\mathcal{N}(\mathcal{K}, \xi)$ denotes an un-directed communican interesting methodation network with N connected buses, designated by $\mathcal{K} = \{1, 2, \ldots N\}$, and $\mathbb{N}_{\mathcal{E}} \subseteq \mathcal{K} \times \mathcal{K}$, which represents a set of edges. The un-directed edge $e_{kn} = (k, n)$ indicates that buses k and n can share information with each other. This means two agents (*i.e.,* buses) should be able to share information when they are connected by a power line.

The Laplacian matrix $L = D - A = \{[l_{kn}]\,|l_{kn} \in R^{P \times P}\}$, where D is a network degree matrix

and A is an adjacency matrix, is defined by (4.26). The element a_{kn} of the adjacency matrix is non zero ($a_{kn} \neq 0$) or zero ($a_{kn} = 0$) if $\forall e_{kn} \in \mathbb{N}_{\mathcal{E}}$, $\forall e_{kn} \notin \mathbb{N}_{\mathcal{E}}$, respectively. As can be seen, the definition of a Laplacian matrix is very similar to that of admittance matrix; thus, any bus can easily use the *conductance* value of a line that is connected to it.

$$L = \begin{cases} l_{kk} = \sum\limits_{\forall n \in (\mathbb{N}_{\mathcal{S}} - \{k\})} a_{kn} & , \quad \forall k \in \mathbb{N}_{\mathcal{S}} \\ l_{kn} = -a_{kn} & , \quad \forall e_{kn} \in \mathbb{N}_{\mathcal{E}} \\ l_{kn} = 0 & , \quad otherwise \end{cases} \tag{4.26}$$

We assume that the $k-th$ bus *only* accesses its own private information, such as its generator's cost function ($\mathcal{C}_k(P_{\mathcal{G}_k})$), generated active power ($P_{\mathcal{G}_k}$) and its local load ($P_{\mathcal{L}_k}$). Any of these pieces of information could be zero depending on the type of bus, such as PV, PQ or connection buses. Each bus will pick an arbitrary positive value as the initial value of its incremental cost (λ_k). Incremental costs are the only piece of information shared with immediate neighbors to be used as a consensus. Hence, all of the buses finally reach an identical value of λ as a consensus (λ_c) no matter whether problem constraint(s) are binding or not. Equation (4.27) demonstrates the consensus-based distributed protocol, where $\vec{\lambda} = \left\{ [\lambda_1, \lambda_2, ..., \lambda_N]^T \, | \lambda_k \in \mathcal{K} \right\}$ and j is the iteration number for the consensus protocol [74].

$$\begin{aligned} \dot{\vec{\lambda}}^{i,j+1} &= -L\vec{\lambda}^{i,j}, \quad \forall i \\ \vec{\lambda}^{i,j+1} &= \vec{\lambda}^{i,j} + \dot{\vec{\lambda}}^{i,j+1}, \quad \forall i \end{aligned} \tag{4.27}$$

When all buses reach the consensus $\lambda_1^{i,j+1} = \lambda_2^{i,j+1} = ... = \lambda_N^{i,j+1} = \lambda_{c,k}^{i}$, generator buses calculate their active power generation using (4.28). Load buses or other connection buses will consider zero generation, *i.e.*, $P_{\mathcal{G}_k}^{i} = 0$, $\forall k \notin \mathbb{N}_{\mathcal{G}}$.

$$P^i_{\mathcal{G}_k} = \begin{cases} \dfrac{\lambda^i_{c,k} - \beta_k + \eta^i_{st,k}}{2\alpha_k} & , \quad \forall k \in \mathbb{N}_{\mathcal{G}} \\ 0 & , \quad \forall k \notin \mathbb{N}_{\mathcal{G}} \end{cases} \tag{4.28}$$

Then, W_{kn} and W_{kk} for the the next iteration are calculated by (4.29) and (4.30), respectively, where $\rho_W \ll 1$.

$$W^{i+1}_{kn} = W^i_{kn} + \rho_W \left(W^i_{kk} \times W^i_{nn} - \left(W^i_{kn}\right)^2 \right), \quad \forall k \in \mathbb{N}_{\mathcal{S}}, \quad \forall n \in (\mathbb{N}_{\mathcal{S}} - \{k\}) \tag{4.29}$$

$$W^{i+1}_{kk} = (P^i_{\mathcal{G}_k} - P_{\mathcal{L}_k} + \sum_{\forall n \in (\mathbb{N}_{\mathcal{S}} - \{k\})}^{N} G_{kn} W^i_{kn}) \times ({}^{1}\!/_{\sum\limits_{\forall n \in (\mathbb{N}_{\mathcal{S}} - \{k\})}^{N} G_{kn}}) \tag{4.30}$$

Afterward, each bus updates its incremental cost for the next iteration using (4.31), based on the private information and consensus.

$$\lambda^{i+1,j}_k = \lambda^i_{c,k} + \rho_\lambda \left(P^i_{\mathcal{G}_k} - P_{\mathcal{L}_k} - \sum_{\forall n \in (\mathbb{N}_{\mathcal{S}} - \{k\})}^{N} G_{kn} (W^{i+1}_{kk} - W^{i+1}_{kn}) \right), \tag{4.31}$$

Then, all λ_k will be identical ($\left|\lambda^{i+1,j}_k - \lambda^i_{c,k}\right| \to 0$) when nodal KCL is satisfied at each bus, and generators will support the total demand.

In addition, equation (4.32) will be effective when constraint (4.10) of the l^{th} line between the s^{th} and t^{th} buses is binding to make sure that the power flow through the l^{th} line does not violate its maximum rating. In this equation, $\varphi_{st,k}$ shows the sensitivity of the line between s^{th} and t^{th} buses to the power changes at the k^{th} bus and $\rho_\eta \ll 1$.

$$\eta^{i+1}_{st,k} = \eta^i_{st,k} + \rho_\eta \varphi_{st,k} \left(P_{st} - P^{max}_{st} \right) \tag{4.32}$$

Finally, all local and global constraints including the power balance constraint, will be satisfied. It is worth mentioning that

- The only information shared with immediate neighbors is the estimated λ_k, W_{kk}.

- Only the two buses connected at either ends of a line are aware of line conductance (G_{kn}), means, agents do not need to know the entire configuration of the DC grids.
- None of the private/financial information of generators, such as $P_{\mathcal{G}_k}$, α_k, β_k, $P_{\mathcal{L}_k}$ is shared.
- The graph's minimum connectivity is required. Hence, islanded part of the system cannot participate in the distributed protocol.

The optimality and convergence analysis of the proposed distributed algorithm will be discussed in the rest of this section, and it is shown that this protocol converges to the global optimal point of the optimization problem.

4.5.1 Optimality Analysis

In this section, a mathematical discussion is provided for optimality analysis of the above OPF problem considering all constraints, including (5.3), (5.9), (5.7), (5.9), (4.11), (4.12), (4.13), and (4.14).

Remark 2. The relaxed optimization problem presented in this chapter is a convex optimization problem with differentiable objective and constraint functions satisfying Slater's condition, and the KKT conditions provide the necessary and sufficient conditions for optimality.

Remark 3. The incremental cost of each bus, indicating the dual variable of the power balance constraint, should be equal at the optimal point, *i.e*, $\lambda_1 = \lambda_2 =, \dots, = \lambda_N$, whether other constraints are binding or not.

Proposition: Given *Remarks* 2 and 3, a dual gradient method (4.34-4.40) will converge to the global optimal point considering the Lagrangian function provided in (4.33).

Here, it is shown that the solution of the proposed distributed consensus algorithm is a global

optimal solution of (5.2) if it satisfies the following KKT conditions.

$$L(\vec{P}_{\mathcal{G}}, \lambda, \mu, \zeta, \nu, \vartheta, \eta) = \sum_{\forall k \in \mathbb{N}_{\mathcal{G}}}^{N} \mathcal{C}_k(P_{\mathcal{G}_k}) + \lambda \left(\sum_{\forall k \in \mathbb{N}_{\mathcal{S}}}^{N} P_{\mathcal{L}_k} - \sum_{\forall k \in \mathbb{N}_{\mathcal{G}}}^{N} P_{\mathcal{G}_k} + \sum_{\forall k \in (\mathbb{N}_{\mathcal{S}})}^{N} \sum_{\forall n \in (\mathbb{N}_{\mathcal{S}} - \{k\})}^{N} G_{kn}(W_{kk} - W_{kn}) \right) + \sum_{\forall k \in \mathbb{N}_{\mathcal{G}}}^{N} \mu_k \left(P_{\mathcal{G}_k} - P_{\mathcal{G}_k}^{max} \right) + \sum_{\forall k \in \mathbb{N}_{\mathcal{G}}}^{N} \zeta_k \left(0 - P_{\mathcal{G}_k} \right) + \sum_{\forall k \in \mathbb{N}_{\mathcal{S}}}^{N} \nu_k \left(W_{kk} - W_{kk}^{max} \right) + \sum_{\forall k \in \mathbb{N}_{\mathcal{S}}}^{N} \vartheta_k \left(W_{kk}^{min} - W_{kk} \right) + \sum_{\forall (s,t) \in \mathbb{N}_{\mathcal{E}}}^{N} \eta_{st} \left(P_{st} - P_{st}^{max} \right) \tag{4.33}$$

$$\vec{P}_{\mathcal{G}}^{i+1} = \underset{P_{\mathcal{G}_k}}{argmin}\ L(\vec{P}_{\mathcal{G}}, \lambda^i, \mu^i, \zeta^i, \nu^i, \vartheta^i, \eta_{st}^i) \Rightarrow$$

$$P_{\mathcal{G}_k}^{i+1} = \frac{\lambda^i - \beta_k - \mu_k^i + \zeta_k^i + \varphi_{st,k}\eta_{st}^i}{2\alpha_k},\ \forall k \in \mathbb{N}_{\mathcal{S}} \tag{4.34}$$

where, $\varphi_{st,k} = {}^{\partial(P_{st} - P_{st}^{max})}/_{\partial(P_{\mathcal{G}_k})}$.

$$\lambda^{i+1} = \lambda^i + \rho_\lambda \left(\sum_{\forall k \in \mathbb{N}_{\mathcal{G}}}^{N} P_{\mathcal{G}_k}^{i+1} - \sum_{\forall k \in (\mathbb{N}_{\mathcal{G}} + \mathbb{N}_{\mathcal{L}})}^{N} P_{\mathcal{L}_k} - \sum_{\forall k \in (\mathbb{N}_{\mathcal{S}})}^{N} \sum_{\forall n \in (\mathbb{N}_{\mathcal{S}} - \{k\})}^{N} G_{kn}(W_{kk}^{i+1} - W_{kn}^{i+1}) \right) \tag{4.35}$$

$$\mu_k^{i+1} = \left[\mu_k^i + \rho_\mu (P_{\mathcal{G}_k}^{i+1} - P_{\mathcal{G}_k}^{max}) \right]^+,\ \forall k \in \mathbb{N}_{\mathcal{S}} \tag{4.36}$$

$$\zeta_k^{i+1} = \left[\zeta_k^i + \rho_\zeta (-P_{\mathcal{G}_k}^{i+1}) \right]^+,\ \forall k \in \mathbb{N}_{\mathcal{S}} \tag{4.37}$$

$$\nu_k^{i+1} = \left[\nu_k^i + \rho_\nu (W_{kk}^{i+1} - W_{kk}^{max}) \right]^+,\ \forall k \in \mathbb{N}_{\mathcal{S}} \tag{4.38}$$

$$\vartheta_k^{i+1} = \left[\vartheta_k^i + \rho_\vartheta (W_{kk}^{min} - W_{kk}^{i+1}) \right]^+,\ \forall k \in \mathbb{N}_{\mathcal{S}} \tag{4.39}$$

$$\eta_{st}^{i+1} = \left[\eta_{st}^i + \rho_\eta (P_{st} - P_{st}^{max}) \right]^+,\ \forall (s,t) \in \mathbb{N}_{\mathcal{E}} \tag{4.40}$$

Theorem 2: The distributed consensus-based method proposed in (4.26)-(4.32) will converge to the global optimal point of the OPF problem.

Proof part-I*:* Equation (4.35), which originates from power balance constraint (5.6), needs information from all buses. As mentioned earlier, each agent can choose a positive random value as the initial value for its λ_k^i in the proposed distributed consensus method.

We consider λ^i in (4.35) as a summation of N (number of buses) random positive values, *i.e.,* $\lambda^i = \lambda_1^i + \lambda_2^i + \cdots + \lambda_N^i = \sum_{\forall k \in \mathbb{N}_S}^{N} \lambda_k^i$. Then, we can rewrite the right side of this statement as (4.41). Therefore, equation (4.35) can be rewritten as (4.42) without loss of generality where ρ_λ is a small value and $\rho_\lambda \ll 1$.

$$\lambda^i = \underbrace{\frac{\sum_{\forall k \in \mathbb{N}_S}^{N} \lambda_k^i}{N} + \frac{\sum_{\forall k \in \mathbb{N}_S}^{N} \lambda_k^i}{N} + \cdots + \frac{\sum_{\forall k \in \mathbb{N}_S}^{N} \lambda_k^i}{N}}_{N-times} \tag{4.41}$$

$$\lambda^{i+1} = \underbrace{\frac{\sum_{\forall k \in \mathbb{N}_S}^{N} \lambda_k^i}{N} + \frac{\sum_{\forall k \in \mathbb{N}_S}^{N} \lambda_k^i}{N} + \cdots + \frac{\sum_{\forall k \in \mathbb{N}_S}^{N} \lambda_k^i}{N}}_{N-times}$$

$$+\rho_\lambda \left(\sum_{\forall k \in \mathbb{N}_\mathcal{G}}^{N} P_{\mathcal{G}_k} - \sum_{\forall k \in (\mathbb{N}_\mathcal{G} + \mathbb{N}_\mathcal{L})}^{N} P_{\mathcal{L}_k} - \sum_{\forall k \in (\mathbb{N}_\mathcal{S})}^{N} \sum_{\forall n \in (\mathbb{N}_\mathcal{S} - \{k\})}^{N} G_{kn}(W_{kk}^{i+1} - W_{kn}^{i+1}) \right) \tag{4.42}$$

Now, we are able to write (4.42) in a decomposition fashion as in (4.43),

$$\begin{aligned}
\lambda_1^{i+1} + \lambda_2^{i+1} + \cdots + \lambda_N^{i+1} = {} & \frac{\sum_{\forall k \in \mathbb{N}_S}^{N} \lambda_k^i}{N} + \rho_\lambda \left(P_{\mathcal{G}_1} - P_{\mathcal{L}_1} - \sum_{\forall n \in (\mathbb{N}_\mathcal{S} - \{1\})}^{N} G_{1n}(W_{11}^{i+1} - W_{1n}^{i+1}) \right) + \\
& \frac{\sum_{\forall k \in \mathbb{N}_S}^{N} \lambda_k^i}{N} + \rho_\lambda \left(P_{\mathcal{G}_2} - P_{\mathcal{L}_2} - \sum_{\forall n \in (\mathbb{N}_\mathcal{S} - \{2\})}^{N} G_{2n}(W_{22}^{i+1} - W_{2n}^{i+1}) \right) + \cdots + \\
& \frac{\sum_{\forall k \in \mathbb{N}_S}^{N} \lambda_k^i}{N} + \rho_\lambda \left(P_{\mathcal{G}_N} - P_{\mathcal{L}_N} - \sum_{\forall n \in (\mathbb{N}_\mathcal{S} - \{N\})}^{N} G_{Nn}(W_{NN}^{i+1} - W_{Nn}^{i+1}) \right)
\end{aligned} \tag{4.43}$$

As can be seen, each bus can take its own dual gradient equation. This $\sum_{\forall k \in \mathbb{N}_S}^{N} \lambda_k^i / N$ is the average of all the λ_k^is and can be distributively calculated by the consensus average-based distributed algorithm

in (4.27).

***Proof part-II**:* Constraint (4.10) of the l^{th} line between the s^{th} and t^{th} buses is binding when the power flow through this line is larger than the line maximum capacity, ($P_{st} > P_{st}^{max}, \forall (s,t) \in \mathbb{N}_{\mathcal{E}}$). To avoid the violation of this constraint, the generation output has to be shifted in favor of the overloaded line to reduce line flow by $\triangle P_{st} = P_{st} - P_{st}^{max}$. The Power Transfer Distribution Factors (PTDFs), representing the sensitivity of the power flow on line l to a shift of power from a source (generator) bus to a sink (slack) bus, is used in equation (4.44) to model $\triangle P_{st}$ based on the generator's power shift $\triangle P_{\mathcal{G}_k}$. It is worth noting that the PTDF depends **only** on the network parameters and is not affected by loading or voltages on the network. Furthermore, the PTDF does not depend on the location of the reference bus in the network [40].

$$\triangle P_{st} = \sum_{\forall k \in \mathbb{N}_{\mathcal{S}}}^{N} \varphi_{st,k} \triangle P_{\mathcal{G}_k} \tag{4.44}$$

where the PTDFs are shown by $\varphi_{st,k}$, and $\triangle P_{\mathcal{G}_k}$ is the generator shifted power. Thus, we may rewrite equation (4.40) as

$$\eta_{st}^{i+1} = \left[\eta_{st}^{i} + \rho_{\eta}(\varphi_{st,1} \triangle P_{\mathcal{G}_1} + \varphi_{st,2} \triangle P_{\mathcal{G}_2} + \cdots)\right]^{+} \tag{4.45}$$

which, if we substitute η_{st}^{i} with the summation of $\eta_{st,1}^{i}+\eta_{st,2}^{i}+\cdots$, the above equation could be easily decomposed and reformulated for each bus as $\eta_{st,k}^{i+1} = \eta_{st,k}^{i}+\rho_{\eta}\varphi_{st,k} \triangle P_{\mathcal{G}_k}$, which is equivalent to $\varphi_{st,k}\eta_{st}^{i}$ in equation (4.34).

***Proof part-III**:* As can be seen, μ, ζ, ν, and ϑ do not need to be updated at all because these parameters could locally be satisfied by each bus. Thus, we do not consider them in updating process. The related parameter variables such as $P_{\mathcal{G}_k}$ and W_{kk} need to be replaced by its boundary when these constraints are binding. In addition, iterative equation (4.29) makes sure that the converged point would be on parabola.

4.6 Performance Assessment

In this section, the proposed method is applied to some power flow test cases, such as, 14, 30, 57, 118, 200-bus system archived by [149] and [150]. First, we discuss the IEEE 30-bus systems in detail and scrutinize its solution graphs then the solution of all cases will be compared with the benchmark.

While conducting this research, we did not have access to realistic data sets for DC systems, which is why we have tried to build our own DC grids based on the existing AC counterparts. To have a DC grid, all lines' reactance data is ignored in all AC test cases; however, some lines have zero resistance ($z = 0 + jx$), such that after removing reactance, no impedance data is left. To resolve this issue in all cases, a random reasonable value is considered for the line resistance. To generate random numbers for missing data, we calculated the mean ($\bar{\mu}_x$) and variance (σ_x^2) of existing data. Then, we use $randn$ function (in MATLAB), which returns random numbers from a normal distribution with mean $\bar{\mu}_x$ and variance σ_x^2. This process ensures that the generated random number does in fact reflect the practical range of the parameters. Additionally, there were several other missing pieces of information, such as the generator maximum capacity and line ratings and generator financial information. All this missing information is accounted for using random data. It is also worth mentioning that active power loss, which is calculated by each bus, is considered as an amount of load reported by each bus for the sake of simplicity. The reason this assumption is that the total losses of the power system are inherently part of the power flow calculation, so there is no need for any specific calculation of these losses.

The IEEE 30-bus system has six generators, which are installed on $\mathbb{N}_{\mathcal{G}} = [1,\ 2,\ 13,\ 22,\ 23,\ 27]$. The coefficient of their cost functions are randomly chosen *i.e.*, $\alpha = [31,\ 74, 66, 63, 69, 14, 41, 52, 32, 25] \times 10^{-4}$, $\beta = [2.71,\ 3.53, 7.58, 2.24, 8.53, 2.25, 6.29, 4.3\, 8.26,\ 5.3]$, and $\gamma_k = 0,\ \forall k \in \mathbb{N}_{\mathcal{G}}$ [28]. Figure (4.2a) demonstrates the evolution of the generators' output power, which finally converge to $P_{\mathcal{G}} = [80,\ 58.75,\ 0,\ 53.84,\ 0,\ 40]$ in kW and support the total load and system power loss $P_{\mathcal{L}}+P_{Loss}=\ 232.6\,[kW]$. Figure (4.2b) shows the convergence of W_{kk} for all buses. The

voltage of all buses can be easily calculated by $\sqrt{W_{kk}}$.

As mentioned earlier, to the best of our knowledge, there exist only a few studies on distributed control methods for OPF of DC distribution networks. The most significant advantage of our method over existing ones is its low number of iterations required for convergence. For comparison, [145], as can be seen in figures (4.2a) and (4.2b), our method requires about 400 iterations to converge in an IEEE 30-bus system while the method proposed in [145] requires about 2.5×10^5 for a 4-bus system.

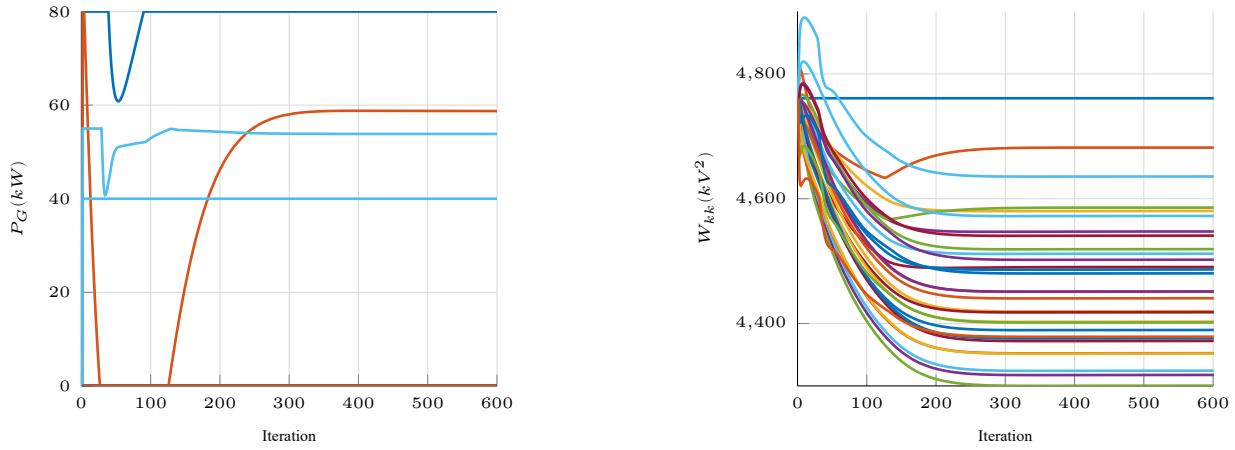

(a) Generators' output power

(b) $W_{kk} = V_K^2$ for all buses

Figure 4.2: Solution graph for the IEEE 30-bus case study, a) Generators' output, and b) Buses' voltage

The consensus value (λ) coordinated among neighbors and the total cost of generators' output is indicated in figures (4.3a) and (4.3b). As proven earlier, all agents reach a similar value of λ as a consensus value whether the constraints of the optimization problem are binding or not. The consensus value represents the incremental cost of the system if none of the constraints is binding, otherwise it is not equal to the incremental cost. For instance, if the upper limit of the k^{th} generator is binding, then the incremental cost would be $\lambda - \mu_k$.

Table 4.1 shows the solution precision between the proposed distributed method and benchmark achieved by any centralized method. In the first two columns, the actual cost function value at the optimal point is compared together; accordingly, the solution mismatch between the total minimum

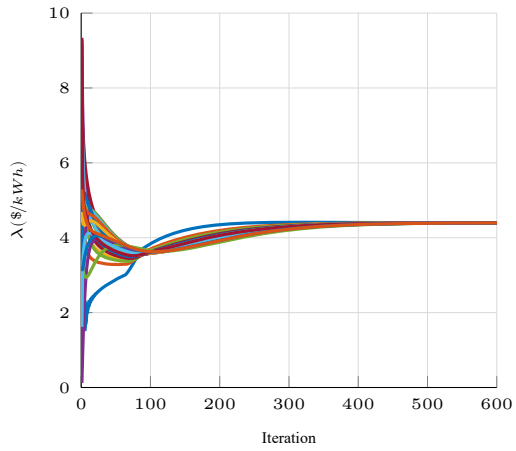

(a) Consensus value λ

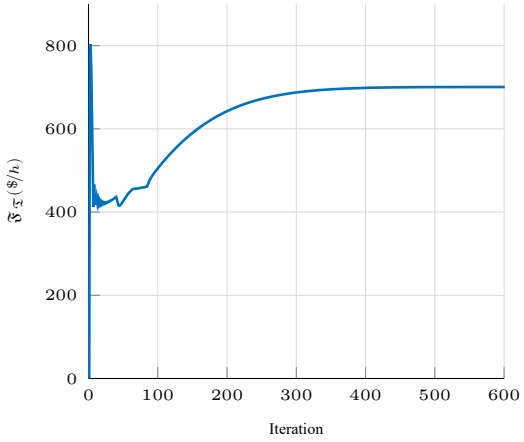

(b) Total cost of generators $\mathfrak{F}_{\mathfrak{T}}$

Figure 4.3: Solution graph for the IEEE 30-bus case study, a) Consensus value λ, and b) Total cost of generators $\mathfrak{F}_{\mathfrak{T}}$

cost of the distributed method and that of the benchmark is 0.005%, 0.032%, 0.0029%, 0.012%, 0.0055% for the 14, 30, 57, 118, 200-bus system, respectfully. These solution mismatches are relatively small. The next two columns indicates total calculated active loss by distributed method and the method used for the benchmark results. The solution mismatch of the total active loss is 0.03 [kW], 0.3 [kW], 0.05 [kW], 9.917 [kW], 0.0837 [kW] for the 14, 30, 57, 118, 200-bus system, respectfully. The last two columns of this table demonstrates the solution average mismatch ($\%$) between DM and the benchmark on the generators' active power output and buses voltage. As can obviously be seen the numbers on these columns are also insignificant. In sum, the simulation results shows the proposed method properly works and converges to global optimal point.

Table 4.1: Simulation test results and comparison with benchmark

	Total cost ($/hr)		Total loss (kW)		Solution average mismatch ($\%$) between DM and Benchmark on	
Case study	Dist. Method	Benchmark	Dist. Method	Benchmark	Active power	Voltage
14-Bus System	1722.12	1722.20	8.65	8.62	0.0046	≈ 0
30-Bus System	700.58	700.32	5.83	5.53	0.0032	≈ 0
57-Bus System	9446.94	9446.66	14.32	14.27	0.0091	≈ 0
118-Bus System	137056.594	137039.58	113.2	103.283	4.8	0.19
200-Bus System	50759.8848	50757.09	9.7347	9.651	0.34227	0.011

4.7 Conclusions

Applying distributed control methods over a DC distribution system improves the privacy of any individual agent either generator or load and the entire system, distributes computational load among all agents, and avoids a single point of failure in a distribution system. We applied our proposed distributed algorithm to a DC distribution system to solve optimal power flow in a fully distributed way without having a central controller or aggregator. The mathematical proof shows it converges to the global optimal point and our simulation case studies demonstrate the high accuracy of the proposed algorithm's performance.

CHAPTER 5
Distributed Optimal Power Flow Algorithm for AC Systems

5.1 Introduction

Optimal generation dispatch is one of the challenging problems in the field of both market and system security due to its non-convexity and uncertainty. Many solutions have been proposed in recent years to solve it by convexification and linearization. Some of these methods fail to be practical, however, due to their specific assumptions. In this chapter, a fully distributed algorithm is proposed for a complete optimal power flow without any convexification or linearization. A mathematical proof for its global optimality is provided for a simple version of the optimization problem; then is extended to consider all constraints. Finally, two test power systems, a synthetic 37-bus case study and an IEEE 118-bus test feeder considering all equality and inequality constraints is simulated to evaluate the proposed algorithm's performance.

5.2 Literature Review

Optimal power flow (OPF), as a fundamental optimization problem in power systems, was introduced by J. L. Carpentier [120] to determine the power levels of all generators to support the requested demand in a system while minimizing the total cost and satisfying all local/global constraints at the same time [121, 122]. In OPF problem, an economic dispatch (ED) problem [28] with a power flow calculation is solved simultaneously. The coupling of these two problems and network/physical constraints make it one of the most insurmountable optimization problems. In sum, the reasons that make it difficult to be solved can be categorized as; 1) Non-linearity: there are nonlinear interrelations (*i.e.*, power flow nodal equations) among powers, voltages and system physical parameters [85]. 2) Non-convexity: the lower/upper bound on the voltage amplitude and

the nonlinear power flow equations cause non-convexity [122, 151]. 3) Computational cost: an OPF not only must be run every year for system planning and every day for a day-ahead market, but also should be run every five minutes for real-time market and system security [123]. 4) Uncertainty: large-scale power systems involve uncertainty due to their integration of renewable energy resources, which make OPF more troublesome [152]. One of the immediate solutions for OPF is DCOPF, which uses DC power flow equations and assumptions in place of AC power flow. It provides us with a rough approximation of the AC power flow and is much faster and easier to solve. Although the power losses are ignored and its accuracy is very dependent on the system and case study, it could be useful for limited contingency analyses and economic studies [40, 104, 152–154]. However, such approximations that ignores system complexities may lead to unrealistic results and analysis. Apart from DCOPF, there are many methods proposed in previous years to solve OPF efficiently, accurately and as fast as possible. As we focus on a distributed ACOPF, this literature review categorizes OPF methods into two main groups: 1) Centralized methods, which need a central controller (*i.e.*, operator) to collect, share and coordinate data among power system components; and 2) Distributed methods, which use a specific algorithm to distributively coordinate information among components to reach an optimal point [24].

Centralized OPF methods have been studied since the early 1960s when a typical OPF was first formulated [123]. In a centralized method, all components directly communicate with a central operator *e.g.*, SCADA. This center should be able to monitor, gather and analyze real-time data and provide all components with appropriate control signals while it records events in a log file. Many methods, including interior point, quadratic programming, Lagrangian relaxation, gradient methods, mixed integer programming, Newton based methods, etc., have been reviewed and classified several times. We only mention four major literature reviews for readers' reference and do not review OPF optimization methods proposed prior to 2010 because these surveys cover all OPF methods. M. Huneault and F. Galiana provided one of the first literature reviews of OPF and investigated the evolution of various methods, such as successive approximation and Newton methods, from 1960 to 1991 [155]. J. A. Momoh *et al.* extensively analyzed the progress of OPF methods

proposed during the 70s, 80s and 90s in two consecutive papers [156,157]. In addition, the comprehensive literature survey by S. Frank *et al*. [158, 159], which reviewed various OPF formulations and solution techniques, their advantages, disadvantages, and computational characteristics, was applied to OPF for 40 years, from 1969 to 2010. Solving OPF using a convex relaxation draws many researchers' attention due to its powerful ability to ensure a solution is global or a lower bound on the global solution. Semidefinite programming (SDP) relaxations of OPF comprehensively evaluated up to 2014 in [124, 125]. S. Bruno *et al.* proposed an unbalanced three-phase optimal power flow (TOPF) based on a quasi-Newton method. TOPF as an extended real-time framework that provides control strategies for distribution radial networks [160]. J. Lavaei *et al*. proposed an SDP optimization method and guaranteed a zero duality gap limited to specific conditions for some IEEE test systems. Furthermore, the sufficiency of condition holds by adding a small resistance to transformers [151]. W. A. Bukhsh *et al.* cover an interesting and challenging topic, possible existence of local optima. They show that standard local optimization techniques can converge to these local optima [129]. Due to the high penetration of renewable generation, the uncertainty level increases in the power system. Chance-constrained AC OPF, as one of the interesting methods, is able to deal with stochastic OPF [130, 131, 161].

Due to the high penetration of distributed energy sources/storage, dynamic topologies of power systems and the need for plug-and-play functionalities, centralized algorithms are no longer effective [45–47]. Consequently, distributed OPF methods have been taken into account by researchers as they are able to overcome these drawbacks. Thanks to the advanced technologies used in communication systems, distributed methods are rapidly maturing [53]. In distributed methods, agents are not required to communicate with a central controller. Instead, they only need to locally connect with their immediate neighbor(s); thus, it can be ensured that no private information is released by a third party. This advantage provides all agents with an opportunity to participate in a fair and competitive market, without any kind of monopoly or monopsony [28]. Apart from the privacy improvement, the single point of failure will naturally be resolved as there is no need for a center to supervise all agents [76, 140]. More ever, computational load will no longer affect a central

controller as it is spread out over the entire network [141]. Dynamic topologies of power systems and plug-and-play functionalities will be requisite features of the future open-access power system, which can easily be supported by distributed algorithms. All of these features make it possible for distributed methods to support high scalability as an urgent need in future power systems.

A growing interest in new distributed algorithms, particularly applicable to OPF problems, can be found in recent research. As we discussed earlier, the non-convexity is a major barrier against finding the global optimality. There is a chain of research trying to resolve this issue. Semi-definite programming, known as the SDP relaxation technique, transforms a non-convex problem in the equivalent convex one. E. Dall'Anese *et al.* built a distributed OPF based on SDP relaxation for an unbalanced distribution system by decomposing a main SDP problem into multiple convex subprograms [85]. A. Lam *et al.* also offered a distributed algorithm by decomposing a main optimization problem into smaller sub-problems tha can be solved by SDP [162]. T. Erseghe proposed a distributed OPF using the alternating direction multiplier method (ADMM). His method is designed based on local optimization, where information only exchanged inside of a region [62]. Another interesting topic has been covered in [163]. The authors discuss synchronization of regions for a distributed OPF problem based on an algorithmic framework that allows each region to perform local updates in an asynchronous fashion. A distributed optimal gas-power flow (OGPF) based on the ADMM, proposed in [164]. At both the power and gas distribution sides, a convex relaxation has been performed and then two problems are coordinated by the ADMM. In [165], both SDP relaxation and the ADMM are used together to build a scheduled-asynchronous algorithm for solving OPF problems in a distributed fashion. SDP relaxation and the ADMM are used to convexify formulated sub-problems and help agents to update their local variables, respectively. The authors of [166] designed an ADMM-based distributed AC-OPF using a linear approximation of power flow equations. They considered two control methods to balance convergence and computational load. A distributed cooperative real-time OPF has been proposed in [167]. This method is able to coordinate the active power of synchronous generators and virtual power plants to cover the nominal frequency while minimizing the generation cost in real time under optimization constraints.

A fully consensus-based distributed OPF is proposed in this chapter. We show that the capacity of line and voltage amplitude limits are no longer areas of non-convexity's concern given a new approach. Power flow constraints, as another reason for non-convexity, are replaced with a local convex optimization problem without loss of generality. The main contributions of our work are as follows:

- Neither convex relaxation nor linear approximation is used; therefore, easy implementation and accurate results, respectively, can be ensured.
- The privacy of each component and, subsequently, the privacy of the entire system, is improved due to very limited shared information.
- In addition, there is no need for any kind of aggregator and/or coordinator.
- No specific assumption is considered for the system topology, e.g., mesh/radial grid, and the proposed method can be applied to both the transmission and distributed level.

The structure for the rest of this chapter is organized as follows: Section 5.3 formulates a comprehensive OPF problem as a global objective function, considering cost functions and constraints. Section 5.4 introduces a distributed consensus-based algorithm with a brief review of graph theory. Section 5.5 provides a mathematical proof for a limited version of OPF and simulation results. This solution extended to a full version of OPF without loss of generality. Section 2.5 demonstrates simulation results for a synthetic 37-bus case study and an IEEE 118-bus test feeder. Finally, section 2.6 summarizes this chapter and presents the concluding remarks.

5.3 System Modeling and Problem Description

In this section, the optimization power flow problem, including cost functions and all equality and inequality constraints, are elaborated.

5.3.1 Generators' Cost Function

Generators need to mathematically represent their costs to participate in an electricity market. Estimated generation cost can be represented by various cost functions, such as a multiple piecewise linear, quadratic or cubic functions. For this study, a known quadratic fuel cost function, shown in (5.1), is considered for all generators.

$$\mathcal{C}_k(P_{\mathcal{G}_k}) = \alpha_k P_{\mathcal{G}_k}^2 + \beta_k P_{\mathcal{G}_k} + \gamma_k, \quad \forall k \in \mathbb{N}_{\mathcal{G}} \tag{5.1}$$

where α \$/(kW)^{2}h, β \$/kWh and γ \$/h are coefficients that customize the cost function for each generator. $P_{\mathcal{G}_k}$ kW is the amount of power generated by the $k-th$ generator and $\mathbb{N}_{\mathcal{G}}$ shows a set of buses associated with a generator.

5.3.2 System Equality and Inequality Constraints

As other optimization problems, OPF has some important constraints due to the topology of the power system, flow capacity of transmission lines , some restrictions on the power generation capacity, etc. Power flow equations, *i.e.*, nodal KCL, and load balance are the equality constraints. Voltage amplitude and generation capacity, along with transmission line flow, constitute the inequality constraints. We also need to consider slack bus voltage amplitude and phase angle constraints.

5.3.3 Statement of the Global Optimization Power Flow Problem

As shown in (5.2), the total cost function ($\mathfrak{F}_{\mathfrak{T}}$, where $\overrightarrow{P_{\mathcal{G}}} = \left[P_{\mathcal{G}_1},\ P_{\mathcal{G}_2},\ \cdots,\ P_{\mathcal{G}_N}\right]^T$) is a summation of all generators' cost functions. Equation (5.3) indicates a box constraint for the power capacity of each generator, where $P_{\mathcal{G}_k}^{max}$ and $P_{\mathcal{G}_k}^{min}$ indicates the maximum and minimum possible generation level. We consider $P_{\mathcal{G}_k}^{min} = 0, \quad \forall k \in \mathbb{N}_{\mathcal{G}}$. The voltage magnitude boundary is shown by (5.4), which makes the optimization problem a non-convex problem. Pre-set values of the slack bus are defined by (5.5). Equation (5.6) shows the power balance between generation and consumption. The first statement on the right side of (5.6) shows the total load installed on the generator and

load buses, where $\mathbb{N}_{\mathcal{L}}$ indicates the load-only buses. The second statement on right side of (5.6) represents the summation of the estimated active power loss of each bus, where $\mathbb{N}_{\mathcal{S}}$ defines the set of all buses, including generator, load, slack and connection buses.

$$\min \quad \mathfrak{F}_{\mathfrak{T}}\left(\overrightarrow{P_{\mathcal{G}}}\right) = \sum_{\forall k \in \mathbb{N}_{\mathcal{G}}}^{N} \mathcal{C}_k(P_{\mathcal{G}_k}), \quad \forall k \in \mathbb{N}_{\mathcal{G}} \tag{5.2}$$

$$P_{\mathcal{G}_k}^{min} \leq P_{\mathcal{G}_k} \leq P_{\mathcal{G}_k}^{max}, \quad \forall k \in \mathbb{N}_{\mathcal{G}} \tag{5.3}$$

$$V_k^{min} \leq \left|V_k\right| \leq V_k^{max}, \quad \forall k \in \mathbb{N}_{\mathcal{G}} \tag{5.4}$$

$$\left|V_{k_s}\right| = 1, \ \delta_{k_s} = 0, \quad k_s \in \mathbb{N}_{\mathcal{G}} \tag{5.5}$$

$$\sum_{\forall k \in \mathbb{N}_{\mathcal{G}}}^{N} P_{\mathcal{G}_k} = \sum_{\forall k \in (\mathbb{N}_{\mathcal{G}} + \mathbb{N}_{\mathcal{L}})}^{N} P_{\mathcal{L}_k} + \sum_{\forall k \in \mathbb{N}_{\mathcal{S}}}^{N} \mathcal{P}_{Loss_k} \tag{5.6}$$

$$P_{net,k} = \begin{cases} P_{\mathcal{G}_k} - P_{\mathcal{L}_k} & , \quad \forall k \in (\mathbb{N}_{\mathcal{G}} + \mathbb{N}_{\mathcal{L}}) \\ 0 & , \quad \forall k \notin (\mathbb{N}_{\mathcal{G}} + \mathbb{N}_{\mathcal{L}}) \end{cases} \tag{5.7}$$

$$Q_{net,k} = \begin{cases} Q_{\mathcal{G}_k} - Q_{\mathcal{L}_k} & , \quad \forall k \in (\mathbb{N}_{\mathcal{G}} + \mathbb{N}_{\mathcal{L}}) \\ 0 & , \quad \forall k \notin (\mathbb{N}_{\mathcal{G}} + \mathbb{N}_{\mathcal{L}}) \end{cases} \tag{5.8}$$

$$\mathcal{S}_{net,k} = P_{net,k} + jQ_{net,k} = V_k \left[\sum_{\forall n \in \mathbb{N}_{\mathcal{S}}}^{N} Y_{kn} V_n\right]^* \tag{5.9}$$

$$\mathcal{S}_{kn} = V_k \left[\left(V_k - V_n\right) Y_{kn}\right]^* \leq \mathcal{S}_{kn}^{max}, \quad \forall k \ \& \ \forall n \in \mathbb{N}_{\mathcal{S}} \tag{5.10}$$

The injected active and reactive power are shown by $P_{net,k}$ and $Q_{net,k}$, respectively. $\mathcal{S}_{net,k}$ in (5.9) shows the power flow nodal equation for the $k-th$ bus. The line flow constraint is formulated by (5.10), where $\mathcal{S}_{kn}^{max}$ indicates the maximum complex power flowing through the line connected the $k-th$ and $n-th$ buses.

5.4 Distributed Algorithm for Optimal Power Flow

As mentioned earlier, a consensus-based distributed algorithm for finding the globally optimal solution is proposed in this chapter. A brief graph theory shows our assumptions and justifies our model for a communication network. Then we show how to apply an average-consensus distributed protocol [74] to an OPF problem without network constraints *i.e.*, the economic dispatch (ED) problem. After optimality analysis, power flow nodal equations, and line flow constraints will be added without loss of generality.

$\mathcal{N}(\mathcal{K}, \xi)$ denotes communication network (undirected graph) with N connected buses, designated by $\mathcal{K} = \{1, 2, ... N\}$ and $\xi \subseteq \mathcal{K} \times \mathcal{K}$, which represents a set of edges. The physical power system is mapped onto the communication network. This means that there is a communication link between two buses connected by a transmission line. The undirected edge $e_{kn} = (k, n)$ indicates that bus k and n can share information with each other. Two matrices will commonly be used to represent the communication topology of a multiple-agent network. The adjacency matrix denoted by $\mathcal{A} = \{[a_{kn}] \, | a_{kn} \in \mathcal{R}^{\mathcal{P}\times\mathcal{P}}\}$ of an undirected network $\mathcal{N}$ is symmetric. The entries of the adjacency matrix is defined by (5.11).

$$\mathcal{A} = \begin{cases} a_{kn} \neq 0 & , \quad \forall e_{kn} \in \xi \\ a_{kn} = 0 & , \quad \forall e_{kn} \notin \xi \\ a_{kk} = 0 & , \quad \forall k \in \mathbb{N}_{\mathcal{S}} \end{cases} \tag{5.11}$$

The second matrix is Laplacian matrix $L = D - \mathcal{A} = \{[l_{kn}] \, | l_{kn} \in \mathcal{R}^{\mathcal{P}\times\mathcal{P}}\}$, where D is a network degree matrix. As can be inferred, the definition of a Laplacian matrix is very similar to admittance matrix. The entries of the Laplacian matrix defined by (5.12).

$$L = \begin{cases} l_{kk} = \sum\limits_{\forall n \in \mathbb{N}_{\mathcal{S}}} a_{kn} & , \quad \forall k \in \mathbb{N}_{\mathcal{S}} \\ l_{kn} = -a_{kn} & , \quad \forall e_{kn} \in \xi \\ l_{kn} = 0 & , \quad otherwise \end{cases} \tag{5.12}$$

A consensus-based distributed protocol helps agents share information with their immediate neighbors to reach a consensus at an optimal point. A consensus is defined as an equal value of the state of the $k-th$ and $n-th$ agents [73, 74]. In other words, $k-th$ and $n-th$ agent will have reached a consensus if and only if the value of the state of the $k-th$ agent (x_k) and the state of the $n-th$ agent (x_n) are equal. If we consider that each bus shares its information with its neighbors, a standard linear distributed protocol [74] can be defined in (5.13), where $\vec{x} = [x_1,\, x_2,\, \ldots,\, x_N]^T$.

$$\dot{\vec{x}} = -\nabla\left(2\vec{x}^T L\vec{x}\right) = -L\vec{x} \tag{5.13}$$

Let us consider the total cost function (5.2), box constraints (5.3) and power balance (5.6) as a simple optimization problem. The rest of the constraints will be added later during the analysis of optimality in section 5.5. We assume that $k-th$ bus *only* accesses its own private information, such as its generator's cost function ($\mathcal{C}_k(P_{\mathcal{G}_k})$), generated active power ($P_{\mathcal{G}_k}$) and its local load ($P_{\mathcal{L}_k}$). Any of these pieces of information could be zero depending on the type of bus, such as PV, PQ or connection buses. They also can pick an arbitrary value for their particular incremental cost (λ_k). Incremental costs are the only piece of information shared with immediate neighbors through the average-consensus distributed protocol in (5.13). Eventually, all of the buses reach an identical value of λ_c as a consensus. Then, each bus estimates its active power generation using (5.15); a bus may have no active power generation. An individual incremental cost (λ_k^{i+1}) for the next iteration is calculate by (5.16), based on the private information and consensus. The whole procedure is shown by (5.14), (5.15) and (5.16), where $\vec{\lambda} = \left\{[\lambda_1,\, \lambda_2,\, \ldots,\, \lambda_N]^T \,|\lambda_k \in \mathcal{K}\right\}$ and i is the iteration number.

$$\dot{\vec{\lambda}}^i = -L\vec{\lambda}^i \tag{5.14}$$

$$P_{\mathcal{G}_k}^i = \frac{\lambda_{c,k}^i - \beta_k}{2\alpha_k},\ \forall k \in \mathbb{N}_{\mathcal{S}} \tag{5.15}$$

$$\lambda_k^{i+1} = \lambda_{c,k}^i + \rho(P_{\mathcal{G}_k}^i - P_{\mathcal{L}_k}),\ \forall k \in \mathbb{N}_{\mathcal{S}} \tag{5.16}$$

Finally, all λ_k will be identical, due to the nature of the distributed algorithm in (5.13), $\sum_{\forall k \in \mathbb{N}_{\mathcal{G}}}^{N} P_{\mathcal{G}_k}$ will cover the total demand, and the power balance constraint will be satisfied It is worth mentioning that

- None of the private information, such as $P_{\mathcal{G}_k}$, α_k, β_k, $P_{\mathcal{L}_k}$ are shared.
- The only information shared with immediate neighbors is estimated λ_k.

In the next section, it is shown that this protocol converges to the global optimal point of the optimization problem.

5.5 Analysis of Optimality

This section is organized as follows: Subsection 5.5.1 provides the optimality analysis for a simple optimization problem (similar to the economic dispatch problem), including the total cost function (5.2), box constraints (5.3) and power balance (5.6). Then, subsection 5.5.2 adds two important constraints, including the voltage amplitude limitation (5.4) and line flow constraint (5.10), in subsections 5.5.2 and 5.5.2.

5.5.1 Simple Optimization Problem

Remark 4. All local constraints (5.1) and the total cost function (5.2) are strictly convex.

Remark 5. As the box constraints and power balance equation are considered in this step, all constraints of the ED problem are affine.

Remark 6. The incremental cost of each bus should be equal at the optimal point, i.e, $\lambda_1 = \lambda_2 =$, ... , $= \lambda_N$, because of the dual variable of the power balance constraint [57].

Lemma: Based on *Remark* (4) and *Remark (5),* the ED optimization problem that satisfies Slater's condition and KKT conditions can provide the necessary and sufficient conditions for optimality.

Proposition: Combining *Remark* (4), *Remark* (*5*), and the lemma, a dual gradient method (5.18-

5.21) will converge to the global optimal given the Lagrangian function provided in (5.17).

$$L(\vec{P}_{\mathcal{G}}, \lambda, \mu, \zeta) = \sum_{\forall k \in \mathbb{N}_{\mathcal{G}}}^{N} \mathcal{C}_k(P_{\mathcal{G}_k}) + \lambda \left(\sum_{\forall k \in \mathbb{N}_{\mathcal{S}}}^{N} \mathcal{P}_{Loss_k} + \sum_{\forall k \in (\mathbb{N}_{\mathcal{G}} + \mathbb{N}_{\mathcal{L}})}^{N} P_{\mathcal{L}_k} - \sum_{\forall k \in \mathbb{N}_{\mathcal{G}}}^{N} P_{\mathcal{G}_k} \right) + \sum_{\forall k \in \mathbb{N}_{\mathcal{G}}}^{N} \mu_k \left(P_{\mathcal{G}_k} - P_{\mathcal{G}_k}^{max} \right) + \sum_{\forall k \in \mathbb{N}_{\mathcal{G}}}^{N} \zeta_k \left(-P_{\mathcal{G}_k} \right) \tag{5.17}$$

$$\vec{P}_{\mathcal{G}}^{i+1} = \underset{P_{\mathcal{G}_k}}{argmin}\ L(\vec{P}_{\mathcal{G}}, \lambda^i, \mu^i, \zeta^i) \Rightarrow$$

$$P_{\mathcal{G}_k}^{i+1} = \frac{\lambda^{i+1} - \beta_k - \mu_k^{i+1} + \zeta_k^{i+1}}{2\alpha_k} \forall k \in \mathbb{N}_{\mathcal{S}} \tag{5.18}$$

$$\lambda^{i+1} = \lambda^i + \epsilon(\sum_{\forall k \in \mathbb{N}_{\mathcal{S}}}^{N} \mathcal{P}_{Loss_k} + \sum_{\forall k \in \mathbb{N}_{\mathcal{G}}}^{N} P_{\mathcal{G}_k} - \sum_{\forall k \in (\mathbb{N}_{\mathcal{G}} + \mathbb{N}_{\mathcal{L}})}^{N} P_{\mathcal{L}_k}) \tag{5.19}$$

$$\mu_k^{i+1} = \left[\mu_k^i + \rho(P_{\mathcal{G}_k} - P_{\mathcal{G}_k}^{max}) \right]^+, \ \forall k \in \mathbb{N}_{\mathcal{S}} \tag{5.20}$$

$$\zeta_k^{i+1} = \left[\zeta_k^i + \rho(-P_{\mathcal{G}_k}) \right]^+, \ \forall k \in \mathbb{N}_{\mathcal{S}} \tag{5.21}$$

Theorem: If the optimization problem presented in (5.2), constrained by box and power balance constraints, has a feasible globally optimal point, then the consensus-based distributed algorithm proposed in section (5.4) will converge to that globally optimal point.

Proof. The decomposition approach of the dual gradient helps us to provide a set of separate equations for each bus . Equations (5.17), (5.20) and (5.21) can easily be calculated, in a parallel fashion, with only private information (no need for shared information among immediate neighbors). However, equation (5.19) needs a kind of coordinator to gather and send bus information and λ (see Remark (6)). This approach obviously violate the privacy and puts extra computational load on a coordinator. We can consider λ^i as a summation of N arbitrary real values

$\lambda^i = \lambda_1^i + \lambda_2^i + \cdots + \lambda_N^i = \sum_{\forall k \in \mathbb{N}_S}^{N} \lambda_k^i$, where the N is number of buses. Then, we can rewrite the right side of this statement as (5.22). Therefore, equation (5.19) can be re-written as (5.23) without loss of generality.

$$\lambda^i = \underbrace{\frac{\sum_{\forall k \in \mathbb{N}_S}^{N} \lambda_k^i}{N} + \frac{\sum_{\forall k \in \mathbb{N}_S}^{N} \lambda_k^i}{N} + \cdots + \frac{\sum_{\forall k \in \mathbb{N}_S}^{N} \lambda_k^i}{N}}_{N-times} \tag{5.22}$$

$$\lambda^{i+1} = \underbrace{\frac{\sum_{\forall k \in \mathbb{N}_S}^{N} \lambda_k^i}{N} + \frac{\sum_{\forall k \in \mathbb{N}_S}^{N} \lambda_k^i}{N} + \cdots + \frac{\sum_{\forall k \in \mathbb{N}_S}^{N} \lambda_k^i}{N}}_{N-times} + \epsilon\Big(\sum_{\forall k \in \mathbb{N}_\mathcal{S}}^{N} \mathcal{P}_{Loss_k} + \sum_{\forall k \in \mathbb{N}_\mathcal{G}}^{N} P_{\mathcal{G}_k} - \sum_{\forall k \in (\mathbb{N}_\mathcal{G} + \mathbb{N}_\mathcal{L})}^{N} P_{\mathcal{L}_k} \Big) \tag{5.23}$$

Now, we are able to write (5.23) in a decomposition fashion as (5.24),

$$\lambda_1^{i+1} + \lambda_2^{i+1} + \cdots + \lambda_N^{i+1} = \frac{\sum_{\forall k \in \mathbb{N}_S}^{N} \lambda_k^i}{N} + \epsilon(\mathcal{P}_{Loss_1} + P_{\mathcal{G}_1} - P_{\mathcal{L}_1}) + \frac{\sum_{\forall k \in \mathbb{N}_S}^{N} \lambda_k^i}{N} + \epsilon(\mathcal{P}_{Loss_2} + P_{\mathcal{G}_2} - P_{\mathcal{L}_2}) + \cdots + \frac{\sum_{\forall k \in \mathbb{N}_S}^{N} \lambda_k^i}{N} + \epsilon(\mathcal{P}_{Loss_N} + P_{\mathcal{G}_N} - P_{\mathcal{L}_N}) \tag{5.24}$$

Based on (5.25), each bus can take its own dual gradient equation. The first righ-side statement is the average of all the estimated λ_ks and can be distributively calculated by introducing the protocol in (5.13) or (5.14) because this protocol always calculate the average.

$$\lambda_k^{i+1} = \frac{\sum_{\forall k \in \mathbb{N}_S}^{N} \lambda_k^i}{N} + \epsilon(\mathcal{P}_{Loss_k}^i + P_{\mathcal{G}_k}^i - P_{\mathcal{L}_k}) \tag{5.25}$$

Equation (5.25) is the one introduced in (5.16), where $\lambda_{c,k}^i = \sum_{\forall k \in \mathbb{N}_S}^{N} \lambda_k^i / N$, $\rho = N\epsilon$. □

For the sake of accuracy assessment, two test networks, network A (14 generators) and network B (21 generators), are randomly generated by the Erdos–Renyi model and the Watts–Strogatz model,

respectively. Figure. (5.1a) and Figure. (5.1b) show their visual topology and related model parameters. All random networks are, in this section, generated by Cytoscape [168]. The demanded load on network A and network B are 2602 kW and 4832 kW, accordingly.

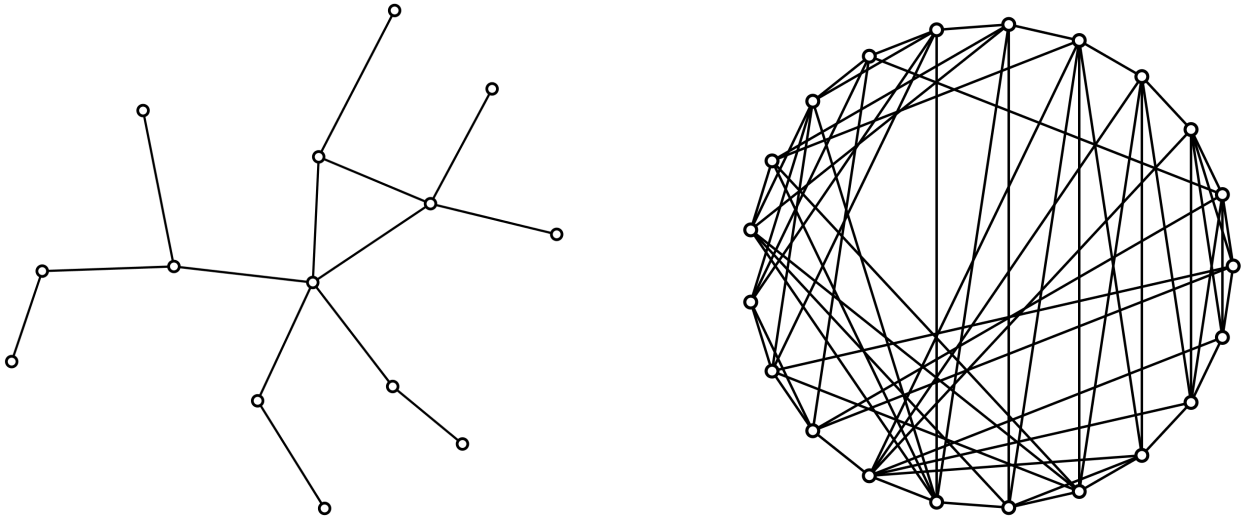

(a) Network A) Erdos–Renyi model

(b) Network B) Watts–Strogatz model

Figure 5.1: Test graph randomly generated by two different models, a) $G_{ER}(n,p):\ n=14,\ p=0.1$, b) $G_{WS}(n,k^{'},\beta^{'}):\ n=21,\ k^{'}=6,\ \beta^{'}=0.1$

Table (5.1) presents the results of the optimization problem given the proposed algorithm and a centralized method (YALMIP is applied [95]) to provide an accuracy evaluation following our proof. As shown in Table (5.1), the solution mismatch between the distributed and centralized methods is less than 0.008% of the average. As can be seen, this value is almost zero and demonstrates our proposed method can find the same optimal point as a centralized method. Figures. (5.2a) and (5.3a) show a visual convergence of dispatched power among the generators for both systems. As shown in Figures. (5.2b) and (5.3b), the incremental cost (λ) finally converges to $6.77\ \$/\text{kWh}$ for network A and $7.13\ \$/\text{kWh}$ for network B.

A bigger system, shown in Figure. (5.4), is used for the sake of scalability study. This network has 1000 nodes, which are randomly generated by the Watts–Strogatz model. In addition, the mean parameters of the coefficients of the generators' cost functions are selected to be $0.0085\ \$/(\text{kW})^2\text{h}$ and $4.21\ \$/\text{kWh}$. The demand is also normally distributed among all buses. The total generation ($450234.1\,kW$), which is achieved after 350 iterations, supports the total demand ($450238\,kW$).

It indicates that although the number of nodes is 50 times bigger than the first two networks, the iteration is only (almost) doubled. The incremental cost of all 1000 agents converges to 13.01 $\$/\text{kWh}$ at the optimal point. The solution mismatch between the distributed and centralized methods is about 0.0062% of the average. Again, this value confirms the precision of the proposed method for large-size networks.

Table 5.1: Numerical comparison of proposed distributed and centralized methods

	Network A		Network B	
Power	Distributed	Centralized	Distributed	Centralized
P_1	219.43	219.45	258.97	258.97
P_2	400.00	400.00	400.00	400.00
P_3	88.98	89.014	160.24	160.26
P_4	425.00	425.00	425.00	425.00
P_5	100.00	100.00	100.00	100.00
P_6	8.016	8.034	58.516	58.533
P_7	170.00	170.00	170.00	170.00
P_8	200.00	200.00	200.00	200.00
P_9	0.00	0.00	0.00	0.00
P_{10}	150.00	150.00	150.00	150.00
P_{11}	240.37	240.39	269.36	269.37
P_{12}	33.55	33.56	55.54	55.55
P_{13}	312.00	312.00	312.00	312.00
P_{14}	254.54	254.55	277.50	277.51
P_{15}	-	-	270.00	270.00
P_{16}	-	-	597.59	597.60
P_{17}	-	-	656.00	656.00
P_{18}	-	-	111.19	111.20
P_{19}	-	-	240.00	240.00
P_{20}	-	-	0.00	0.00
P_{21}	-	-	120.00	120.00
Total	2601.89	2601.998	4831.906	4831.993

5.5.2 Voltage Amplitude and Line Flow Constraints

As known, the OPF problem is more complex than what has been discussed here. One of the important groups of constraints is the power flow nodal equations and voltage amplitude limitation, as expressed in (5.9) and (5.4). It may perhaps be observed that without having limitation on voltage amplitude (5.4), nodal equations (5.9) are not effective because voltage of buses can choose any

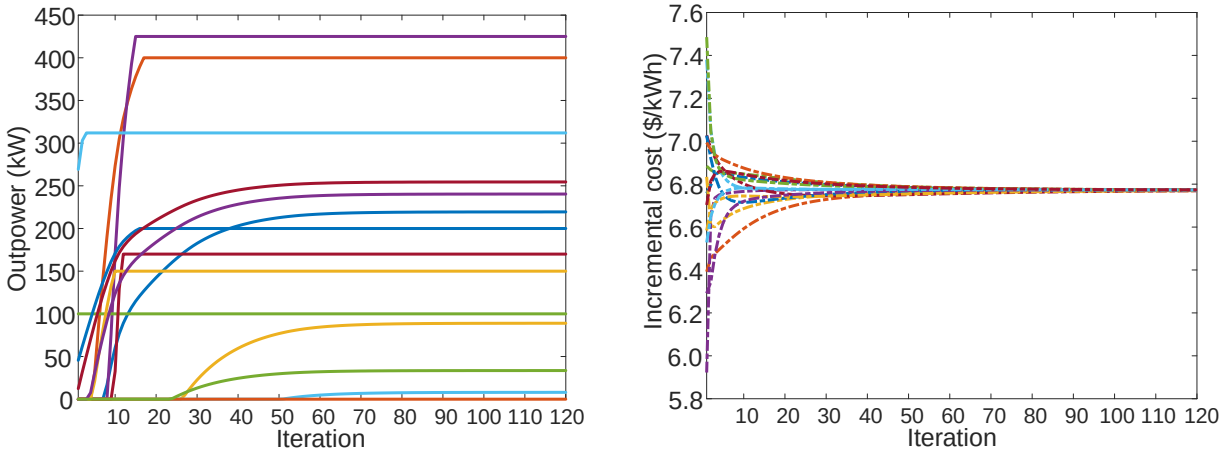

(a) Output powers of generators (kW)

(b) Consensus on λ $^{\$}/_{kWh}$

Figure 5.2: Network A: convergence of parameters

values, satisfying nodal equations. This can be calculated by power flow easily.

Voltage amplitude constraints

As it is known, in a transmission network, the flow of active power depends on the voltage angle, and the flow of reactive power depends on the voltage amplitude. Hence, active power moves from a larger voltage angle bus to a smaller voltage angle bus. On the other hand, reactive power flows from a higher voltage amplitude bus to a smaller voltage magnitude bus.

There are two general approaches for controlling the voltage amplitude at a bus, a local voltage controller and power re-dispatching, to make sure that the voltage amplitude satisfies the constraints provided by equation (5.4). Preferably, the voltage amplitude is controlled locally by changing the reactive power of a given bus as is the case with PV buses. However, it is not possible to have a voltage controller on all buses, like PQ buses and connection buses. Therefore, re-dispatching active and reactive power could be a potential alternative solution. Any re-dispatching of active power, other than the solution found by ED, increases the price of total generation. Additionally, the re-dispatching of active power cannot effectively change the voltage amplitude at the target bus because, as has been discussed, voltage amplitudes are more sensitive to reactive power than active

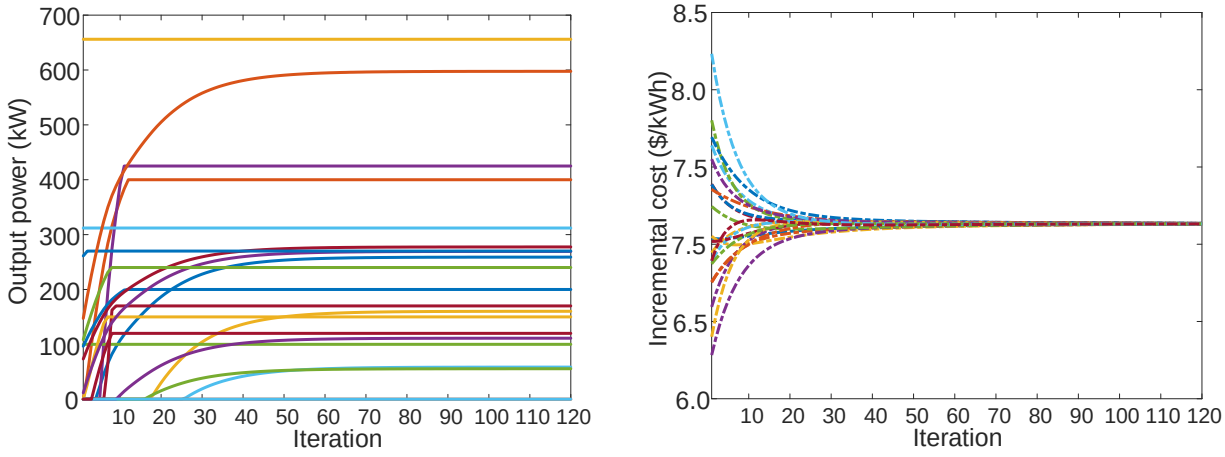

(a) Output powers of generators (kW)

(b) Consensus on λ $^{\$}/_{kWh}$

Figure 5.3: Network B: convergence of parameters

power. This fact can also be investigated by calculation of the sensitivity of the voltage amplitude to active and reactive power changes. On the other hand, re-dispatching of reactive power can be very effective in comparison with re-dispatching of active power because it does not change the optimal point calculated by ED. In this part, the set point voltage of the generators is used to compensate for the violation of voltage amplitude in other buses. We assume that there is enough amount of the reactive power to control voltage. When the voltage amplitude in a bus violates its limitation, the amount of violation can be used as a factor to change the set point voltage of the generators and consequently change the reactive power injected by each generator. Equation (5.26) shows the simple relation used to compensate for violated voltage amplitude, where α parameters can be any number with absolute value less than unity. Using a sensitivity index for α, which measures the sensitivity of bus voltages to changes in generator voltage set points could be very effective. $\left|V_n^{limit}\right|$ indicates the $\left|V_n^{min}\right|$ or $\left|V_n^{max}\right|$.

$$V_k^{Gen,\,i+1} = V_k^{Gen,\,i} + \sum_{i=1}^{i} \sum_{\forall n \in \mathbb{N}_S}^{N} \alpha_{n,k} \left| \left|V_n^i\right| - \left|V_n^{limit}\right| \right|, \quad \forall k \tag{5.26}$$

The new voltage set point of a generator installed on k^{th} bus will be supported by the reactive

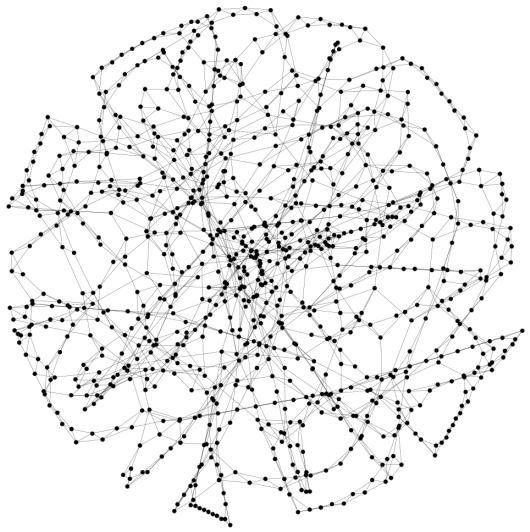

Figure 5.4: 1000 node network by the Watts\textendash Strogatz model, $G_{WS}(n, k^{'}, \beta^{'}) : n = 1000,\ k^{'} = 4,\ \beta^{'} = 0.05$

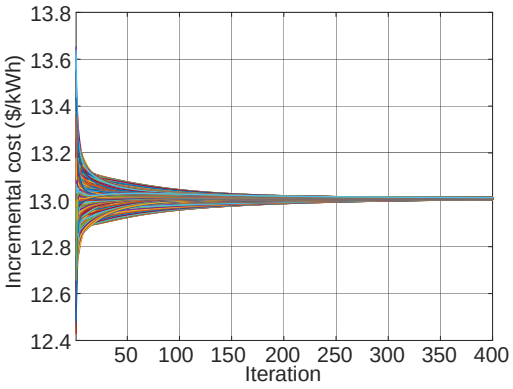

Figure 5.5: Consensus on incremental cost for random network with 1000 nodes

power injected at the respective bus.

As discussed earlier, re-dispatching of reactive power would not affect the ED solution, which is a global optimal point. However, it may change the total loss because it is changing the voltage magnitude. It is worth mentioning that we are not minimizing the active loss function as it is not in the scope of this chapter.

Line flow constraints

Now, the line flow constraints shown in (5.10) are the only group of constraints causing non-convexity. There is no easy way to convexify these constraints without linearization. In this section, an intuitive method is used to easily replace these constraints. We define another optimization problem, whose solution satisfies constraint (10). This optimization problem only replaces the line flow constraints and does not replace whole optimization problem. To alleviate overloading, the output power of generators connected to the network must be re-dispatched in a cost-effective way. This means each generator should change its output by $\triangle P_{\mathcal{G}_k}$, compared to its output in the solution of

the unconstrained problem (*i.e.* the ED problem), to reduce the power flow through the congested lines.

Assumption: the global optimal solution of the unconstrained problem (without constraint (5.10)) is $\{P_{\mathcal{G}_1},\ P_{\mathcal{G}_2},\ \cdots,\ P_{\mathcal{G}_n}\}$, whose total minimum cost is $\mathfrak{F}_{\mathfrak{T}} = \mathcal{C}_1 + \mathcal{C}_2 + \cdots + \mathcal{C}_n$.

Theorem: in a constrained problem (with constraint (5.10)), a set of re-dispatching generators *i.e.*, $\{\triangle P_{\mathcal{G}_1},\ \triangle P_{\mathcal{G}_2},\ \cdots,\ \triangle P_{\mathcal{G}_n}\}$ which has minimal price changes from the unconstrained problem, among feasible solutions, is global optimal point. This re-dispatching should not violate constraint (5.6); therefore, $\sum\limits_{\forall k \in \mathbb{N}_{\mathcal{G}}} \triangle\ P_{\mathcal{G}_k} = 0$.

Each $\triangle P_{\mathcal{G}_k}$ causes a price change ($\triangle \mathcal{C}_k$) in the respective generator. The summation of all $\triangle \mathcal{C}_k$ should be minimized to guarantee the closest feasible solution to the solution of the unconstrained problem, which is the global optimal point. The line flow constraint (5.10) is replaced by (5.27), subject to constraint (5.28) and other local constraints from the main problem, where $\triangle \mathcal{C}_k = \mathcal{C}_k(\triangle P_{\mathcal{G}_k}) = \alpha_k(\triangle P_{\mathcal{G}_k})^2 + \beta_k(\triangle P_{\mathcal{G}_k}) + \gamma_k, \quad \forall k \in \mathbb{N}_{\mathcal{G}}$.

$$\min \quad \sum_{\forall k \in \mathbb{N}_{\mathcal{G}}}^{N} \mathcal{C}_k(\triangle P_{\mathcal{G}_k}), \quad \forall k \in \mathbb{N}_{\mathcal{G}} \tag{5.27}$$

$$\triangle P_{\mathcal{G}_1} + \triangle P_{\mathcal{G}_2} + \cdots + \triangle P_{\mathcal{G}_n} = 0 \tag{5.28}$$

Equation (5.27) shows that the cost of the power changes should be minimal and equation (5.28) indicates the power changes should not violate power balance constraints. The dual ascent solution for this convex optimization problem is (5.29), where χ is the dual variable related to the equality constraint in (5.28).

$$\triangle\ P^i_{\mathcal{G}_k} = \frac{\chi^i - \beta_k}{2\alpha_k}, \quad \forall k \in \mathbb{N}_{\mathcal{G}} \tag{5.29}$$

Overloading is the only reason that (5.29) comes into play; thus, $\chi = P_{kn} - P^{max}_{kn}$ to satisfy line maximum flow constraints. It is worth mentioning that χ is calculated by sending and receiving end buses and distributed among their neighbors. Thus, privacy is not violated. Furthermore, the

whole problem (5.27) is still convex. The value calculated in (5.29) is added to (5.15).

5.6 Performance Assessment

In this section, we apply the proposed method to two test models of a power system, a synthetic 37-bus case study [1] and an IEEE 118-bus test feeder [150], to evaluate the recently introduced constraints in section (5.5.2).

In the first case study, the set of generators, load and connection buses are, $\mathbb{N}_{\mathcal{G}} = \{7$,17, 20, 30, 32, 33, 34, $35\}$, $\mathbb{N}_{\mathcal{L}} = \{2, 3, 4, 5, 6, 7, 8, 9, 10, 11, 12, 13, 14, 15, 16, 19, 22, 23, 25, 30, 32, 33, 34, 35, 36, $37\}$ and $\mathbb{N}_{\mathcal{S}} - (\mathbb{N}_{\mathcal{G}} \cup \mathbb{N}_{\mathcal{L}}) = \{1, 18, 21, 24, 26, 27, 28, 29, 31\}$, respectively. In addition, bus 20 is selected as a slack bus, *i.e.*, $\delta_{k_s} = 0$, $k_s = 20$. Figure. (5.6) shows the network configuration. There is no assumption regarding transmission line resistance or inductance. Hence, the algorithm can be applied to both transmission and distribution systems. There are some parallel lines in the system, such as the lines between buses 8 and 35, which are considered as a single line.

It is worth mentioning that active power loss, which is estimated by each bus, is considered as an amount of load reported by each bus, as shown by (5.30), for the sake of simplicity. The reason is that the total losses of the power system are inherently part of the power flow calculation and there is no need for any specific calculation.

$$\mathcal{P}_{Loss_k} = \sum_{n \neq k} (1/2)\, G_{kn} \left| V_k - V_n \right|^2, \ \forall k \,\&\, n \in \mathbb{N}_{\mathcal{S}} \tag{5.30}$$

Table (5.2) compares the generators' output calculated by the proposed method and those of the centralized method, obtained from MATPOWER [169] as benchmark results. The solution mismatch between the distributed and centralized methods is almost less than 3.9% of the average. The total cost found by the proposed method (26090.7195 \$/hr) is close to that of centralized methods (26090.60 \$/hr). The total generation is about $1480.7412\ kW$, which covers the total demand ($1447.1\ kW$) plus total loss ($33.641\ kW$). The mismatch between the total estimated power loss between the distributed methods and the benchmark is 0.52%.

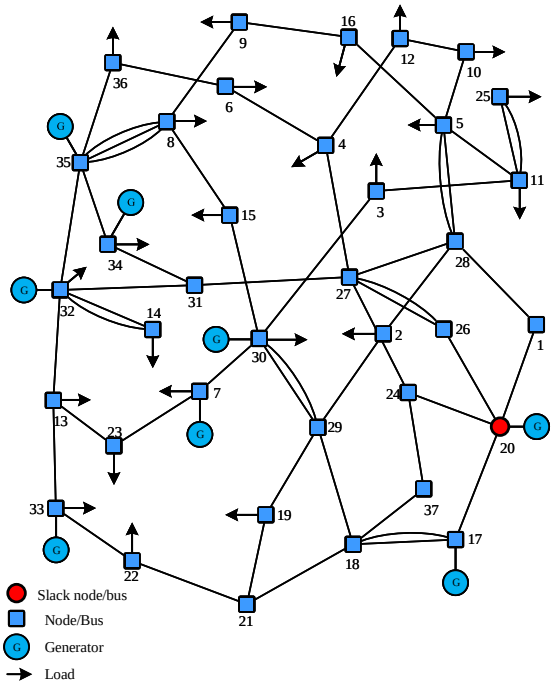

Figure 5.6: 37-bus network [1] for OPF performance evaluation

The overloaded transmission line between buses 13 and 32 is detected by the proposed method and loaded up to its maximum capacity. Figure. (5.8) shows the evolution of the line flow congestion and output power of the all generators. As shown in Figure. (5.7a), the algorithm detects the line overloading and tries to shift power in both sides of the line. As can be seen, the power flow is decreased around the $10th$ iteration and reaches maximum line capacity within 20 iteration. Figure. (5.7b) demonstrates how generators change their output to avoid line overloading. The final consensus value for the entire system is $\lambda = 22.6\,\$/\text{kWh}$.

In the second case study, we test the proposed algorithm on a larger and more realistic power system model, *i.e.*, the IEEE 118-bus, and compare our results with those obtained by the MATPOWER toolbox as a benchmark. The financial information of the generators' cost function (*i.e.,* $\alpha\,\$/(\text{kW})^2\text{h}$, $\beta\,\$/\text{kWh}$) are randomly generated. More information about the system data including bus types, line electrical impedance and other required information regarding, topology can be found in [150]. The comparison between the results obtained by the proposed algorithm and those obtained by

Table 5.2: Numerical comparison of the proposed distributed and centralized methods

Power (kW)	Distributed Method	Centralized Method
P_7	35	35
P_{17}	343.9884	348.75
P_{20}	279.2432	284.09
P_{30}	205.5574	195.01
P_{32}	350	350
P_{33}	34.23851	35.74
P_{34}	98.21342	87.52
P_{35}	134.5003	144.78
Total loss	33.641	33.817
Total generation	1480.7412	1480.89

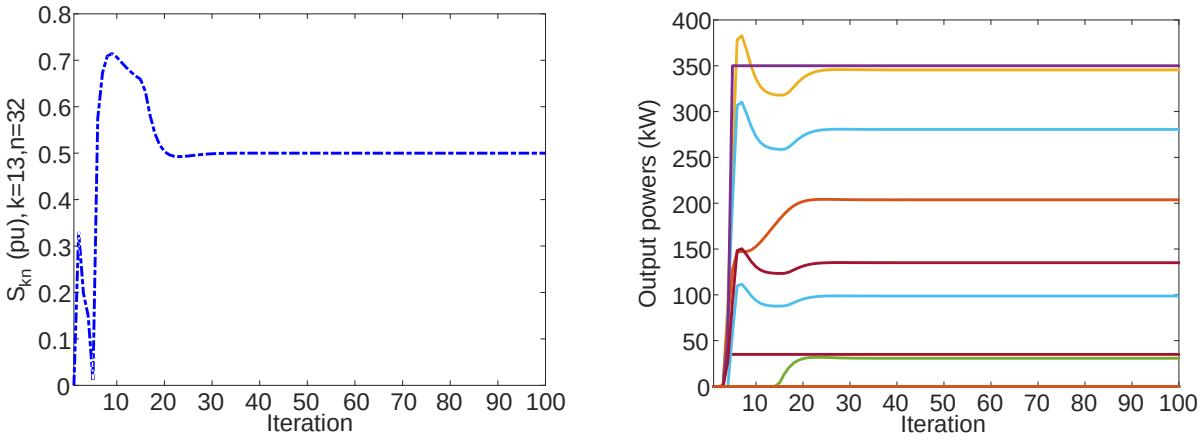

(a) Complex power flow through the line between buses 13 and 32 (pu)

(b) Output powers of generators kW

Figure 5.7: OPF simulaion results for a synthetic 37-bus system system

MATPOWER shows the accuracy and efficiency of our algorithm. The solution mismatch of the generators' output calculated by the distributed methods and those of the benchmark is almost less than 6% of the average. The total cost found by the distributed methods is different from the benchmark results by 0.26%. The total generation is about $4380.55\,kW$, which covers the total demand $(4242.00\,kW)$ plus total loss $(138.55\,kW)$. We should note here that our algorithm is only minimizing the total cost of generation and does not consider minimizing power loss in systems.

As can be seen, the number of iterations required for converging to the final solution does not significantly change with the system size. The number of iterations required for convergence is

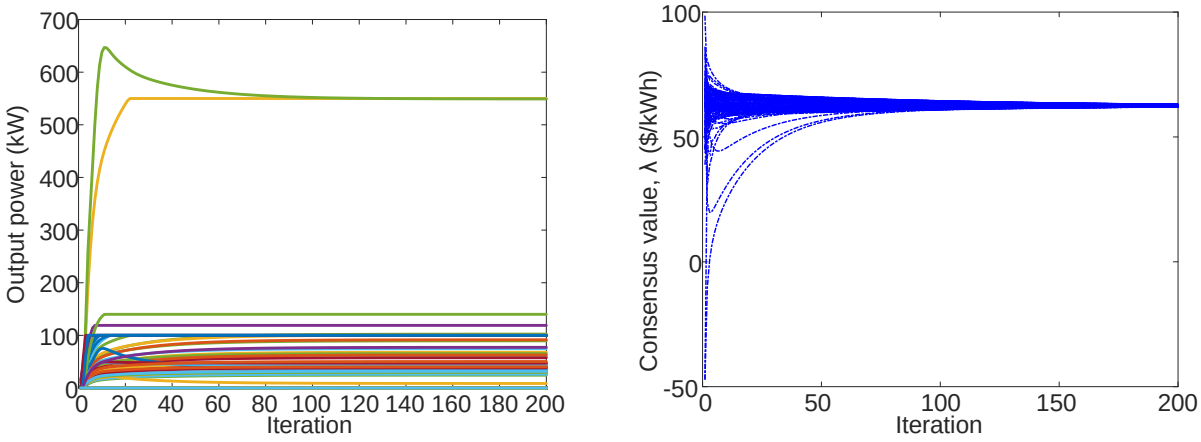

(a) The consensus value of all buses

(b) Output powers of generators kW

Figure 5.8: OPF simulaion results for IEEE 118-bus system system

about 30 in the synthetic 37-bus system. This number is about 42 in the IEEE 118-bus system, while the size of this system is almost 3 times bigger than the first case study. This means the proposed algorithm can efficiently work for bigger systems.

5.7 Conclusions

This work shows that an OPF problem can be solved without linearization and convexification, which in turn does not limit OPF to some specific network and assumptions. As voltage amplitudes are more sensitive to reactive power than active power, the set point voltage of the generators is used to compensate for the violation of voltage amplitude in other buses assuming there is enough amount of the reactive power to control voltage. In addition, line flow constraints are replaced with a local convex problem to pave the way for generalizing the mathematical proof. Simulation results of a synthetic 37-bus case study and an IEEE 118-bus test feeder confirm the optimality analysis.

CHAPTER 6
Conclusion and Future Trends

The foreseeable future of smart grids and energy Internet will significantly affected by Internet of Things (IoT), big data, blockchain, and Cyber-security technologies. The Internet of Things (IoT) is becoming a promising technology for addressing upcoming challenges of power systems by connecting smart devices and leveraging Big data analytic to create giant energy networks. It is also predicted that Blockchain and the Internet of Things (IoT), as key technologies, that will have a huge impact in the next few years for companies in the industrial market [170]. As the IoT scales up as well as energy networks, it's important to provide a flexible and real-time interoperability among different agents in the system. To the the best of my knowledge, distributed control methods could be an effective control method to cope with such giant networks. At the same time, blockchain and Cyber-security technologies have limitless potential to improve privacy in both agent and system level. In addition, digital signature provided by blockchain technology ease most of burden on participation of prosumers and consumers in a real-time retail electricity market.

Thus, researchers can focus on two main areas: Cyber-security (data protection) and intelligent energy management systems. That said, future research will not be limited to these areas. The detailed information is as follows:

6.1 Cyber-Security (Data Protection) for Smart Grids:

In recent years, privacy protection has become more important due to the massive and ceaseless flow of confidential information among a power system's components. Thus, stored and transmitted data must be kept secure with minimal loss and latency for the sake of effective control and monitoring because: 1) it helps entities (e.g, energy producers) protect their technological and

confidential information against adversaries, and 2) it grants autonomy in an electrical competitive market for protection against adversaries.

A) Cryptography is a practice concerned with the enhancement of secret communication in the presence of adversaries. Encryption, as one of the subfields of cryptography, protects stored or transferred data across communications networks to shield confidential data against unauthorized viewing. Quantum key distribution (QKD), as an effective encryption method offers a new secure method for the data protection. In quantum cryptography, two authorized parties are capable of generating a random secret key at the quantum level for data encryption. In this method, security is guaranteed by the laws of physics.

B) Blockchain technology provides opportunities to have a distributed peer-to-peer network where non-trusting members can interact with each other without a trusted leader in a verifiable manner. Application of blockchain technology in smart grids could revolutionize the electrical market in term of security and safety.

6.2 Intelligent Energy Management Systems for Energy Internet

To achieve commercialization and widespread use of renewable energy sources, an efficient energy management strategy based on distributed control method needs to be addressed.

A) Renewable generation integration: This energy management system integrates all possible and remote renewable energy sources to increase energy **independency** from large sources and with its modern tools, it provides agents with the latest information to control their electricity bills and increase their social welfare.

B) Secured communication system: An intelligent energy management system uses Cyber-Security methods to improve the reliability and security of the entities confidential information and the nation's power grid data infrastructure.

C) Power flow management: This system will be equipped with **energy routers**, which are responsible for dynamically adjusting the energy distribution in the grid by rerouting energy flows in transmission and distribution networks.

BIBLIOGRAPHY

[1] J. D. Glover, T. J. Overbye, and M. S. Sarma, *Power system analysis & design*. Boston, MA: Cengage Learning, 6th ed., 2017.

[2] R. J. Hamidi, H. Livani, S. Hosseinian, and G. Gharehpetian, "Distributed cooperative control system for smart microgrids," *Electric Power Systems Research*, vol. 130, pp. 241–250, jan 2016.

[3] S&C Electric Company, "Microgrids: an old idea with new potential," tech. rep., S&C Electric Company, Chicago, IL, USA, 2013.

[4] P. F. Schewe and T. J. Brennan, *The grid: A journey through the heart of our electrified world*, vol. 47. Washington, D.C.: J. Henry Press, 2008.

[5] W. Su, "The Role of Customers in the U.S. Electricity Market: Past, Present and Future," *The Electricity Journal*, vol. 27, pp. 112–125, aug 2014.

[6] W. Su and J. Wang, "Energy Management Systems in Microgrid Operations," *The Electricity Journal*, vol. 25, pp. 45–60, oct 2012.

[7] Navigantresearch, "Market Data: Microgrids," tech. rep., 2016.

[8] L. H. Tsoukalas and R. Gao, "From smart grids to an energy internet: Assumptions, architectures and requirements," in *2008 Third International Conference on Electric Utility Deregulation and Restructuring and Power Technologies*, pp. 94–98, IEEE, apr 2008.

[9] Z. Hu, L. Lu, G. Liu, J. Yi, and L. Zhaoc, "Research on Adaptability Evaluation Method of New Communication Technology Applied to Energy Internet Communication Network," in *2017 IEEE International Conference on Energy Internet (ICEI)*, pp. 250–255, IEEE, apr 2017.

[10] Q. Tang, W. Xu, L. Shen, X. Ye, Y. Xiang, J. Liu, Y. Niu, and J. Hong, "Urban energy internet: Concept and key technology," in *2016 3rd International Conference on Systems and Informatics (ICSAI)*, pp. 318–323, IEEE, nov 2016.

[11] S. Rahman, "Smart grid expectations [In My View]," *IEEE Power and Energy Magazine*, vol. 7, pp. 88, 84–85, sep 2009.

[12] J. Zhu, "Operation of Smart Grid," in *OPTIMIZATION OF POWER SYSTEM OPERATION*, pp. 579–628, Hoboken, NJ, USA: John Wiley & Sons, Inc, jan 2015.

[13] V. Agarwal and L. H. Tsoukalas, "Smart Grids: Importance of Power Quality," in *Lecture Notes of the Institute for Computer Sciences, Social-Informatics and Telecommunications Engineering, LNICST*, vol. 54, pp. 136–143, 2011.

[14] N. Hatziargyriou, A. Dimeas, T. Tomtsi, and A. Weidlich, *Energy-Efficient Computing and Networking*, vol. 54 of *Lecture Notes of the Institute for Computer Sciences, Social Informatics and Telecommunications Engineering*. Berlin, Heidelberg: Springer Berlin Heidelberg, 2011.

[15] S. Borlase, "Smart Grids: Infrastruture, Technology, and Solutions," p. 559, CRC Press, 2013.

[16] J. Rifkin, "The third industrial revolution: how lateral power is transforming energy, the economy, and the world," 2013.

[17] A. Q. Huang, M. L. Crow, G. T. Heydt, J. P. Zheng, and S. J. Dale, "The Future Renewable Electric Energy Delivery and Management (FREEDM) System: The Energy Internet," *Proceedings of the IEEE*, vol. 99, pp. 133–148, jan 2011.

[18] Yi Xu, Jianhua Zhang, Wenye Wang, A. Juneja, and S. Bhattacharya, "Energy router: Architectures and functionalities toward Energy Internet," in *2011 IEEE International Conference on Smart Grid Communications (SmartGridComm)*, pp. 31–36, IEEE, oct 2011.

[19] K. Wang, J. Yu, Y. Yu, Y. Qian, D. Zeng, S. Guo, Y. Xiang, and J. Wu, "A Survey on Energy Internet: Architecture, Approach, and Emerging Technologies," *IEEE Systems Journal*, vol. 12, pp. 2403–2416, sep 2018.

[20] E. Foruzan, S. Asgarpoor, and J. M. Bradley, "Hybrid system modeling and supervisory control of a microgrid," in *2016 North American Power Symposium (NAPS)*, no. 1, pp. 1–6, IEEE, sep 2016.

[21] B. Kroposki, R. Lasseter, T. Ise, S. Morozumi, S. Papathanassiou, and N. Hatziargyriou, "Making microgrids work," *IEEE Power and Energy Magazine*, vol. 6, pp. 40–53, may 2008.

[22] A. Dehghan Banadaki, F. D. Mohammadi, and A. Feliachi, "State space modeling of inverter based microgrids considering distributed secondary voltage control," in *2017 North American Power Symposium (NAPS)*, (Morgantown, WV, USA), pp. 1–6, IEEE, sep 2017.

[23] P. Peng, "Microgrids: A bright future," *Huawei Communicate*, no. 63, pp. 6–8, 2011.

[24] H. Pourbabak, T. Chen, B. Zhang, and W. Su, "Control and energy management system in microgrids," in *Clean Energy Microgrids*, ch. 3, pp. 109–133, Institution of Engineering and Technology, 2017.

[25] M. Higgs, "Electrical SCADA systems from the operators perspective," in *International Conference on People in Control (Human Interfaces in Control Rooms, Cockpits and Command Centres)*, vol. 1999, pp. 458–461, IEE, 1999.

[26] E. Vaahedi, "Power System Monitoring," in *Practical Power System Operation*, ch. 2, pp. 6–20, Hoboken, NJ: John Wiley & Sons, mar 2014.

[27] W. N. S. E. W. Jusoh, M. R. A. Ghani, M. A. M. Hanafiah, and S. H. Raman, "Remote Terminal Unit (RTU) hardware design and development for distribution automation system," in *2014 IEEE Innovative Smart Grid Technologies - Asia, ISGT ASIA 2014*, (Kuala Lumpur, Malaysia), pp. 572–576, IEEE, may 2014.

[28] H. Pourbabak, J. Luo, T. Chen, and W. Su, "A Novel Consensus-Based Distributed Algorithm for Economic Dispatch Based on Local Estimation of Power Mismatch," *IEEE Transactions on Smart Grid*, vol. 9, pp. 5930–5942, nov 2018.

[29] G. Taylor, M. Irving, P. Hobson, C. Huang, P. Kyberd, and R. Taylor, "Distributed monitoring and control of future power systems via grid computing," in *2006 IEEE Power Engineering Society General Meeting*, p. 5 pp., IEEE, 2006.

[30] E. Aladesanmi and K. Folly, "Overview of non-intrusive load monitoring and identification techniques," *IFAC-PapersOnLine*, vol. 48, no. 30, pp. 415–420, 2015.

[31] A. Zoha, A. Gluhak, M. Imran, and S. Rajasegarar, "Non-Intrusive Load Monitoring Approaches for Disaggregated Energy Sensing: A Survey," *Sensors*, vol. 12, pp. 16838–16866, dec 2012.

[32] H. Cao, S. Liu, R. Zhao, H. Gu, J. Bao, and L. Zhu, "A Privacy Preserving Model for Energy Internet Base on Differential Privacy," in *2017 IEEE International Conference on Energy Internet (ICEI)*, pp. 204–209, IEEE, apr 2017.

[33] D. Egarter, C. Prokop, and W. Elmenreich, "Load hiding of household's power demand," in *2014 IEEE International Conference on Smart Grid Communications (SmartGridComm)*, pp. 854–859, IEEE, nov 2014.

[34] W. Yang, N. Li, Y. Qi, W. Qardaji, S. McLaughlin, and P. McDaniel, "Minimizing private data disclosures in the smart grid," in *Proceedings of the 2012 ACM conference on Computer and communications security - CCS '12*, (New York, New York, USA), p. 415, ACM Press, 2012.

[35] S. Finster and I. Baumgart, "Elderberry: A peer-to-peer, privacy-aware smart metering protocol," in *2013 Proceedings IEEE INFOCOM*, pp. 3411–3416, IEEE, apr 2013.

[36] C.-K. Chu, J. K. Liu, J. W. Wong, Y. Zhao, and J. Zhou, "Privacy-preserving smart metering with regional statistics and personal enquiry services," in *Proceedings of the 8th ACM SIGSAC symposium on Information, computer and communications security - ASIA CCS '13*, (New York, New York, USA), p. 369, ACM Press, 2013.

[37] C. Dwork and A. Roth, "The Algorithmic Foundations of Differential Privacy," *Foundations and Trends® in Theoretical Computer Science*, vol. 9, no. 3-4, pp. 211–407, 2013.

[38] A. G. Tsikalakis and N. D. Hatziargyriou, "Centralized Control for Optimizing Microgrids Operation," *IEEE Transactions on Energy Conversion*, vol. 23, pp. 241–248, mar 2008.

[39] B. Saravanan, S. Das, S. Sikri, and D. P. Kothari, "A solution to the unit commitment problem—a review," *Frontiers in Energy*, vol. 7, pp. 223–236, jun 2013.

[40] A. J. Wood, B. F. Wollenberg, and G. B. Sheble, *Power generation, operation, and control*. John Wiley & Sons, Inc., Hoboken, New Jersey, 3rd ed., 2014.

[41] R. Sioshansi, R. O'Neill, and S. Oren, "Economic Consequences of Alternative Solution Methods for Centralized Unit Commitment in Day-Ahead Electricity Markets," *IEEE Transactions on Power Systems*, vol. 23, pp. 344–352, may 2008.

[42] D. E. Olivares, C. A. Canizares, and M. Kazerani, "A Centralized Energy Management System for Isolated Microgrids," *IEEE Transactions on Smart Grid*, vol. 5, pp. 1864–1875, jul 2014.

[43] R. Palma-Behnke, C. Benavides, F. Lanas, B. Severino, L. Reyes, J. Llanos, and D. Saez, "A Microgrid Energy Management System Based on the Rolling Horizon Strategy," *IEEE Transactions on Smart Grid*, vol. 4, pp. 996–1006, jun 2013.

[44] H. Pourbabak and A. Kazemi, "A new technique for islanding detection using voltage phase angle of inverter-based DGs," *International Journal of Electrical Power & Energy Systems*, vol. 57, pp. 198–205, may 2014.

[45] M. Warnier, S. Dulman, Y. Koç, and E. Pauwels, "Distributed monitoring for the prevention of cascading failures in operational power grids," *International Journal of Critical Infrastructure Protection*, vol. 17, pp. 15–27, jun 2017.

[46] H. Pourbabak, Tao Chen, and W. Su, "Consensus-based distributed control for economic operation of distribution grid with multiple consumers and prosumers," in *2016 IEEE Power and Energy Society General Meeting (PESGM)*, vol. 2016-Novem, (Boston, MA), pp. 1–5, IEEE, jul 2016.

[47] R. Mudumbai, S. Dasgupta, and B. B. Cho, "Distributed Control for Optimal Economic Dispatch of a Network of Heterogeneous Power Generators," *IEEE Transactions on Power Systems*, vol. 27, pp. 1750–1760, nov 2012.

[48] A. X. Sun, D. T. Phan, and S. Ghosh, "Fully decentralized AC optimal power flow algorithms," in *2013 IEEE Power & Energy Society General Meeting*, pp. 1–5, IEEE, 2013.

[49] W. Ren and R. W. Beard, *Distributed Consensus in Multi-vehicle Cooperative Control*. Communications and Control Engineering, London: Springer London, 2008.

[50] W. Su, J. Wang, K. Zhang, and A. Q. Huang, "Model predictive control-based power dispatch for distribution system considering plug-in electric vehicle uncertainty," *Electric Power Systems Research*, vol. 106, pp. 29–35, jan 2014.

[51] T. Senjyu, R. Kuninaka, N. Urasaki, H. Fujita, and T. Funabashi, "Power system stabilization based on robust centralized and decentralized controllers," in *2005 International Power Engineering Conference*, pp. 905–910 Vol. 2, IEEE, 2005.

[52] H. Pourbabak, S. Xu, T. Chen, Z. Liang, and W. Su, "Distributed control algorithm for optimal power allocation of EV parking lots," in *2017 IEEE Power & Energy Society General Meeting*, vol. 2018-Janua, (Chicago, IL), pp. 1–5, IEEE, jul 2017.

[53] S. Xu, H. Pourbabak, and W. Su, "Distributed cooperative control for economic operation of multiple plug-in electric vehicle parking decks," *International Transactions on Electrical Energy Systems*, vol. 27, p. e2348, sep 2017.

[54] Y. Yan, Y. Qian, H. Sharif, and D. Tipper, "A Survey on Smart Grid Communication Infrastructures: Motivations, Requirements and Challenges," *IEEE Communications Surveys & Tutorials*, vol. 15, no. 1, pp. 5–20, 2013.

[55] R. Deng, Z. Yang, F. Hou, M.-Y. Chow, and J. Chen, "Distributed Real-Time Demand Response in Multiseller–Multibuyer Smart Distribution Grid," *IEEE Transactions on Power Systems*, vol. 30, pp. 2364–2374, sep 2015.

[56] G. Hug, S. Kar, and C. Wu, "Consensus + Innovations Approach for Distributed Multiagent Coordination in a Microgrid," *IEEE Transactions on Smart Grid*, vol. 6, pp. 1893–1903, jul 2015.

[57] N. Rahbari-Asr, U. Ojha, Z. Zhang, and M.-Y. Chow, "Incremental Welfare Consensus Algorithm for Cooperative Distributed Generation/Demand Response in Smart Grid," *IEEE Transactions on Smart Grid*, vol. 5, pp. 2836–2845, nov 2014.

[58] H. Dagdougui and R. Sacile, "Decentralized Control of the Power Flows in a Network of Smart Microgrids Modeled as a Team of Cooperative Agents," *IEEE Transactions on Control Systems Technology*, vol. 22, pp. 510–519, mar 2014.

[59] R. de Azevedo, M. H. Cintuglu, T. Ma, and O. A. Mohammed, "Multiagent-Based Optimal Microgrid Control Using Fully Distributed Diffusion Strategy," *IEEE Transactions on Smart Grid*, vol. 8, pp. 1997–2008, jul 2017.

[60] D. K. Molzahn, F. Dorfler, H. Sandberg, S. H. Low, S. Chakrabarti, R. Baldick, and J. Lavaei, "A Survey of Distributed Optimization and Control Algorithms for Electric Power Systems," *IEEE Transactions on Smart Grid*, vol. 8, pp. 2941–2962, nov 2017.

[61] B. Yang and M. Johansson, "Distributed optimization and games: A tutorial overview," in *Lecture Notes in Control and Information Sciences*, vol. 406, pp. 109–148, 2010.

[62] T. Erseghe, "Distributed Optimal Power Flow Using ADMM," *IEEE Transactions on Power Systems*, vol. 29, pp. 2370–2380, sep 2014.

[63] N. Rahbari-Asr and M.-Y. Chow, "Cooperative Distributed Demand Management for Community Charging of PHEV/PEVs Based on KKT Conditions and Consensus Networks," *IEEE Transactions on Industrial Informatics*, vol. 10, pp. 1907–1916, aug 2014.

[64] P. Yi, Y. Hong, and F. Liu, "Distributed gradient algorithm for constrained optimization with application to load sharing in power systems," *Systems & Control Letters*, vol. 83, pp. 45–52, sep 2015.

[65] A. B. Bondi, "Characteristics of scalability and their impact on performance," in *Proceedings of the second international workshop on Software and performance - WOSP '00*, (New York, New York, USA), pp. 195–203, ACM Press, 2000.

[66] H. Pourbabak, A. Ajao, T. Chen, and W. Su, "Fully distributed AC power flow (ACPF) algorithm for distribution systems," *IET Smart Grid*, vol. 2, pp. 155–162, jun 2019.

[67] H. Pourbabak, Q. Alsafasfeh, and W. Su, "A Distributed Consensus-based Algorithm for Optimal Power Flow in DC Distribution Grids," *Under Review*, 2019.

[68] H. Pourbabak, Q. Alsafasfeh, and W. Su, "Fully Distributed AC Optimal Power Flow," *IEEE Access*, vol. 7, pp. 97594–97603, 2019.

[69] S. Aman, Y. Simmhan, and V. K. Prasanna, "Holistic Measures for Evaluating Prediction Models in Smart Grids," *IEEE Communications Surveys & Tutorials*, vol. 14, pp. 944–980, jun 2014.

[70] C. W. Potter, A. Archambault, and K. Westrick, "Building a smarter smart grid through better renewable energy information," in *2009 IEEE/PES Power Systems Conference and Exposition*, pp. 1–5, IEEE, mar 2009.

[71] A. Asadinejad, K. Tomsovic, and C.-f. Chen, "Sensitivity of incentive based demand response program to residential customer elasticity," in *2016 North American Power Symposium (NAPS)*, no. September, pp. 1–6, IEEE, sep 2016.

[72] L. I. Millett, B. Fischhoff, and P. J. Weinberger, *Foundational Cybersecurity Research*. Washington, D.C.: National Academies of Sciences, Engineering and Medicine, jul 2017.

[73] R. Saber and R. Murray, "Consensus protocols for networks of dynamic agents," in *Proceedings of the 2003 American Control Conference, 2003.*, vol. 2, pp. 951–956, IEEE, 2003.

[74] R. Olfati-Saber, J. A. Fax, and R. M. Murray, "Consensus and Cooperation in Networked Multi-Agent Systems," *Proceedings of the IEEE*, vol. 95, pp. 215–233, jan 2007.

[75] G. Binetti, A. Davoudi, F. L. Lewis, D. Naso, and B. Turchiano, "Distributed Consensus-Based Economic Dispatch With Transmission Losses," *IEEE Transactions on Power Systems*, vol. 29, pp. 1711–1720, jul 2014.

[76] Y. Xu, J. Hu, W. Gu, W. Su, and W. Liu, "Real-Time Distributed Control of Battery Energy Storage Systems for Security Constrained DC-OPF," *IEEE Transactions on Smart Grid*, pp. 1–1, 2016.

[77] Z. Zhang and M.-Y. Chow, "Convergence Analysis of the Incremental Cost Consensus Algorithm Under Different Communication Network Topologies in a Smart Grid," *IEEE Transactions on Power Systems*, vol. 27, pp. 1761–1768, nov 2012.

[78] Wente Zeng and Mo-Yuen Chow, "Resilient Distributed Control in the Presence of Misbehaving Agents in Networked Control Systems," *IEEE Transactions on Cybernetics*, vol. 44, pp. 2038–2049, nov 2014.

[79] D. S. Kirschen and G. Strbac, *Fundamentals of power system economics*. Chichester: John Wiley & Sons, 2004.

[80] P. Samadi, H. Mohsenian-Rad, R. Schober, and V. W. S. Wong, "Advanced Demand Side Management for the Future Smart Grid Using Mechanism Design," *IEEE Transactions on Smart Grid*, vol. 3, pp. 1170–1180, sep 2012.

[81] Y. Xu, W. Zhang, G. Hug, S. Kar, and Z. Li, "Cooperative Control of Distributed Energy Storage Systems in a Microgrid," *IEEE Transactions on Smart Grid*, vol. 6, pp. 238–248, jan 2015.

[82] W. Ren and Y. Cao, *Distributed Coordination of Multi-agent Networks*. Communications and Control Engineering, London: Springer London, 2011.

[83] A. Kazemi and H. Pourbabak, "Islanding detection method based on a new approach to voltage phase angle of constant power inverters," *IET Generation, Transmission & Distribution*, vol. 10, pp. 1190–1198, apr 2016.

[84] F. Guo, C. Wen, J. Mao, and Y.-D. Song, "Distributed Economic Dispatch for Smart Grids With Random Wind Power," *IEEE Transactions on Smart Grid*, vol. 7, pp. 1572–1583, may 2016.

[85] E. Dall'Anese, Hao Zhu, and G. B. Giannakis, "Distributed Optimal Power Flow for Smart Microgrids," *IEEE Transactions on Smart Grid*, vol. 4, pp. 1464–1475, sep 2013.

[86] W. T. Elsayed and E. F. El-Saadany, "A Fully Decentralized Approach for Solving the Economic Dispatch Problem," *IEEE Transactions on Power Systems*, vol. 30, no. 4, pp. 2179–2189, 2014.

[87] W. Zhang, W. Liu, X. Wang, L. Liu, and F. Ferrese, "Online Optimal Generation Control Based on Constrained Distributed Gradient Algorithm," *IEEE Transactions on Power Systems*, vol. 30, pp. 35–45, jan 2015.

[88] S. Yang, S. Tan, and J.-X. Xu, "Consensus Based Approach for Economic Dispatch Problem in a Smart Grid," *IEEE Transactions on Power Systems*, vol. 28, pp. 4416–4426, nov 2013.

[89] N. Cai, Nguyen Thi Thanh Nga, and J. Mitra, "Economic dispatch in microgrids using multi-agent system," in *2012 North American Power Symposium (NAPS)*, pp. 1–5, IEEE, sep 2012.

[90] T.-H. Chang, A. Nedic, and A. Scaglione, "Distributed Constrained Optimization by Consensus-Based Primal-Dual Perturbation Method," *IEEE Transactions on Automatic Control*, vol. 59, pp. 1524–1538, jun 2014.

[91] M. Fahrioglu and F. Alvarado, "Using utility information to calibrate customer demand management behavior models," *IEEE Transactions on Power Systems*, vol. 16, pp. 317–322, may 2001.

[92] P. Samadi, A.-H. Mohsenian-Rad, R. Schober, V. W. S. Wong, and J. Jatskevich, "Optimal Real-Time Pricing Algorithm Based on Utility Maximization for Smart Grid," in *2010 First IEEE International Conference on Smart Grid Communications*, pp. 415–420, IEEE, oct 2010.

[93] F. L. Lewis, H. Zhang, K. Hengster-Movric, and A. Das, *Cooperative Control of Multi-Agent Systems*. Communications and Control Engineering, London: Springer London, 2014.

[94] S. P. Boyd and L. Vandenberghe, *Convex optimization*. Cambridge Cambridge University, 2018.

[95] J. Lofberg, "YALMIP : a toolbox for modeling and optimization in MATLAB," in *2004 IEEE International Conference on Robotics and Automation (IEEE Cat. No.04CH37508)*, pp. 284–289, IEEE, 2004.

[96] Jingwei Luo, H. Pourbabak, and W. Su, "The application of distributed control algorithms using VOLTTRON-based software platform," in *2017 8th International Renewable Energy Congress (IREC)*, (Dead Sea, Jordan), pp. 1–6, IEEE, mar 2017.

[97] H. Glavitsch and R. Bacher, "Optimal Power Flow Algorithms," in *Analysis and control system techniques for electric power systems*, vol. 41, pp. 135–205, 1991.

[98] W. Tinney and C. Hart, "Power Flow Solution by Newton's Method," *IEEE Transactions on Power Apparatus and Systems*, vol. PAS-86, pp. 1449–1460, nov 1967.

[99] V. da Costa, N. Martins, and J. Pereira, "Developments in the Newton Raphson power flow formulation based on current injections," *IEEE Transactions on Power Systems*, vol. 14, no. 4, pp. 1320–1326, 1999.

[100] J. B. Ward and H. W. Hale, "Digital Computer Solution of Power-Flow Problems [includes discussion]," *Transactions of the American Institute of Electrical Engineers. Part III: Power Apparatus and Systems*, vol. 75, jan 1956.

[101] R. Klump and T. Overbye, "A new method for finding low-voltage power flow solutions," in *2000 Power Engineering Society Summer Meeting (Cat. No.00CH37134)*, vol. 1, pp. 593–597, IEEE, 2000.

[102] M. Matos, "A new power flow method for radial networks," in *2003 IEEE Bologna Power Tech Conference Proceedings,*, vol. 2, pp. 359–363, IEEE, 2003.

[103] N. Ghadimi, "Two new methods for power flow tracing using bus power balance equations," *Journal of Central South University*, vol. 21, pp. 2712–2718, jul 2014.

[104] B. Stott, J. Jardim, and O. Alsac, "DC Power Flow Revisited," *IEEE Transactions on Power Systems*, vol. 24, pp. 1290–1300, aug 2009.

[105] N. Hatziargyriou, H. Asano, R. Iravani, and C. Marnay, "Microgrids," *IEEE Power and Energy Magazine*, vol. 5, pp. 78–94, jul 2007.

[106] Guofang Zhu, Guibin Zou, Baoguang Zhao, Houlei Gao, and Bingbing Tong, "Directional pilot protection method for distribution grid with DG," in *12th IET International Conference on Developments in Power System Protection (DPSP 2014)*, no. 1, pp. 12.07–12.07, Institution of Engineering and Technology, 2014.

[107] W. Su, J. Wang, and D. Ton, "Smart Grid Impact on Operation and Planning of Electric Energy Systems," in *Handbook of Clean Energy Systems*, pp. 1–13, Chichester, UK: John Wiley & Sons, Ltd, jul 2015.

[108] S. D. J. McArthur, E. M. Davidson, V. M. Catterson, A. L. Dimeas, N. D. Hatziargyriou, F. Ponci, and T. Funabashi, "Multi-Agent Systems for Power Engineering Applications—Part I: Concepts, Approaches, and Technical Challenges," *IEEE Transactions on Power Systems*, vol. 22, pp. 1743–1752, nov 2007.

[109] M. Kleinberg, Karen Miu, and C. Nwankpa, "Distributed Multi-Phase Distribution Power Flow: Modeling, Solution Algorithm and Simulation Results," *SIMULATION*, vol. 84, pp. 403–412, aug 2008.

[110] C. P. Nguyen and A. J. Flueck, "A Novel Agent-Based Distributed Power Flow Solver for Smart Grids," *IEEE Transactions on Smart Grid*, vol. 6, pp. 1261–1270, may 2015.

[111] E. Iggland and G. Andersson, "On using reduced networks for distributed DC power flow," in *2012 IEEE Power and Energy Society General Meeting*, pp. 1–6, IEEE, jul 2012.

[112] K. Nakayama, C. Zhao, L. F. Bic, M. B. Dillencourt, and J. Brouwer, "Distributed power flow loss minimization control for future grid," *International Journal of Circuit Theory and Applications*, vol. 43, pp. 1209–1225, sep 2015.

[113] V. R. Disfani, L. Fan, and Z. Miao, "Distributed DC Optimal Power Flow for radial networks through partial Primal Dual algorithm," in *2015 IEEE Power & Energy Society General Meeting*, pp. 1–5, IEEE, jul 2015.

[114] "The War of the Currents: AC vs. DC Power, Department of Energy, https://www.energy.gov/articles/war-currents-ac-vs-dc-power," 2014.

[115] V. Vossos, S. Pantano, R. Heard, and R. Brown, "DC Appliances and DC Power Distribution: A Bridge to the Future Net Zero Energy Homes," Tech. Rep. September, Lawrence Berkeley National Laboratory, 2017.

[116] L. Mackay, N. H. van der Blij, L. Ramirez-Elizondo, and P. Bauer, "Toward the Universal DC Distribution System," *Electric Power Components and Systems*, vol. 45, pp. 1032–1042, jun 2017.

[117] L. Piao, M. de Weerdt, and L. de Vries, "Electricity market design requirements for DC distribution systems," in *2017 IEEE Second International Conference on DC Microgrids (ICDCM)*, pp. 95–101, IEEE, jun 2017.

[118] K. Kim, K. Park, G. Roh, and K. Chun, "DC-grid system for ships: a study of benefits and technical considerations," *Journal of International Maritime Safety, Environmental Affairs, and Shipping*, vol. 2, pp. 1–12, nov 2018.

[119] L. Mackay, *Steps towards the universal direct current distribution system*. doctoral thesis, Delft University of Technology, 2018.

[120] J. CARPENTIER, "Optimal power flows," *International Journal of Electrical Power & Energy Systems*, vol. 1, pp. 3–15, apr 1979.

[121] A. Engelmann, T. Mühlpfordt, Y. Jiang, B. Houska, and T. Faulwasser, "Distributed AC Optimal Power Flow using ALADIN * *TF is indebted to the Baden-Württemberg Stiftung for the financial support of this research by the Elite Programme for Postdocs. TF and BH are supported by the Deutsche Forschungsgemeinschaft, Grants WO 20," *IFAC-PapersOnLine*, vol. 50, pp. 5536–5541, jul 2017.

[122] A. S. Zamzam, X. Fu, E. Dall'Anese, and N. D. Sidiropoulos, "Distributed optimal power flow using feasible point pursuit," in *2017 IEEE 7th International Workshop on Computational Advances in Multi-Sensor Adaptive Processing (CAMSAP)*, pp. 1–5, IEEE, dec 2017.

[123] M. Cain, R. O'Neill, and A. Castillo, "History of Optimal Power Flow and Formulations," Tech. Rep. December, 2012.

[124] S. H. Low, "Convex Relaxation of Optimal Power Flow—Part I: Formulations and Equivalence," *IEEE Transactions on Control of Network Systems*, vol. 1, pp. 15–27, mar 2014.

[125] S. H. Low, "Convex Relaxation of Optimal Power Flow—Part II: Exactness," *IEEE Transactions on Control of Network Systems*, vol. 1, pp. 177–189, jun 2014.

[126] S. Galvani and S. Rezaeian Marjani, "Optimal power flow considering predictability of power systems," *Electric Power Systems Research*, vol. 171, pp. 66–73, jun 2019.

[127] T. Liu, B. Sun, and D. H. K. Tsang, "Rank-One Solutions for SDP Relaxation of QCQPs in Power Systems," *IEEE Transactions on Smart Grid*, vol. 10, pp. 5–15, jan 2019.

[128] Q. Xia, Z. Yang, C. Kang, H. Zhong, and A. Bose, "Optimal Power Flow in AC-DC Grids With Discrete Control Devices," *IEEE Transactions on Power Systems*, vol. 33, no. 2, pp. 1461–1472, 2017.

[129] W. A. Bukhsh, A. Grothey, K. I. M. McKinnon, and P. A. Trodden, "Local Solutions of the Optimal Power Flow Problem," *IEEE Transactions on Power Systems*, vol. 28, pp. 4780–4788, nov 2013.

[130] L. Roald and G. Andersson, "Chance-Constrained AC Optimal Power Flow: Reformulations and Efficient Algorithms," *IEEE Transactions on Power Systems*, vol. 33, pp. 2906–2918, may 2018.

[131] A. Venzke, L. Halilbasic, U. Markovic, G. Hug, and S. Chatzivasileiadis, "Convex Relaxations of Chance Constrained AC Optimal Power Flow," *IEEE Transactions on Power Systems*, vol. 33, pp. 2829–2841, may 2018.

[132] Y. Tang, K. Dvijotham, and S. Low, "Real-Time Optimal Power Flow," *IEEE Transactions on Smart Grid*, vol. 8, pp. 2963–2973, nov 2017.

[133] K. Fleischer and R. Munnings, "Power systems analysis for direct current (DC) distribution systems," *IEEE Transactions on Industry Applications*, vol. 32, no. 5, pp. 982–989, 1996.

[134] C. Jayarathna, P. Binduhewa, J. Ekanayake, and J. Wu, "Load flow analysis of low voltage dc networks with photovoltaic," in *2014 9th International Conference on Industrial and Information Systems (ICIIS)*, no. 1, pp. 1–6, IEEE, dec 2014.

[135] L. Gan and S. H. Low, "Optimal Power Flow in Direct Current Networks," *IEEE Transactions on Power Systems*, vol. 29, pp. 2892–2904, nov 2014.

[136] J. Li, F. Liu, Z. Wang, S. H. Low, and S. Mei, "Optimal Power Flow in Stand-Alone DC Microgrids," *IEEE Transactions on Power Systems*, vol. 33, no. 5, pp. 5496–5506, 2018.

[137] J. Ma, L. Yuan, Z. Zhao, and F. He, "Transmission Loss Optimization-Based Optimal Power Flow Strategy by Hierarchical Control for DC Microgrids," *IEEE Transactions on Power Electronics*, vol. 32, pp. 1952–1963, mar 2017.

[138] B. Han and Y. Li, "Power flow optimization for DC distribution grid with distributed energy access based on Newton–Raphson method through upper level control," *Cluster Computing*, vol. 0, feb 2018.

[139] L. Mackay, A. Dimou, R. Guarnotta, G. Morales-Espania, L. Ramirez-Elizondo, and P. Bauer, "Optimal power flow in bipolar DC distribution grids with asymmetric loading," in *2016 IEEE International Energy Conference (ENERGYCON)*, pp. 1–6, IEEE, apr 2016.

[140] H. Han, H. Wang, Y. Sun, J. Yang, and Z. Liu, "Distributed control scheme on cost optimisation under communication delays for DC microgrids," *IET Generation, Transmission & Distribution*, vol. 11, pp. 4193–4201, nov 2017.

[141] B. Kim and R. Baldick, "A comparison of distributed optimal power flow algorithms," *IEEE Transactions on Power Systems*, vol. 15, pp. 599–604, may 2000.

[142] A. Engelmann, Y. Jiang, T. Muhlpfordt, B. Houska, and T. Faulwasser, "Toward Distributed OPF Using ALADIN," *IEEE Transactions on Power Systems*, vol. 34, pp. 584–594, jan 2019.

[143] X. Fang, B.-M. Hodge, H. Jiang, and Y. Zhang, "Decentralized wind uncertainty management: Alternating direction method of multipliers based distributionally-robust chance constrained optimal power flow," *Applied Energy*, vol. 239, pp. 938–947, apr 2019.

[144] S. Kar and G. Hug, "Distributed robust economic dispatch in power systems: A consensus \& innovations approach," in *2012 IEEE Power and Energy Society General Meeting*, pp. 1–8, IEEE, jul 2012.

[145] S. Karambelkar, L. Mackay, S. Chakraborty, L. Ramirez-Elizondo, and P. Bauer, "Distributed Optimal Power Flow for DC Distribution Grids," in *2018 IEEE Power & Energy Society General Meeting (PESGM)*, pp. 1–5, IEEE, aug 2018.

[146] E. Sindi, L. Y. Wang, M. Polis, G. Yin, and L. Ding, "Distributed Optimal Power and Voltage Management in DC Microgrids: Applications to Dual-Source Trolleybus Systems," *IEEE Transactions on Transportation Electrification*, vol. 4, pp. 778–788, sep 2018.

[147] N. Meyer-Huebner, M. Suriyah, and T. Leibfried, "Decentralized Optimal Power Flow in Hybrid AC-DC Grids," *IEEE Transactions on Power Systems*, vol. X, no. X, pp. 1–1, 2019.

[148] Z.-q. Luo, W.-k. Ma, A. So, Y. Ye, and S. Zhang, "Semidefinite Relaxation of Quadratic Optimization Problems," *IEEE Signal Processing Magazine*, vol. 27, pp. 20–34, may 2010.

[149] "Electric Grid Test Cases, Texas A\&M UNiversity, "https://electricgrids.engr.tamu.edu/electric-grid-test-cases/"."

[150] "Power Systems Test Case Archive, Univesity of Washington, "https://labs.ece.uw.edu/pstca/"."

[151] J. Lavaei and S. H. Low, "Zero Duality Gap in Optimal Power Flow Problem," *IEEE Transactions on Power Systems*, vol. 27, pp. 92–107, feb 2012.

[152] M. Lubin, Y. Dvorkin, and L. Roald, "Chance Constraints for Improving the Security of AC Optimal Power Flow," *IEEE Transactions on Power Systems*, vol. 34, pp. 1908–1917, may 2019.

[153] D. Van Hertem, "Usefulness of DC power flow for active power flow analysis with flow controlling devices," in *8th IEE International Conference on AC and DC Power Transmission (ACDC 2006)*, vol. 2006, pp. 58–62, IEE, 2006.

[154] T. Overbye, Xu Cheng, and Yan Sun, "A comparison of the AC and DC power flow models for LMP calculations," in *37th Annual Hawaii International Conference on System Sciences, 2004. Proceedings of the*, p. 9 pp., IEEE, 2004.

[155] M. Huneault and F. Galiana, "A survey of the optimal power flow literature," *IEEE Transactions on Power Systems*, vol. 6, pp. 762–770, may 1991.

[156] J. Momoh, R. Adapa, and M. El-Hawary, "A review of selected optimal power flow literature to 1993. I. Nonlinear and quadratic programming approaches," *IEEE Transactions on Power Systems*, vol. 14, no. 1, pp. 96–104, 1999.

[157] J. Momoh, M. El-Hawary, and R. Adapa, "A review of selected optimal power flow literature to 1993. II. Newton, linear programming and interior point methods," *IEEE Transactions on Power Systems*, vol. 14, no. 1, pp. 105–111, 1999.

[158] S. Frank, I. Steponavice, and S. Rebennack, "Optimal power flow: a bibliographic survey I," *Energy Systems*, vol. 3, pp. 221–258, sep 2012.

[159] S. Frank, I. Steponavice, and S. Rebennack, "Optimal power flow: a bibliographic survey II," *Energy Systems*, vol. 3, pp. 259–289, sep 2012.

[160] S. Bruno, S. Lamonaca, G. Rotondo, U. Stecchi, and M. La Scala, "Unbalanced Three-Phase Optimal Power Flow for Smart Grids," *IEEE Transactions on Industrial Electronics*, vol. 58, pp. 4504–4513, oct 2011.

[161] D. Bienstock, M. Chertkov, and S. Harnett, "Chance-Constrained Optimal Power Flow: Risk-Aware Network Control under Uncertainty," *SIAM Review*, vol. 56, pp. 461–495, jan 2014.

[162] A. Y. Lam, B. Zhang, and D. N. Tse, "Distributed algorithms for optimal power flow problem," in *2012 IEEE 51st IEEE Conference on Decision and Control (CDC)*, pp. 430–437, IEEE, dec 2012.

[163] J. Guo, G. Hug, and O. Tonguz, "Impact of communication delay on asynchronous distributed optimal power flow using ADMM," in *2017 IEEE International Conference on Smart Grid Communications (SmartGridComm)*, pp. 177–182, IEEE, oct 2017.

[164] C. Wang, W. Wei, J. Wang, L. Bai, Y. Liang, and T. Bi, "Convex Optimization Based Distributed Optimal Gas-Power Flow Calculation," *IEEE Transactions on Sustainable Energy*, pp. 1–1, 2017.

[165] C.-Y. Chang, J. Cortes, and S. Martinez, "A scheduled-asynchronous distributed optimization algorithm for the optimal power flow problem," in *2017 American Control Conference (ACC)*, pp. 3968–3973, IEEE, may 2017.

[166] Y. Zhang, M. Hong, E. Dall'Anese, S. V. Dhople, and Z. Xu, "Distributed Controllers Seeking AC Optimal Power Flow Solutions Using ADMM," *IEEE Transactions on Smart Grid*, vol. 9, pp. 4525–4537, sep 2018.

[167] Y. Liu, Z. Qu, H. Xin, and D. Gan, "Distributed Real-Time Optimal Power Flow Control in Smart Grid," *IEEE Transactions on Power Systems*, vol. 32, pp. 3403–3414, sep 2017.

[168] P. Shannon, "Cytoscape: A Software Environment for Integrated Models of Biomolecular Interaction Networks," *Genome Research*, vol. 13, pp. 2498–2504, nov 2003.

[169] R. D. Zimmerman, C. E. Murillo-Sanchez, and R. J. Thomas, "MATPOWER: Steady-State Operations, Planning, and Analysis Tools for Power Systems Research and Education," *IEEE Transactions on Power Systems*, vol. 26, pp. 12–19, feb 2011.

[170] D. Miller, “Blockchain and the Internet of Things in the Industrial Sector,” *IT Professional*, vol. 20, pp. 15–18, may 2018.